CHALMERS

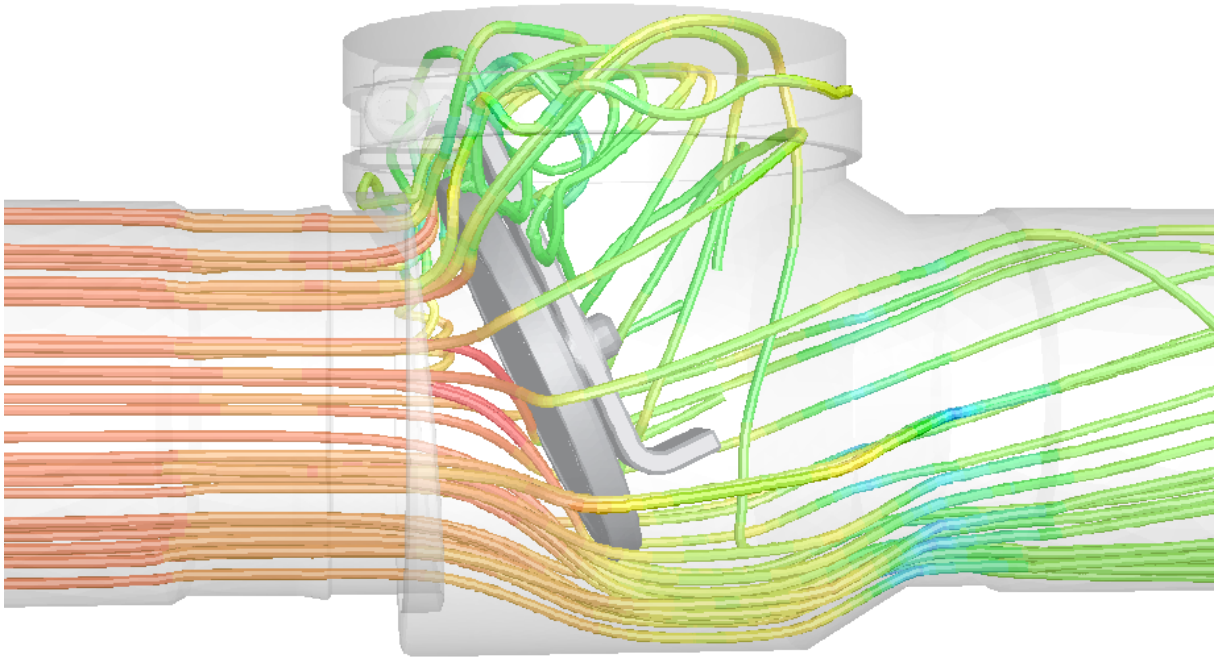

Dynamic simulation of check valve using CFD and evaluation of check valve model in RELAP5

Master of Science Thesis [Nuclear Engineering]

Martin Turesson

Department of Chemistry and Bioscience
Division of chemical reaction engineering
CHALMERS UNIVERSITY OF TECHNOLOGY
Göteborg, Sweden, 2011

Dynamic simulation of check valve using CFD and evaluation of check valve model in RELAP5

Master's Thesis

Martin Turesson

Department of Chemistry and Bioscience
Chalmers University of Technology
SE-412 96 Göteborg
Sweden
Telephone + 46 (0)31-772 1000

Göteborg, Sweden 2011

The picture on the front page describes the flow at a disc angle of 20° where the pathlines are colored by static pressure.

Summary

Check valves are widely used within the nuclear industry to prevent back flow and by doing so protect sensitive components such as pumps or prevent inadvertent draining of tanks. A check valve is a passive component that admits flow in one direction only. An ideal check valve will close exactly when the flow is reversed. However in reality some back flow often occurs and when the valve closes completely a pressure surge will result. This pressure surge will affect the piping system both through unbalanced forces and increased/decreased internal pressure. The size of pressure surge is largely dependent on the amount of back flow through the valve prior to closing. Hydraulic transients are often simulated using 1D code. The most widely used code in Sweden for hydraulic transients in nuclear power plants is the RELAP5 code. These codes are fast but the description of components such as a swing check valve is not complete which introduces inaccuracy in the simulated results. This inaccuracy has been known for many years and with the computer power that is today there is really no problem to simulate a real size swing check valve in all three dimensions, using appropriate CFD software.

Three different RELAP5 swing check valves models have been investigated and compared to the corresponding CFD simulations. The first model is the built-in description of a swing check valve in RELAP5, while the other two are models based on either another 1D code named DRAKO or on quasi-stationary CFD simulations. All three of these models are shown to under-predict the time for closure and thus also the maximum reverse velocity. Three different valve sizes have been simulated together with four different flow transients and they all show the same behavior. A more detailed study of the steady state behavior at a variety of disc angles also show that the forces and corresponding torques on the swing disc differs for forward and backward flows, where the forward flow gives the largest torque. This is found to be mainly due to different stagnation zones at the two sides of the disc.

The RELAP5 model based on stationary CFD simulation at different angles shows that the rotational movement is of great importance but modeled poorly. This is also the fact for the other two models where there is no specific term in the torque balance equations describing the rotation.

Keywords: Swing check valve, computational fluid dynamics, RELAP5, stationary, transient

Acknowledgement

I would like to express my thankfulness to my two supervisors Dr. Jonas Bredberg and Daniel Edebro at Epsilon UC Väst AB for their great support and patience during these months. A special thank also goes out to my dear friend and now co-worker Henrik Alfredsson for clearing the way and creating this opportunity.

I would also like to thank my examiner Prof. Bengt Andersson at Chalmers University of Technology for first of all introducing me to the world of CFD and secondly for the support I received during this Master's thesis.

Last but not least I would like to thank the love of my life for her outstanding support on the home front during especially all the Sundays that I spent with this thesis.

Nomenclature

Roman

A	Area
C	Virtual mass coefficient
C_p	Heat capacity
d	Perpendicular distance between two axes
D	Diffusion coefficient
E	Specific internal energy
g	Acceleration due to gravity
h	Enthalpy
I	Rotational inertia
k	Spring constant
k_{eff}	Heat coefficient
L	Characteristic length
m	Mass
m_n	Mass fraction
N	Magnitude of the normal force
P	Pressure
ΔP_{cr}	Cracking pressure
P_K, P_L	Pressure on either side of the valve
Q	Heat transfer rate per unit volume
r	Distance to the rotational axis
S	Source term
T	External torque
U	Velocity
V	Volume
Δx	Displacement from equilibrium
z	Height difference

Greek

α	Void fraction
ω	Rotational velocity
ρ	Density
θ	Angle
μ^{kin}	Coefficient of kinetic friction
σ_k	Model coefficient
ν_T	Turbulent viscosity
ν	Kinematic viscosity
μ	Dynamic viscosity
Γ	Vaporization/condensation rate
τ_{ij}	Viscous stress tensor
δ_{ij}	Kronecker's delta function

Abbreviations

$DISS$	Wall friction dissipations
FIG	Interface drag coefficient

General subscript

g	Gas
f	Fluid
w	Wall
i	Interface
cm	Center of mass
p	Projection

Contents

1 Introduction

1.1 Background

The nuclear industry is perhaps the most safety concern industry there is. Strict government regulations stipulate that each time a change is made to a system the consequences of this change must be evaluated and the structural integrity of the system must be checked. The pipes and other components need to be designed to withstand the normal operation loads during long time and extreme conditions due to unlikely flow transients.

Often calculations must be performed. These calculations are usually performed in two steps. First the hydraulic loads are calculated. This is usually done using a 1D computer code that determines the transient flow and thus the forces acting on the piping system. Pumps, valves etc is modelled in a simplistic way. The second step is to calculate the stresses caused by these loads. Depending on the likelihood of an event different margins are permitted. This thesis focuses on improving the quality of the first step – the hydraulic load calculations.

Check valves are often used in piping system to avoid the fluid to flow backwards. However they can also cause hydraulic loads when they close. An ideal check valve closes exactly when the flow is reversed. However in reality, this is not always the case. Due to non-ideal properties of the valve some back flow often occurs. When the valve slams shut a pressure surge occurs. The severity of this pressure surge is largely dependent on the back flow prior to the closing. For the hydraulic load calculations the modelling of the check valve closure is very important.

There exist several different codes for flow simulations that are common within the nuclear industry. The RELAP5 code is perhaps the most widely used but its focus is not on one specific component but rather system transients. The behavior of specific components such as a check valve may however be of importance and a detailed study of the flow causing the valve to close can be performed using computational fluid dynamic (CFD). From the knowledge obtained by a 3D CFD simulation the simpler RELAP5 model can be evaluated without the use of time-consuming and expensive experiments.

1.2 Objective and method

The main objective of this Master's thesis is to model a full scale swing check valve using both 1D and 3D computer codes. The 3D simulations are performed using the CFD software FLUENT v12.1 while the 1D calculations are performed by the RELAP5 code. With results from the 3D simulations in both steady state and transient flows the aim is to improve the behavior of the 1D model of a swing check valve. This problem involves some methodology development.

1.3 Thesis outline

In this report the reader is first introduced to what a check valve is, what problems that are associated with its operation and some commonly used check valve designs. The important physics and corresponding equations are then presented, followed by the different check valve models used in the 1D code RELAP5. A more in depth review regarding the CFD simulation and the equations solved is made along with some important flow and fluid characteristics. When the reader is well acquainted with the problem at hand and the methods used the report continues with presenting the results. These are mainly presented as plots of the angle of the swing disc as a function of time but also some colorful pictures are provided by the CFD run. The results are thereafter discussed and some final conclusions are made.

2 Swing check valve

2.1 Basics of check valves

Some characteristics of a check valve in general and swing check valve in specific are presented along with some different valve designs.

2.1.1 Property of check valves

Check valves are used to prevent reverse flow in piping systems. Reverse flow can typically occur after shutdown of a pump or closure of a control valve. The occurrence of reverse flow may cause damage to seals and to the brush gear of the pumps (Thorley, 1989) and inadvertently drain tanks and reservoirs. Due to the physical properties of a check valve such as friction and inertia the valve will not close immediately and some reverse flow will still occur (Rahmeyer, 1996).

There are some problems related to the closing of check valves since a sudden closure may lead to large pressure surges downstream of the check valve and negative pressures upstream (Rahmeyer, 1996). The pressure upstream may drop to the vapor pressure of the liquid causing vapor production. Normally these gas bubbles will collapse rapidly and by doing so creating large pressure pulses in the system which in turn may cause the valve to momentarily reopen (Thorley, 1989). Large pressure transients may also cause pipe to break.

Check valve slam is a phenomenon caused by the reverse flow. As the valve nears its seat, a pressure rise builds up and further accelerates the closure. This acceleration causes the valve to "slam" onto its seat causing a water hammer in the system. To prevent this slam from happen the check valve should close either very rapidly or very slowly. The closure of a check valve is strongly dependent on the valve design. A larger mass of the valve components lead to greater reverse velocities as well as pressure surges. Reverse velocities are less for those check valves which are spring assisted. This is also true for those valves where the closing component have a smaller distance to move (Rahmeyer, 1996) , (Thorley, 1989).

The magnitude of the pressure surge caused by the check valve slam can be calculated using the Joukowsky equation given in equation 2.1 (Thorley, 2004).

$$\Delta P = \rho a U_{reverse} \qquad (2.1)$$

The pressure will thus depend on the density, speed of sound, a, in the fluid and the reverse velocity prior to the valve closure. The normal speed of sound for cold water in completely rigid pipes is approximately 1500 m/s. With a reverse velocity of 1 m/s this will cause a pressure surge of about 15 bar in addition to the normal system pressure. To avoid large check valve slams, the reverse velocity should be minimized. The reverse velocity is affected by the flow transient in the piping system as well as the time it take for the valve to close.

Usually the flow transient in the piping system is not affected by the check valve until the valve is almost completely closed. This feature makes it possible to study the closing behaviour of the check valve independently of the piping system. In other words, the flow transient affects the valve but the valve does not affect the system flow until it is almost completely closed. This is however not true for damped check valves.

2.1.2 Check valve design

Categorizing check valves is not easy since different manufacturers have different specifications. However the most common types can be divided into: swing, lift, tilting disc, duo/double disc, stop and nozzle. The distribution of these can be seen in figure 2.1 where the data is taken from (McElhaney, 2000).

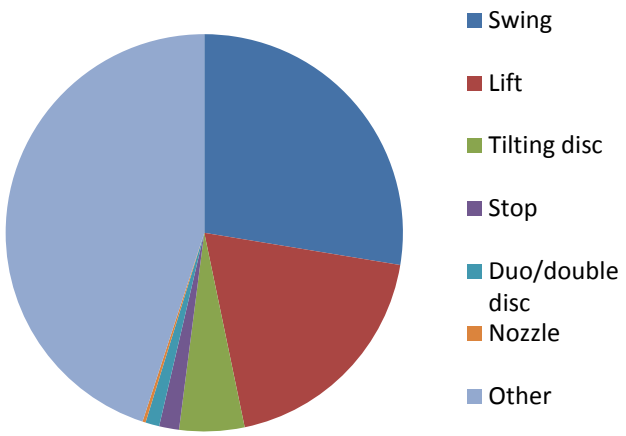

Figure 2.1. Population distribution of check valve in the nuclear industry in 1991 .

Swing check valves

There are a couple of different reasons why the swing check valve is such a common component in the nuclear industry. Primarily it is because of a simple design, low pressure drop, economy, reliable sealing and available in a wide range of sizes. The basic design is a disc suspended from a hinge pin located above the flow stream, see figure 2.2. The closure of these types of valves is dependent on the gravity force. The main disadvantage of the swing check valve is that the closing is the slowest of all check valves. This is due to the relative large mass of the disc and the long distance to travel from fully open to fully closed (McElhaney, 2000).

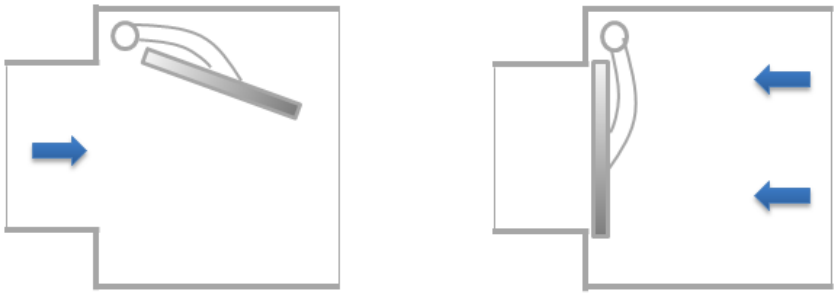

Figure 2.2. Swing check valve.

Tilted disc check valve

The tilting disc check valve differs from the swing check valve in that the hinge pin is located in the flow stream, see figure 2.3. This gives a much quicker closing since the distance to travel is smaller. However there might be some sealing problems with this design. Another disadvantage compared to the swing check valve is that it is more expensive and more difficult to repair. Due to these disadvantages this type of valve is normally limited to applications that the swing check valves cannot handle. (Zappe, et al., 2004)

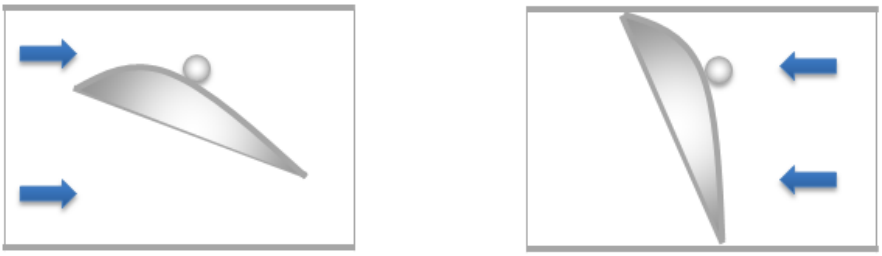

Figure 2.3. Tilted disc check valve.

Duo/double disc check valve

The duo/double disc check valve, seen in figure 2.4 relies on spring-loaded doors for closure even though it is possible to close due to back flow. This design has a larger pressure drop and also leak tight sealing is difficult. These types of valves will close more quickly than both the swing and tilted disc check valves due to the lower inertia and smaller distance. Since the closure normally relies on the aid of a spring, failure of this spring may cause severe operational problems. The spring also provides a constraining force that decreases disc quiver (McElhaney, 2000).

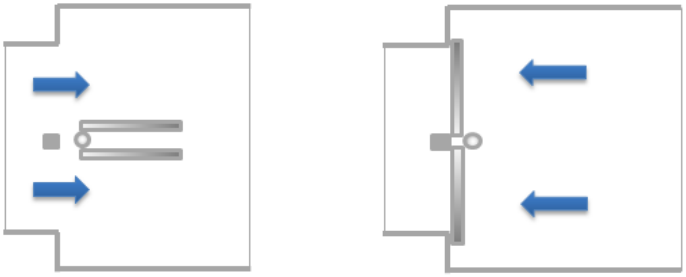

Figure 2.4. Duo/double disc check valve.

Lift check valve

The disc in a lift check valve is normally piston shaped and moves within a guided surface. This guide mechanism can get hindered by dirt entering the valve or slowed down by viscous fluids. One large advantage compared to many other check valves is that the distance to travel between fully open and fully closed is small and is therefore potentially fast closing. Considering the disadvantages of the lift check valves they are most suitable for low viscosity fluids which are solid free (Zappe, et al., 2004).

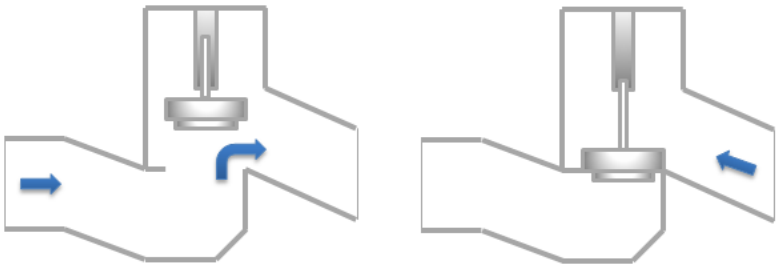

Figure 2.5. Lift check valve

2.1.3 Dynamic characteristic of check valve

The most popular and frequently used method to study the transient behavior of check valves and to categorize them is to apply different flow decelerations and measure the maximum reverse velocity. An experimental study is typically performed by closing a main valve and having a pump in a secondary pipeline create the reverse flow according to figure 2.6. From the start the main valve is opened and the pump is running. The water runs from the upper reservoir to the lower reservoir and through the pump to the lower reservoir. When the main valve is closed the pump forces the fluid to reverse in the direction towards the upper reservoir. This causes the check valve to close. By closing the main valve at different rates different flow decelerations can be produced. The reverse flow is either measured directly with a flow meter or deduced using the Joukowsky equation described in section 2.1.1. The reverse velocity is plotted against the flow acceleration producing a dynamic characteristic curve as displayed in figure 2.7

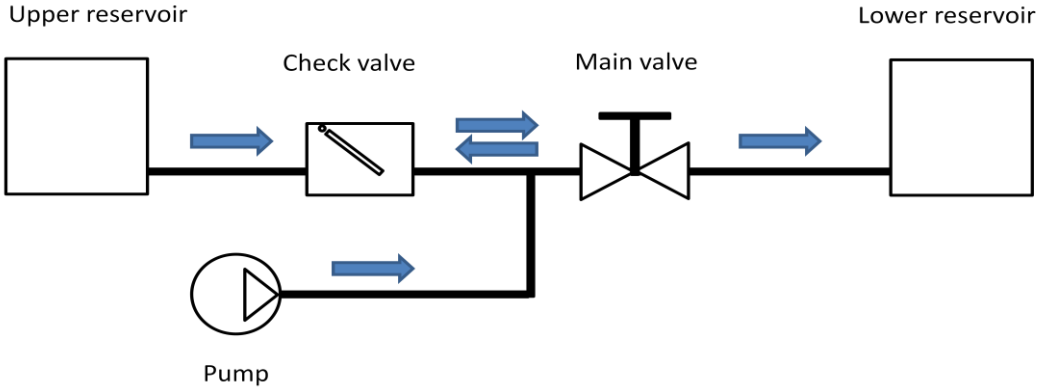

Figure 2.6. Schematics of an experimental setup to study transient behavior of check valves.

There are many aspects affecting the flow deceleration in a piping system. Typically a flow deceleration occurs when a pump is stopped. For instance, if two pumps are working in parallel and one of the pumps stops this will cause the flow to reverse through the pump that is stopped. The deceleration of that flow will then depend on the rotational inertia of the pump rotors, magnitude of driving pressure and the total mass of water that is reversed. According to (Val-Matic Valve and Manufacturing Corp, 2003) the flow deceleration in case of a single-pump, low-head system is less than 6 m/s^2 but for a multiple-pump, high-head system the deceleration may go up to as high as 12 m/s^2.

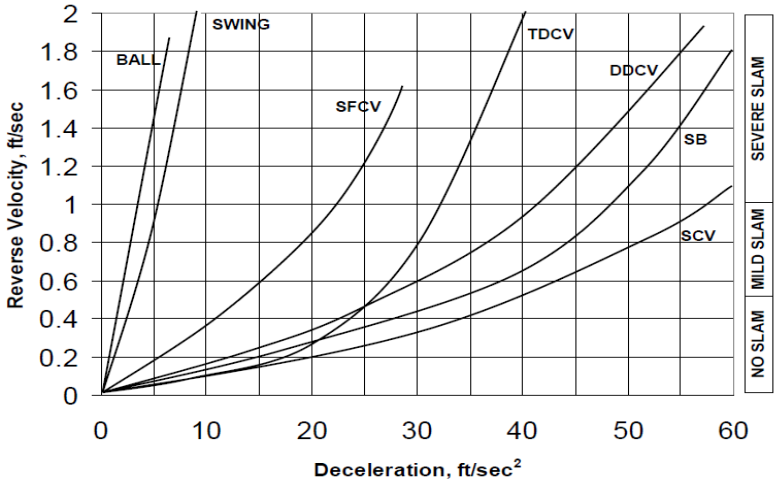

Figure 2.7. Maximum reverse velocity as a function of deceleration for different check valves used in the industry. The abbreviations are as follows; SFCV= swing flex check valve, TDCV= tilted disc check valve, DDCV= dual disc check valve, SB= surge buster check valve and SCV= silent check valve. (Val-Matic Valve and Manufacturing Corp, 2003)

3 Check valve modeling

3.1 Equation of motion

Newton's second law of motion states that a body of mass m that is affected by an external force, F, will undergo acceleration in the same direction as that force. The magnitude is proportional to the force and inversely proportional to the mass. This law is written as:

$$F = ma = m\frac{dU}{dt} \tag{3.1}$$

In order to put up a theoretical model for the closure of a swing check valve first the physics must be evaluated. There are a number of different forces and corresponding torques related to the behavior of the moving disc. By applying Newton's second law to a rotational motion the equation becomes (Cummings, et al., 2004):

$$T = I\frac{d\omega}{dt} \tag{3.2}$$

Where T is the torque, I the rotational inertia and ω the angular velocity.

3.2 Inertia

The concept of rotational inertia is introduced together with added mass, also known as virtual mass or apparent mass.

3.2.1 Rotational inertia

When an object is rotating there is a resistance within the system to change that rotation, this resistance is referred to as the rotational inertia. The concept of rotational inertia is closely related to that of the inertia which is the resistance to change in velocity. The inertia of an object is quantified by its mass. The general expression for the rotational inertia is written as:

$$I = \sum_i m_i r_i^2 = \int_M r^2 dm = \int_V \rho r^2 dV \tag{3.3}$$

Thus the expression of the rotational inertia depends on the mass, shape and distance to the rotational axis. Also due to the summation in the formula, the rotational inertia is an additive property. Since the rotation will not be about the center of any of the bodies, the parallel axis theorem can be applied. This theorem states that the rotational inertia can be determined about any axis according to (Boyd, et al., 1985):

$$I = I_{cm} + md^2 \tag{3.4}$$

Further three shapes are of special interest; disc, rod and sphere. The closing equipment of the swing check valve is shaped as a disc, the arm connecting the disc to the hinge has roughly the shape of a rod and the adjacent fluid of the disc is approximated with a sphere. The fact that the adjacent fluid must be taken into the consideration is explained more in section 3.2.2. How these three geometries are rotating is displayed in Figure 3. 1 below.

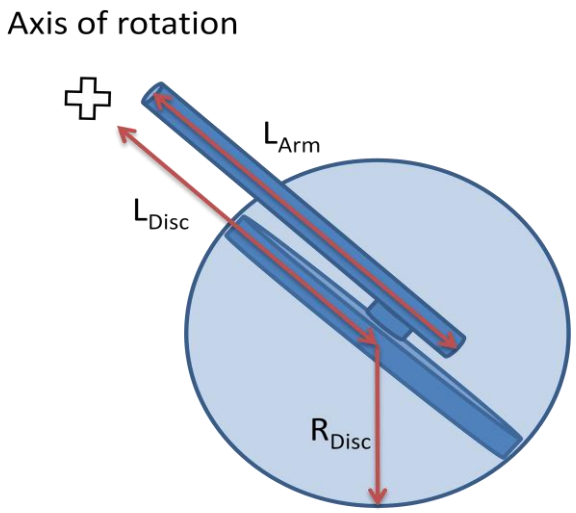

Figure 3. 1. Schematics of the different rotational inertias.

The rotational inertias about the axis of rotation are then written as equation 3.5 through 3.9.

$$I_{flapper} = I_{disc} + I_{rod} \tag{3.5}$$

$$I_{added\ mass} = I_{fluid,sphere} \tag{3.6}$$

$$I_{disc} = \frac{1}{4} m_{disc} R_{Disc}^2 + m_{disc} L_{Disc}^2 \tag{3.7}$$

$$I_{rod} = \frac{1}{12} m_{arm} L_{Arm}^2 + m_{arm} \left(\frac{L_{Arm}}{2}\right)^2 \tag{3.8}$$

$$I_{fluid,sphere} = \frac{2}{5} m_{fluid,sphere} R_{Disc}^2 + m_{fluid,sphere} L_{Disc}^2 \tag{3.9}$$

3.2.2 Added mass

As a solid body is accelerating or decelerating in a fluid, a force will arise due to the acceleration or deceleration of the surrounding fluid. This extra force can be seen as an extra mass to the system (Andersson, et al., 2010). The magnitude of this added mass depends mainly on the geometry of the moving body, the density of the fluid and the type of motion (translational or rotational). Thus in a solid-gas system this component can be neglected due to the large density difference whereas this may not be the case in a solid-liquid system (Panton, 2003), (Brennen, 1982).

The added mass of a swing check valve is not straight forward due to the complexity of the rotating disc and behavior of the flow. However the effect of the added mass on the system is proposed by (Thorley, 1989) to be approximated with a sphere of fluid having the same diameter as the valve door and with identical geometric centers.

The general form of the expression giving the added mass is shown in equation 3.10.

$$T_{added\ mass} = -C_{added\ mass} \rho V L \frac{D}{Dt} \left(U_{flapper} - U_{fluid}\right) \tag{3.10}$$

Where V is the volume of the flapper and C is the added mass force coefficient. The last term correspond to the relative acceleration between the fluid and the swing disc. By assuming that only the acceleration of the disc is of importance the expression can be rewritten into equation 3.11.

$$T_{added\ mass} = -C_{added\ mass}\rho VL\frac{dU_{flapper}}{dt} = -I_{added\ mass}\frac{d\omega}{dt} \quad (3.11)$$

Equation 3.11 is the same as the approximation described by (Thorley, 1989) however the problem is to model the rotational inertia of the added mass correctly.

Test case for added mass

A test case has been performed in order to really understand the importance of the added mass. This case is composed of a cylinder that is rotating about its center at different angular velocities in stagnant water. The magnitude of the added mass is investigated by considering a power balance equation. Note here that for simplicity the torque of the added mass is the total torque of both the cylinder and the adjacent fluid.

$$P = T_{added\ mass}d\omega = \frac{dW}{dt} \quad (3.12)$$

Where *P* is the power, *T* the torque, ω the angular velocity and *W* the energy in the water. By using the results from equation 3.11 this expression can be rewritten resulting in equation 3.13. Notice also here that the differential is replaced by a difference but the expressions are equal at limes.

$$I_{added\ mass}\frac{d\omega}{dt}d\omega = I_{added\ mass}\frac{\omega_2+\omega_1}{2\Delta t}\omega_2 - \omega_1 = \frac{W_2+W_1}{\Delta t} \quad (3.13)$$

And finally the expression for the added mass can be calculated according to equation 3.14.

$$I_{added\ mass} = 2\frac{W_2+W_1}{\omega_2^2-\omega_1^2} \quad (3.14)$$

Observe that the energy in the water is calculated based on the dynamic pressure according to equation 3.15.

$$W = mU^2 \quad (3.15)$$

The result of this test case is summarized in Table 3. 1 and shows that the rotational inertia of the added mass is larger than the rotational inertia of only the cylinder. If the effect of accelerating the adjacent fluid is not taken into consideration the calculations will be misguiding.

Table 3. 1. The results of a test case with the intention to investigate the effect of added mass.

Angular velocity (rad/s)	***Energy in the water (kJ)***	***Rotational inertia of cylinder (kgm^2)***	***Rotational inertia of added mass (kgm^2)***	***Ratio of rotational inertias (-)***
0.5	220	0.19 E6	1.6 E6	8.4
1	821			

3.3 Forces of important

A torque is initialized when a force, *F*, is acting on an object at a distance, *r*, from the rotational axis, defined as:

$$T = r \times F \quad (3.16)$$

The forces of interest are those due to gravity, fluid pressure, friction, buoyancy and an attached spring. The inertias that need to be taken into the calculations are the inertia of the disc and the adjacent fluid (Thorley, 1989). The direction of the acting forces can be seen in Figure 3. 2.

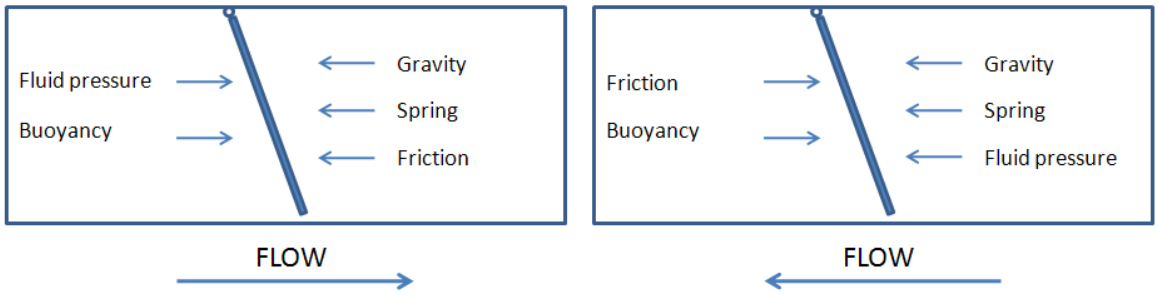

Figure 3. 2. Simplified swing check valve showing the directions of the important forces for different flow directions.

3.3.1 Hydrodynamic force

As the moving fluid strikes the check valve disc it will exert a force on the disc. This force is due to the change in linear momentum of the system according to Newton's second law of motion. In the CFD software that is used it is however more convenient to calculate the force of the fluid in terms of pressure and area. The magnitude of the force due to pressure of a fluid is written as:

$$|F| = P \cdot A \tag{3.17}$$

Note that for the expression to hold the force must be uniform over the area and perpendicular to it. For non-uniform forces and surfaces the same equation can be applied, given that the area segment is small (lim A→0). The corresponding torque then depends on where on the disc this area segment is situated and the total torque is the sum over the disc area (Cummings, et al., 2004).

Drag force

Another way of describing a flow striking a solid object is to relate the force to a drag coefficient, C_d, which depends on the shape of the object. This drag coefficient is assumed to be constant at high Reynolds number (Re>1000). The drag force can then be written as equation 3.18.

$$F_{drag} = \frac{1}{2} C_d \rho A_p |U| U \tag{3.18}$$

Where C_d is the drag coefficient (1.1 for circular disc), A_p is the projected area in the flow direction, ρ the density and U the bulk velocity (Welty, et al., 2001). The concept of drag force and drag coefficient will be adopted in the attempt to develop a new 1D check valve model. In this model the drag coefficient will be replaced with a stationary torque coefficient (which will depend on the angle of the disc) and will be used to instead help describe the torque on the disc. This new model is further described in section 3.4.3.

Impinging flow and stagnation point

As the water travels through the piping system and enters the valve housing, it will strike the valve disc causing the flow to separate. This flow impingement on a solid body will cause a stagnation point to form. A stagnation point is a point at the surface of the disc where the local velocity of the fluid is zero and thus is brought to rest. By applying Bernoulli's equation for incompressible flow given by equation 3.19 it can be shown that the static pressure has its highest value at the point where the velocity is zero (Janna, 2010). Flow impingement on a vertical disc that causes the flow to separate can be seen in Figure 3. 3.

$$\frac{v^2}{2} + gz + \frac{p}{\rho} = constant \tag{3.19}$$

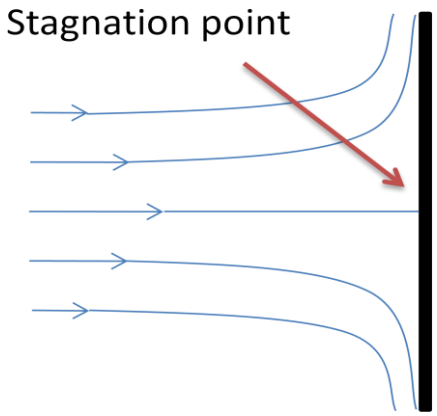

Figure 3. 3. Flow striking a vertical surface and by doing so creating a stagnation point.

3.3.2 Weight force

The weight force consists of two contributions; the gravitational force and the buoyant force. The swing check valve is oriented so that the gravitational force will tend to close it since this will cause the distance from the mass center of the disc to the mass center of the earth to be minimized. The force due to gravity is expressed as:

$$F_{grav} = m_{flapper} g \tag{3.20}$$

Buoyancy is the concept of a submerged body in a fluid. A submerged body with a certain volume will experience a force that acts in the opposite direction of the gravity. This is the buoyant force, a concept also referred to as Archimedes' principle. The magnitude of the buoyant force depends on the mass of the displaced fluid and can be expressed as (Cummings, et al., 2004):

$$F_{buoy} = m_{fluid} g \tag{3.21}$$

The weight force can then be written as equation 3.22.

$$F_{weight} = \left(m_{flapper} - m_{fluid}\right) g \tag{3.22}$$

When considering the implementation of the weight force into a computer code it might be important to know the location of the mass centre since this will probably not be the same as the center of the disc.

3.3.3 Friction force

There are two types of friction, static and kinetic. Static corresponds to a stationary body and kinetic to a moving one. The kinetic friction force acts on bodies that are in motion and the direction is opposite of that of the motion. The magnitude of this force depends on the roughness of the surfaces that are in contact with each other. In general the friction force is expressed as (Cummings, et al., 2004):

$$F_{fric} = \mu^{kin} N \tag{3.23}$$

Another approach to the friction force in a swing check valve is to relate it to the minimum pressure difference that is required in order for the disc to start moving. This pressure difference is called the cracking pressure. The frictional force can then be written as (Information Systems Laboratories, Inc, 2003):

$$F_{fric} = \Delta P_{cr} A_{disc} \tag{3.24}$$

The frictional force is located to the part of the check valve where the valve door is suspended. The impact of the frictional force on the motion of the valve door is however not modeled since no experimental data was available and this term was thereby neglected.

3.3.4 Spring force

In some swing check valve there is a spring attached to the disc, making it close faster and smoother. The force that the spring exerts on the disc depends on two things; the stiffness of the spring and the displacement. The spring equation is also referred to as Hooke's law for an ideal spring (Cummings, et al., 2004):

$$F_{spring} = -k\Delta x \tag{3.25}$$

The corresponding torque then depends on where the spring is attached to the disc.

3.4 1D check valve models

When modeling using a 1D code the system properties are most commonly evaluated at the center of each volume cell where the number of such cells are counted in tens. Thus there is no possibility of evaluating the pressure and corresponding force directly on the flapper surface. This includes also other types of forces and these quantities therefore must be modeled accordingly. Force modeling in RELAP5 is performed using control variables, where in fact these control variables can be any quantity that is needed to control the simulation or of interest later in post-processing. The control variables can call upon quantities provided by the solver such as mass flow and time step and use these to calculate the average force of the flow acting within the system. The control variables are only the top of the procedure of calculating specific quantities in RELAP5. A control variable need input of what kind of mathematical operation that is performed and one control variable can only handle one operator. This tends to make even the simplest calculation require a bit of code writing.

3.4.1 Inertial swing check valve (inrvlv)

The normal way of modeling a non-ideal swing check valve in RELAP5 is to use the built-in hydrodynamic component *inertial swing check valve* (inrvlv). This component uses the angular version of Newton´s second law of motion to calculate the position of the disc according to equation 3.26 below.

$$T_{Hydro} + T_F + T_W = I\frac{d\omega}{dt} \tag{3.26}$$

The torque due to friction is calculated according to:

$$T_F = \Delta P_{cr} A_{disc} L \tag{3.27}$$

Instead of giving a value of the friction directly the *cracking pressure* is used as input. For the sake of the analysis the cracking pressure is neglected in this thesis.

Torque due to weight:

$$T_W = -\left(m_d - m_f\right) gLsin(\theta) \tag{3.28}$$

The weight is considered to be the submerged weight of all of the moving parts. The actual mass is only used for the calculation of the moment of inertia, *I*. Finally, the torque due to the hydrodynamic force/drag is given by:

$$T_{Hydro} = (P_1 - P_2) A_p L \tag{3.29}$$

where $(P_1\text{-}P_2)$ is the pressure difference across the valve, *Ap* is the projected area of a disk hinged at the top end and *L* is the length to the centre of mass. The pressure difference $(P_1\text{-}P_2)$ the valve is controlled by the pressure loss in the valve and will affect the torque on the valve. A 1D code usually calculates the pressure loss in valves based on the opening area of the valve according to some idealised case. RELAP5 assumes an orifice like geometry as shown in Figure 3. 4.

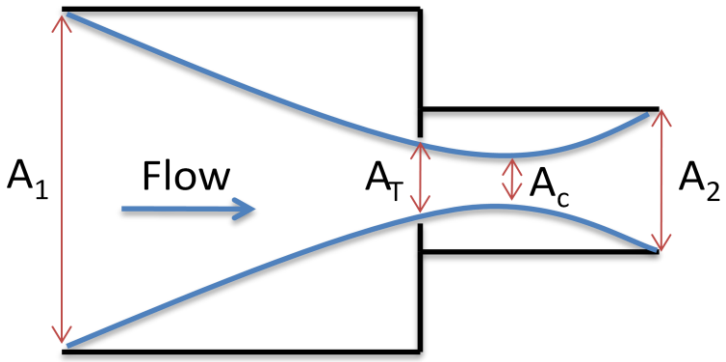

Figure 3. 4. Abrupt area change at an orifice.

The areas A_1 and A_2 are given to the code as input but A_T and A_C are calculated, and thus depend on the position of the valve door. By using these different areas, three area ratios can be formed:

$$\varepsilon_c = \frac{A_c}{A_T}, \qquad \varepsilon_T = \frac{A_T}{A_1}, \qquad \varepsilon = \frac{A_2}{A_1}$$

The pressure loss can be calculated according to:

$$\Delta P_f = \frac{1}{2}\rho\left(1 - \frac{\varepsilon}{\varepsilon_c \varepsilon_T}\right)^2 v_2^2 \tag{3.30}$$

RELAP5 then uses a relation between ε_c and ε_T given by the empirical expression below to calculate the pressure loss due to an abrupt area change:

$$\varepsilon_c = 0.62 + 0.38(\varepsilon_T)^3 \tag{3.31}$$

For the inertial swing check valve the throat area is assumed calculated according to:

$$A(\theta) = \frac{min(A_1|A_2)}{A_{junction}}\big(1 - cos(\theta)\big)C_c\big(1 - cos(\theta)\big) \tag{3.32}$$

where C_c is interpolated from the following table (area fraction open = 1 – cos(θ)).

Table 3. 2. The contraction coefficient for different area fraction openings.

Area fraction open	0.0	0.1	0.2	0.3	0.4	0.5	0.6	0.7	0.8	0.9	1.0
C_C	0.617	0.624	0.632	0.643	0.659	0.681	0.712	0.755	0.813	0.892	1.0

Input requirements

Input data to the model is cracking pressure, leakage fraction, minimum and maximum angles, rotational inertia of the flapper, moment length of flapper, radius of the disc and mass of the disc. These quantities are summarized in Table 3. 1 where also the actual inputs for the simulation are presented. It should be noted that there is no way of controlling the pressure loss and thus the hydrodynamic torque on the disc.

Table 3. 3. Input data to the RELAP5 simulations

Input variable	***Data***
Cracking pressure	0 Pa
Leackage fraction	0
Minumum angle	5 °
Maximum opening angle[1]	57 °
Rotational inertia	0.1875 kgm^2
Moment length	0.155 m
Radius of the flapper	0.112 m
Submerged weight of the flapper	6.15 kg

Inaccuracies in the RELAP5 inertial check valve model

The pressure on both sides of the valve used to determine the hydrodynamic torque is calculated at the center of the computational cell. This procedure leads to a false pressure difference that is related to the flow acceleration and results in an earlier closure of the valve. This leads to a volume length dependancy that makes the valve close faster for longer adjacent volume lengths. To correct these pressures equations 3.33 and 3.34 can be implemented. The mass flow change is taken in the valve junction.

$$P_{1,adjusted} = P_1 - 0.5\frac{dm}{dt}\frac{dx_1}{A_1} \quad (3.33)$$

$$P_{2,adjusted} = P_2 + 0.5\frac{dm}{dt}\frac{dx_2}{A_2} \quad (3.34)$$

The node length dependence for a typcical valve closure can be seen in Figure 3. 5 where a smaller distance between the computing nodes gives a later closure.

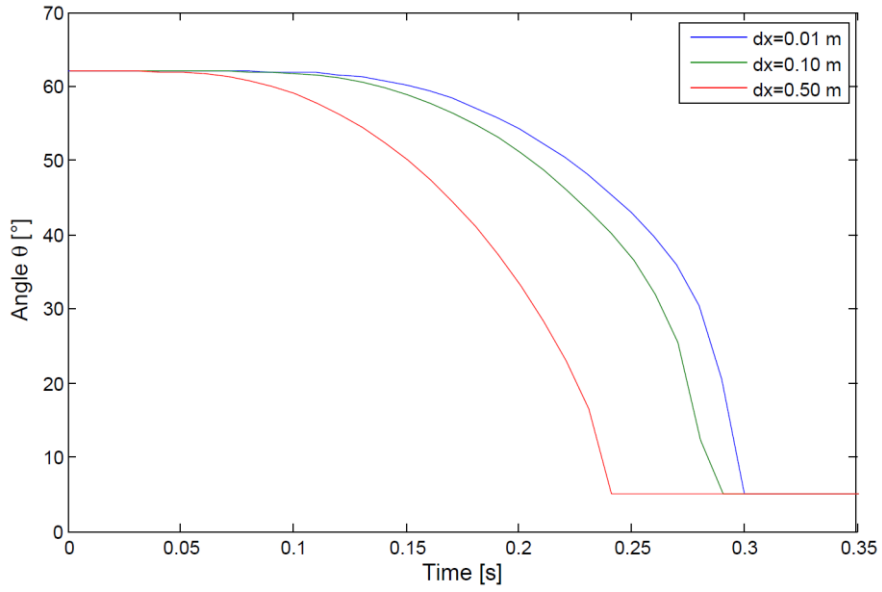

Figure 3. 5. The RELAP5: inrvlv model is dependent upon the node length.

The evaluation at the volume centre will also give a false value if the valve is mounted in a vertical line because of the hydrostatic pressure difference. Also, the weight term should contain a cosine for vertically mounted check valves. This is not accounted for in the inertial swing check valve.

[1] Maximum opening angle refers to the angle between fully closed and fully open. Since the angle for closed valve is 5˚ the maximum angle will be 62˚.

RELAP5 implementation

A model using control variables has previously been developed at Ringhals and is used to reproduces the behaviour of the built-in model. This procedure is required in order to be able to monitor certain quantities such as the opening angle and closing torque. The input-file can be found in Appendix C.

3.4.2 DRAKO swing check valve model

The water hammer software DRAKO also has a swing check valve component. The main difference between it and the RELAP5 inertial swing check valve model is the term for the hydrodynamic torque. In addition to a pressure difference term it also includes a term corresponding to the diversion of the flow according equation 3.35 below (KAE, 2005). The importance of the two phenomena is displayed in Figure 3. 6 at different angles.

$$T_{Hydro} = (P_K - P_L)A_{disc}L + |U_{rel}|U_{rel}\rho A_{seat}cos^2(\theta)L \quad (3.35)$$

Where

$$U_{rel} = \frac{U_K A_K}{A_{seat}} - L\omega cos(\theta) \quad (3.37)$$

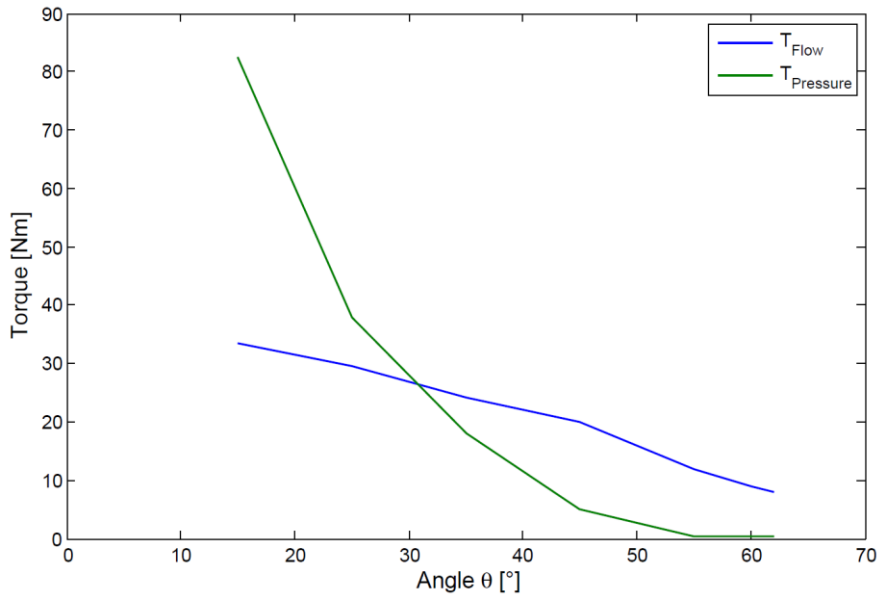

Figure 3. 6. Torque due to pressure and flow diversion for the DRAKO model.

The area function used to calculate the flow resistance is not the same as the one used in RELAP5. The RELAP5 area function is solely based on an empirical relation using the abrupt area change model. The DRAKO model required more input data and a complete review of the procedure is given in equations 3.38 to 3.40. The input requirements are the diameter of the disc (D_{disc}), valve seat diameter (D_{seat}) and valve house diameter (D_{vh}) along with the distance from the axis of rotation to the center of the disc (L_{cod}) and the maximum opening angle (θ_{max}).

First of all the different areas are defined:

$$A_{seat} = \frac{\pi}{4}D_{seat}^2 \quad A_{disc} = \frac{\pi}{4}D_{disc}^2 \quad A_{vh} = \frac{\pi}{4}D_{vh}^2$$

For smaller openings:

$$Ak(\theta) = \pi^2 D_{seat} L_{cod} \frac{\theta}{180} \quad (3.38)$$

For larger openings:

$$Ag(\theta) = \frac{\pi}{4} D_{vh}^2 - \frac{\pi}{4} D_{disc}^2 cos\left(\theta \frac{\pi}{180}\right) \quad (3.39)$$

The intersection between Ak and Ag is calculated and denoted θ_l which marks the lower limit later in the area function. The upper limit is marked by the intersection between Ag and A_{seat}. The area function F(θ) is obtained using the relation in equation 3.40.

$$\begin{aligned} &if\ \theta \leq \theta_l \\ &\quad F(\theta) = Ak(\theta) \\ &elseif\ \theta_l < \theta \leq \theta_u \\ &\quad F(\theta) = Ag(\theta) \\ &else \\ &\quad F(\theta) = A_{seat} \end{aligned} \quad (3.40)$$

This area function, F(θ) is the same representation as the area at the vena contracta, A_C in the RELAP5 model. Since the DRAKO model is implemented into the RELAP5 code the area function must be transformed to a suitable form by using the empirical formula connecting the vena contracta area to the normalized area function, $A_{KAE}(\theta)$. This is achieved by saying that the head loss, K is the same for the two methods according to equations 3.41 and 3.42.

$$K_{KAE} = A_2^2 \left(\frac{1}{F(\theta)^2} - \frac{1}{A_1^2}\right) \quad (3.41)$$

$$K_{RELAP5} = \left(1 - \frac{\varepsilon}{\varepsilon_c \varepsilon_T}\right)^2 \quad (3.42)$$

From these expressions the throat area, A_T can be solved and the normalized area function corresponding to the DRAKO code is written as equation 3.43.

$$A_{KAE}(\theta) = \frac{A_T}{A_{junction}} \quad (3.43)$$

Area functions used in the 1D code

In Figure 3. 7 below there are three area functions displayed; the function used by RELAP5 with default settings, the function recommended by the developer KAE according to equation 3.40 and an additional function using both the empirical relation given in equation 3.31 and stationary CFD simulations to calculate the head loss. This last method is thus more complicated since it requires CFD calculations but has the possibility to better describe the area function. The procedure of obtaining this area function is reviewed in equation 4.56 through 4.57.

Start by assuming that the torque can be described by a pressure difference and the diversion of the flow according to equation 3.55 above. The diversion of the flow is written as:

$$T_{flow} = |U_{rel}| U_{rel} \rho A_{seat} cos^2(\theta) L \quad (3.56)$$

Leading to a pressure force according to:

$$F_{pressure} = \frac{T_{CFD} - T_{flow}}{L} \quad (3.57)$$

The pressure force can also be described using the head loss, K according to:

$$F_{pressure} = \frac{1}{2} K \rho A U^2 \quad (3.58)$$

By putting these last to equations equal, a valve of K can be obtained. This K values is then used to calculate the corresponding normalized area function, $A_{CFD}(\theta)$ by using equation 3.42.

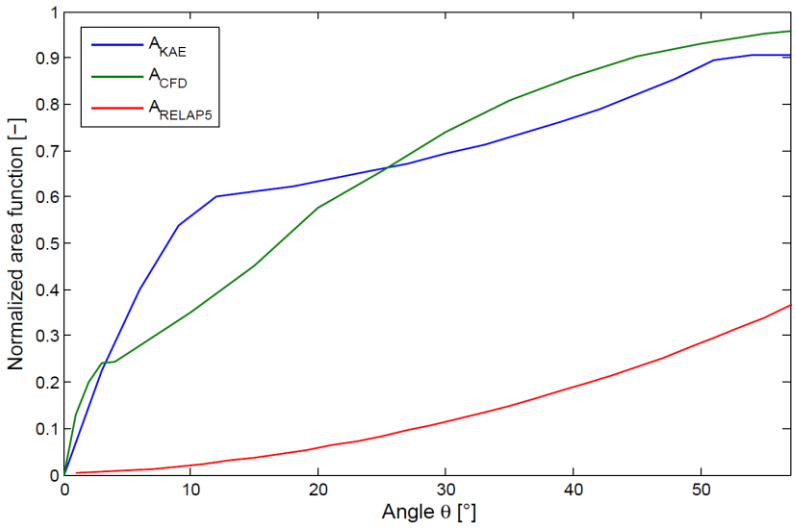

Figure 3. 7. The normalized area functions as a function of angle.

Input requirements

The input requirements for the DRAKO model are summarized in Table 3. 4 below where also the values are displayed. It is noteworthy that the number of inputs for the DRAKO model exceeds those for the RELAP5 model.

Table 3. 4. Input data to the DRAKO simulations.

Input variable	***Data***
Area of the disc	0.0394 m
Area of the valve seat	0.0324 m
Area of the valve housing	0.0568 m
Moment length to center of disc	0.155 m
Moment length to center of gravity	0.152 m
Angle for closed valve	5 °
Maximum opening angle	57 °
Submerged weight of the flapper	6.15 kg
Moment of inertia	0.1875 kgm^2
Bearing friction torque	0
Friction coefficient for plate overflow	0
Accereration of gracity	9.81 m/s^2

3.4.3 Quasi-stationary model

The torque balance and the included terms are presented and explained for a third RELAP5 swing check valve model.

Quasi-stationary

After going through the work of (Liou, et al., 2003) and (Lim, et al., 2006) the transient behavior of a swing check valve is proposed to be divided into separate parts, where each part describe a physical property. The torque is separated into parts corresponding to a steady state pressure force and weight. The new equation of motion thus becomes:

$$I_{flapper}\frac{d\omega}{dt} = T_{flow} + T_W \qquad (3.44)$$

The torque corresponding to the flow striking the tilted disc will be described with an equation similar to the drag force according to equation 3.45.

$$T_{flow} = T_{drag} = \frac{1}{2} C_d \rho A_p L |U| U \quad (3.45)$$

The drag coefficient C_d will however change with the angle of the disc and thus a new coefficient is introduced called the stationary torque coefficient C(θ). This coefficient is assumed to completely handle the angle dependence of the drag and thus the projected area is replaced with the disc area.

$$T_{flow} = \underbrace{\frac{1}{2} C_d A_p}_{C(\theta)A} L\rho|U|U = C(\theta) A L \rho |U| U \quad (3.46)$$

The torque due to the weight force is written as:

$$T_W = -V_{flapper}\left(\rho_{flapper} - \rho_{fluid}\right) g L sin(\theta) \quad (3.47)$$

The only unknown variable that needs to be modeled is the coefficient C and only depends on the angle of the disc. This variable is acquired through steady state CFD simulations at different angles resulting in the following relation:

$$T_{CFD}(\theta) = C(\theta) A L \rho |U| U \quad (3.48)$$

From the work of (Rahmeyer, 1993) based on experiments it has been proposed that the coefficient C(θ) should have the form of:

$$C(\theta) = (K\theta)^{-3} \quad (3.49)$$

In the proposed model this form has been loosely adopted resulting in a new relation given by:

$$C(\theta) = X\theta^{-Y} \quad (3.50)$$

Where the variables *X* and *Y* are found by fitting the equation to the data obtained by the CFD simulation and can be found in the result chapter in section 6.1.2.

Input requirements

The quasi-stationary model requires less input data than the other two models and the exact variables and their values is presented in Table 3. 5.

Table 3. 5. Input data to the quasi-stationary simulations.

Input variable	***Data***
Diameter of the disc	0.224 m
Moment length	0.155 m
Moment length to center of gravity	0.152 m
Angle for closed valve	5 °
Maximum opening angle	57 °
Submerged weight of the flapper	6.15 kg

Expanding the quasi-stationary model

Further to investigate also the transient behavior of a moving swing disc the rotation and acceleration of surrounding fluid should be described. The effect of these two phenomena is described by adding an added mass term as described in section 3.2.2 and instead of using the flow velocity in equation 3.48 use the relative velocity given by equation 3.50.

$$U_{rel} = U - \omega L cos(\theta) \quad (3.51)$$

In order to fully investigate the effect of these new terms, three new balances are formed in equation 3.52 through 3.55.

Using added mass:

$$\left(I_{flapper} + I_{added\ mass}\right)\frac{d\omega}{dt} = T_{flow} + T_{weight} \tag{3.52}$$

Using relative velocity:

$$I_{flapper}\frac{d\omega}{dt} = T^{*}_{flow} + T_{weight} \tag{3.53}$$

Using both added mass and relative velocity

$$\left(I_{flapper} + I_{added\ mass}\right)\frac{d\omega}{dt} = T^{*}_{flow} + T_{weight} \tag{3.54}$$

Where

$$T^{*}_{flow} = C(\theta)AL\rho|U_{rel}|U_{rel} \tag{3.55}$$

3.5 3D check valve models

Modeling using a 3D code solves for a numerous number of variables in the domain including millions computational cells. Two of these variables are the area and pressure of the surface cells located on the flapper. Thus the solver directly provides the force acting on the flapper and no additional calculations have to be performed. The correct forces can be sorted out by an appropriate function (UDF) and used for its purpose. The usage of these UDF's are explained more in section 5.5. The general torque formula is written in the same way as the 1D code but is repeated for clarity in equation 3.59.

$$I_{flapper}\frac{d\omega}{dt} = T_{Hydro} + T_{W} \tag{3.59}$$

The flow field in the check valve is solved completely by the code and thus there is no need to model the rotation in any way. The torque balance equation will thus be written in the most simple way according, where only the fluid pressure and the flapper weight are considered. The rest is handled by the CFD solver. The hydrodynamic component of the torque equation is described by equation 3.60.

$$T_{Hydro} = PAr = \sum_i P_i\left(-A_{x,i}y_i + A_{y,i}x_i + A_{z,i}0\right) \tag{3.60}$$

Where $\left(-A_{x,i}y_i + A_{y,i}x_i + A_{z,i}0\right)$ is the z-component of the cross product r x PA. Equation 3.60 can be more easily understood by looking at Figure 3. 8 where a simplified check valve and the interesting quantities are drawn.

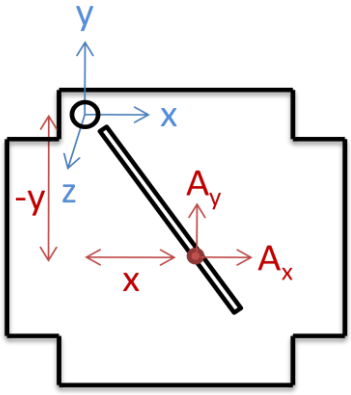

Figure 3. 8. Sketch of how to calculate the torque due to pressure in the CFD modeling.

Input requirements

The input requirements of the CFD simulation are listed in Table 3. 6 and are fed to solver in a proper UDF. All other valve dimensions are found in the mesh that is required for the simulation to run.

Table 3. 6. Input data to CFD simulation.

Input variable	***Data***
Moment length to center of gravity	0.152 m
Angle for closed valve	5 °
Maximum opening angle	57°
Submerged weight of the flapper	6.15 kg
Rotational inertia	0.1875 kgm^2
Acceleration of gravity	9.81 m/s^2

4 Code description

4.1 One-dimensional code: RELAP5

The most important equations in the RELAP5 code are reviewed together with some general information.

4.1.1 Basics about the code

RELAP5 is a thermo-hydraulic software developed by Idaho National Engineering Laboratory for the U.S government during the early 1980's. The code is designed for best-estimate transient simulation of light water reactor (LWR) coolant system. This means that it is capable of solving systems with mixtures of water, steam, noncondensable and solute. In addition the code is written in a generic way, making it also applicable to nonnuclear systems (Information Systems Laboratories, Inc, 2003).

The RELAP5 code is based on cards where each card has a specific number and function. The reason behind this disposition is that during the early computer age the programming was performed using cards with holes symbolizing the binary system. There are some mandatory cards that are used to start the simulation but then the user provides the system that is to be modeled. Such systems are built up by different components each with different numbers in order for the code to solve it in correct order. These components can be pumps, valves or other common part in a piping system. A typical description can be found in section 6.6 where the investigated system is presented. It is also important for the code to know what components that are linked together and this is performed with different junction components.

4.1.2 Mathematics in RELAP5

The governing equations in the two-fluid nonequilibrium model are two phasic continuity equations, two phasic momentum equations and two phasic energy equations which are displayed in equation 4.1 through 4.7. The equations are solved using time and volume-averaged dependent variables and time and one space dimension as independent variables.

Phasic continuity equation

$$\frac{\partial}{\partial t}\left(\alpha_g \rho_g\right) + \frac{1}{A}\left(\alpha_g \rho_g U_g A\right) = \Gamma_g \tag{4.1}$$

$$\frac{\partial}{\partial t}\left(\alpha_f \rho_f\right) + \frac{1}{A}\left(\alpha_f \rho_f U_f A\right) = \Gamma_f \tag{4.2}$$

Further no mass sources or sinks are concerned, meaning that positive liquid generation required negative vapor generation according to:

$$\Gamma_f = -\Gamma_g \tag{4.3}$$

Phasic momentum equations

$$\begin{aligned}&\alpha_g \rho_g \frac{\partial U_g}{\partial t} + \frac{1}{2}\alpha_g \rho_g A \frac{\partial U_g^2}{\partial t} = \\ &-\alpha_g A \frac{\partial P}{\partial x} + \alpha_g \rho_g B_x A - \left(\alpha_g \rho_g A\right) FWG\left(U_g\right) + \Gamma_g A\left(U_{gI} - U_g\right) \\ &-\left(\alpha_g \rho_g A\right) FIG\left(U_g - U_f\right) - C\alpha_g \alpha_f \rho_m A\left[\frac{\partial\left(U_g - U_f\right)}{\partial t} + U_f \frac{\partial U_g}{\partial x} + v_g \frac{\partial U_f}{\partial x}\right]\end{aligned} \tag{4.4}$$

$$\alpha_f \rho_f \frac{\partial U_f}{\partial t} + \frac{1}{2}\alpha_f \rho_f A \frac{\partial U_f^2}{\partial t} =$$
$$-\alpha_f A \frac{\partial P}{\partial x} + \alpha_f \rho_f B_x A - (\alpha_f \rho_f A) FWG(U_f) + \Gamma_f A(U_{fI} - U_f)$$
$$-(\alpha_f \rho_f A) FIG(U_f - U_g) - C\alpha_f \alpha_g \rho_m A \left[\frac{\partial (U_f - U_g)}{\partial t} + v_g \frac{\partial U_f}{\partial x} + v_f \frac{\partial U_g}{\partial x}\right] \quad (4.5)$$

Phasic energy equations

$$\frac{\partial}{\partial t}(\alpha_g \rho_g E_g) + \frac{1}{A}\frac{\partial}{\partial x}(\alpha_g \rho_g E_g U_g A) =$$
$$-P\frac{\partial \alpha_g}{\partial t} - \frac{P}{A}\frac{\partial}{\partial x}(\alpha_g U_g A) + Q_{wg} + Q_{ig} + \Gamma_{ig} h_g^* + DISS_g \quad (4.6)$$

$$\frac{\partial}{\partial t}(\alpha_f \rho_f E_f) + \frac{1}{A}\frac{\partial}{\partial x}(\alpha_f \rho_f E_f U_f A) =$$
$$-P\frac{\partial \alpha_f}{\partial t} - \frac{P}{A}\frac{\partial}{\partial x}(\alpha_f U_f A) + Q_{wf} + Q_{if} + \Gamma_{if} h_f^* + DISS_f \quad (4.7)$$

4.1.3 Boundary conditions

The boundary conditions of a RELAP5 simulation are most usually set by having time-dependent volumes at the inlet(s) and outlet(s). In these components the user can specify pressure and temperature variation. This approach controls the pressure of the flow but for some applications it is more valuable to control the velocity. The inlet velocity at the boundaries of the computational domain is set by adding a time dependent junction which is attached to a time-dependent volume.

4.2 Alternative one-dimensional code: DRAKO

A short description will be given here of an alternative one-dimensional code developed by KAE and capable of simulating a swing check valve. This code however is not used for the simulation but instead the RELAP5 code uses the swing check valve model from the DRAKO code.

The DRAKO code has been developed to handle unsteady flows in complex piping system and is thus commonly used for calculating water and steam hammer loadings in nuclear power plants. In addition to the three conservation equations for mass, momentum and energy the code uses a material law. This law describes the density and enthalpy as functions of both pressure and entropy.

4.3 Mathematics in computational fluid dynamics (CFD)

A brief description will be given about the main equations that need to be solved for both the flow and fluid. This includes the general flow equations and more specific turbulent models equations. For more information the reader is referred to (Andersson, et al., 2010) or any other CFD literature.

4.3.1 Basic behavior of a moving fluid

For laminar flows it is the viscous forces that dominate and it is possible to obtain very accurate simulations in CFD for single phase. However the transition between laminar and turbulent flow is difficult to model correctly. The dimensionless Reynolds number (Re) is the ratio between inertial and viscous forces and thus describes the relative importance of these two for a given flow. A laminar flow is characterized by low Re and thus the viscous forces

dominate resulting in a smooth constant fluid motion. At high Re the fluid motion is more influenced by the inertial forces and the flow becomes turbulent, leading to instabilities in the flow. The Reynolds number can be written as:

$$Re = \frac{inertial\ forces}{viscous\ forces} = \frac{\rho v^2 L^2}{\mu v L} = \frac{\rho v L}{\mu} \tag{4.8}$$

The transition between laminar and turbulent flow depends on where the flow is situated. In case of an internal flow in a pipe the characteristic length is the diameter of the pipe.

4.3.2 Governing equations

The general transport equation in tensor notation for a scalar, vector or tensor φ can be formulated in its continuous form as:

$$\frac{\partial \phi}{\partial t} + U_i \frac{\partial \phi}{\partial x_i} = D \frac{\partial^2 \phi}{\partial x_i \partial x_i} + S(\phi) \tag{4.9}$$

Here the terms correspond to accumulation, convection, diffusion and source respectively. The continuity equation is obtained by specifying φ=ρ and recognizing that the transport by diffusion is zero as well as the source term resulting in:

$$\frac{\partial \rho}{\partial t} + \frac{\partial \rho U_j}{\partial x_j} = 0 \tag{4.10}$$

The momentum equation which is also known as Navier-Stokes equations is obtained by setting $\varphi_i = \rho U_i$ and specifying the source term:

$$\frac{\partial U_i}{\partial t} + U_j \frac{\partial U_i}{\partial x_j} = -\frac{1}{\rho}\frac{\partial P}{\partial x_i} - \frac{1}{\rho}\frac{\partial \tau_{ij}}{\partial x_j} + g_i \tag{4.11}$$

The Navier-Stokes equations are based on Newton's second law of motion saying that the rate of change of momentum is due to the forces applied. Forces that need to be considered are those due to pressure, stresses and gravity. It is these two equations that are the foundation of all CFD simulations.

To make the description of the flow complete one additional equation is required, namely the energy transport equation. Included in this equation is the kinetic, thermal, chemical and potential energy and is written according to:

$$\frac{\partial h}{\partial t} = -\frac{\partial}{\partial x_j}\left[hU_j - k_{eff}\frac{\partial T}{\partial x_i} + \sum_n m_n h_n D_n \frac{\partial C_n}{\partial x_j} - \tau_{kj} U_k\right] + S_h \tag{4.12}$$

In order to solve these continuous equations numerically they need to be transferred into discrete variables. This can be done using different schemes and then obtaining different level of accuracy of the calculations.

4.3.3 Reynolds-Averaged Navier-Stokes equations

RANS is an abbreviation for Reynolds Averaged Navier-Stokes equations and is a method where the instantaneous variables are divided in to one mean part and one fluctuating part according to:

$$U_i = \langle U_i \rangle + u_i \tag{4.13}$$

$$P = \langle P \rangle + p \tag{4.14}$$

The Navier-Stokes equation can then be written as:

$$\frac{\partial\langle U_i\rangle}{\partial t} + \langle U_j\rangle\frac{\partial\langle U_i\rangle}{\partial x_j} = -\frac{1}{\rho}\frac{\partial}{\partial x_j}\left\{\langle P\rangle\delta_{ij} + \mu\left[\frac{\partial\langle U_i\rangle}{\partial x_j} + \frac{\partial\langle U_j\rangle}{\partial x_i}\right] - \rho\langle u_i u_j\rangle\right\} \quad (4.15)$$

The last term $-\rho\langle u_i u_j\rangle$ also denoted as τ_{ij} is referred to as the Reynolds stresses and is important since it introduces a coupling between the mean and fluctuating parts of the flow. In all RANS based turbulence models this term must be modeled in order to close equation 4.15. One way to do this is to relate the Reynolds stress tensor to the mean velocity itself.
The Boussinesq approximation relates the Reynolds stress tensor to the mean flow by assuming that the tensor is proportional to the mean velocity gradients. It is assumed that the Reynolds stresses can be modeled using a turbulent viscosity analogous to molecular viscosity.

$$\frac{\tau_{ij}}{\rho} = -\langle u_i u_j\rangle = \nu_T\left(\frac{\partial\langle U_i\rangle}{\partial x_j} + \frac{\partial\langle U_j\rangle}{\partial x_i}\right) - \frac{2}{3}k\delta_{ij} \quad (4.16)$$

With the introduction of turbulent viscosity to describe the fluctuating parts of the flow another closure problem has arose. This problem is handled differently in various turbulence models. However the different turbulence models based on the Boussinesq approximation have that in common that the turbulent viscosity is calculated from the use of local appropriate length and velocity scales. With the assumption introduced by Boussinesq and the phenomena of turbulent viscosity the RANS equation can now be written as:

$$\frac{\partial\langle U_i\rangle}{\partial t} + \langle U_j\rangle\frac{\partial\langle U_i\rangle}{\partial x_j} = -\frac{1}{\rho}\frac{\partial\langle P\rangle}{\partial x_j} - \frac{2}{3}\frac{\partial k}{\partial x_i} + \frac{\partial}{\partial x_j}\left[(\nu + \nu_T)\left(\frac{\partial\langle U_i\rangle}{\partial x_j} + \frac{\partial\langle U_j\rangle}{\partial x_i}\right)\right] \quad (4.17)$$

The turbulent kinetic energy k has also been introduced according to:

$$k = \frac{1}{2}\langle u_i u_j\rangle \quad (4.18)$$

4.3.4 Alternative approach to RANS

The Navier-Stokes equations are able to describe turbulent flows but due to the complexity of the flow the equations are not possible to solve for real engineering purposes with the computer power that is today. For instance in a stirred tank reactor the lifetime for the smallest turbulent eddies are about 5 ms and the size of those eddies (describes by the Kolmogorov scales) are about 50 μm resulting in a very fine space and time resolution. The Navier-Stokes equations are thus only solved directly for very small systems in order to understand turbulence better and develop new models. This method is called Direct Numerical Simulation (DNS) and this means that no turbulence models are used.

By filtering out the smallest turbulent scales and model these as flow dependent a more cost effective method is obtained. This procedure is referred to as Large Eddy Simulation (LES) but is also time consuming and for more complex flows the turbulence fluctuations is not resolved at all and the RANS based models are used even though higher order of accuracy can be achieved with DNS and LES.

4.3.5 Turbulence models

A various number of turbulence models exist and to categorize them, they are separated by the number of additional partial differential equations in addition to the RANS and continuity equation. Hence zero-equation and one-equation models are the simplest ones, but they will not be discussed further since they are not considered to be complete models and are not used

for general purpose flow simulations. Two-equation-models however have the ability to model both velocity and length scale making them complete in that sense.

Realizable k-ε model

As the name of the model implies, the modeled parameters are the turbulent kinetic energy, k, and the turbulent dissipation rate, ε. The transport equation for turbulent kinetic energy can be deduced from the equation for kinetic energy by Reynolds decomposition and is written as:

$$\underbrace{\frac{\partial k}{\partial t}}_{A} + \underbrace{\langle U_j \rangle \frac{\partial k}{\partial x_j}}_{B} = \underbrace{-\langle u_i u_j \rangle \frac{\partial \langle U_i \rangle}{\partial x_j}}_{C} \underbrace{- \nu \left\langle \frac{\partial u_i}{\partial x_j} \frac{\partial u_i}{\partial x_j} \right\rangle}_{D} + \frac{\partial}{\partial x_j} \left(\underbrace{\nu \frac{\partial k}{\partial x_j}}_{E} \underbrace{- \frac{\langle u_i u_i u_j \rangle}{2}}_{F} \underbrace{- \left\langle \frac{u_j p}{\rho} \right\rangle}_{G} \right) \quad (4.19)$$

Where the physical interpretation is given below:

A. Accumulation of *k*.
B. Convection of *k* by mean velocity.
C. Production of *k*.
D. Dissipation of *k* by viscous stress.
E. Molecular diffusion of *k*.
F. Turbulent transport by velocity fluctuations.
G. Turbulent transport by pressure fluctuations.

Closures are required for production, dissipation and turbulent transport in order to solve the k-equation. The Boussinesq-approximation is used to relate the production term the gradients of the mean flow according to:

$$-\langle u_i u_j \rangle = \nu_T \left(\frac{\partial \langle U_i \rangle}{\partial x_j} + \frac{\partial \langle U_j \rangle}{\partial x_i} \right) - \frac{2}{3} k \delta_{ij} \quad (4.20)$$

And further the production of turbulent kinetic energy is written as:

$$-\langle u_i u_j \rangle \frac{\partial \langle U_i \rangle}{\partial x_j} = \nu_T \left(\frac{\partial \langle U_i \rangle}{\partial x_j} + \frac{\partial \langle U_j \rangle}{\partial x_i} \right) \frac{\partial \langle U_i \rangle}{\partial x_j} - \frac{2}{3} k \frac{\partial \langle U_i \rangle}{\partial x_j} \quad (4.21)$$

The destruction of k is related to the energy dissipation of turbulent kinetic energy as:

$$\varepsilon = \nu \left\langle \frac{\partial u_i}{\partial x_j} \frac{\partial u_i}{\partial x_j} \right\rangle \quad (4.22)$$

The turbulent transports due to velocity and pressure fluctuations are modeled by assuming a gradient diffusion transport mechanism:

$$-\frac{\langle u_i u_i u_j \rangle}{2} - \left\langle \frac{u_j p}{\rho} \right\rangle = \frac{\nu_T}{\sigma_k} \frac{\partial k}{\partial x_j} \quad (4.23)$$

Finally the resulting k-equation used in the modeled is expressed according to:

$$\frac{\partial k}{\partial t} + \langle U_j \rangle \frac{\partial k}{\partial x_j} = \nu_T \left[\left(\frac{\partial \langle U_i \rangle}{\partial x_j} + \frac{\partial \langle U_j \rangle}{\partial x_i} \right) \frac{\partial \langle U_i \rangle}{\partial x_j} \right] - \varepsilon + \frac{\partial}{\partial x_j} \left[\left(\nu + \frac{\nu_T}{\sigma_k} \right) \frac{\partial k}{\partial x_j} \right] \quad (4.24)$$

A similar treatment involving several closures is required for the turbulent dissipation rate to be modeled. These closures are those terms responsible for production, destruction rate and turbulent transport by velocity and pressure fluctuations. The different equations for these closures will however not be given here but instead the final result with all the closure coefficients given in Appendix B:

$$\underbrace{\frac{\partial \varepsilon}{\partial t}}_{A} + \underbrace{\langle U_j \rangle \frac{\partial \varepsilon}{\partial x_j}}_{B} =$$

$$\underbrace{C_1 S \varepsilon}_{C} - \underbrace{C_2 \frac{\varepsilon^2}{k+\sqrt{\nu\varepsilon}}}_{D} - \underbrace{C_{1\varepsilon} \frac{\varepsilon}{k} C_{3\varepsilon} g \left(\frac{\partial \rho}{\partial T}\right)_p \frac{\nu_T}{Pr_t} \frac{\partial T}{\partial x_j}}_{E} + \underbrace{\frac{\partial}{\partial x_j}\left[\left(\nu + \frac{\nu_T}{\sigma_\varepsilon}\right)\frac{\partial \varepsilon}{\partial x_j}\right]}_{F} \quad (4.25)$$

A. Accumulation of ε.
B. Convection of ε by the mean velocity
C. Production of ε.
D. Dissipation of ε.
E. Generation of k due to buoyancy
F. Diffusion of ε.

The turbulent viscosity is present in both of the transport equations previously described. In order to close this turbulence model the turbulent viscosity is modeled according to:

$$\nu_T = C_\mu \frac{k^2}{\varepsilon} \quad (4.26)$$

Unlike the standard k-ε model the parameter Cμ is not a constant but instead a function of the local state that can be found in more detail in Appendix B. This approach results in that the normal component of the Reynold stress tensor is never negative and thus the Schwarz's inequality is fulfilled. This constrain therefore ensures realizability, thus explaining the model name.

The realizable k-ε model is capable of predicting axisymmetrical jets contrary to the standard k-ε model. This model is also better for flows where the strain rate is large, including flows with strong streamline curvature and rotation. For near wall modeling where both k and ε approaches zero, the model may behave poorly but this can be overcome by using wall functions which is discussed more in section 264.3.6.

SST k-ω model

A short description will be given for an alternative turbulence model that has been used to some extent to investigate the dependence of turbulence models. This model uses the specific dissipation, ω, instead of the turbulent dissipation rate, ε, as the length determining quantity. The abbreviation SST stands for Shear-Stress Transport and means that the turbulent viscosity is modified to also account for the transport of the principal turbulent shear stress. The SST k-ω model is based on both the k-ω and the k-ε models. This means that in the free stream the model uses k-ε and for wall bounded regions k-ω is used. The k-ω model does not need wall functions but in return required a very fine mesh close to the walls for near wall modeling. This model works well for both adverse pressure gradient and separating flow.

The general k- and ω- transport equations are shown below but for a complete description of the equations solved in this turbulence model the reader is referred to any of (Wilcox, 2006) , (Menter, 1994) or FLUENT v12.1 manual. The equation for turbulent kinetic energy is given by:

$$\frac{\partial k}{\partial t} + \langle U_j \rangle \frac{\partial k}{\partial x_j} = \nu_T \left[\left(\frac{\partial \langle U_i \rangle}{\partial x_j} + \frac{\partial \langle U_j \rangle}{\partial x_i}\right)\frac{\partial \langle U_i \rangle}{\partial x_j}\right] - \beta k\omega + \frac{\partial}{\partial x_j}\left[\left(\nu + \frac{\nu_T}{\sigma_k}\right)\frac{\partial k}{\partial x_j}\right] \quad (4.27)$$

The modeled ω-equation is:

$$\frac{\partial \omega}{\partial t} + \langle U_j \rangle \frac{\partial \omega}{\partial x_j} = \alpha \frac{\omega}{k} \nu_T \left[\left(\frac{\partial \langle U_i \rangle}{\partial x_j} + \frac{\partial \langle U_j \rangle}{\partial x_i} \right) \frac{\partial \langle U_i \rangle}{\partial x_j} \right] - \beta^* \omega^2 + \frac{\partial}{\partial x_j} \left[\left(\nu + \frac{\nu_T}{\omega_k} \right) \frac{\partial \omega}{\partial x_j} \right] \quad (4.28)$$

The values of the closure coefficients are given in appendix B.

4.3.6 Near wall modeling with wall functions

Wall functions are used to bridge the near wall region. For RANS models the estimated parameters are k, ε, the mean velocities and the Reynold stresses and these estimates are made in the first cell close to the wall. There exist different kinds of wall functions capable of handling a variety of flows. In case of a more complex flow condition involving phenomena such as flow separation, strong pressure gradient or flow impingement the use of modified wall functions is necessary. These wall functions are referred to as non-equilibrium boundary layers wall functions and typically consists of a logarithmic law for the mean velocity.

4.3.7 Boundary conditions

For turbulent flow simulations the turbulent quantities must be known at all boundaries where the flow enters the computational domain. In case of a two-equation model this means that both the turbulent kinetic energy and the energy dissipation rate should be given. However the inputs are not required to be these specific values since the turbulence is defined by the turbulent time, velocity and length scale. Instead the turbulent intensity is often used, and for a pipe at high Reynolds number estimated by equation 3.28:

$$I = \frac{u'}{\bar{U}} = 0.16 Re^{-1/8} \quad (4.29)$$

The turbulent length scale (l) is approximated with the hydraulic diameter (L) according to:

$$l = 0.07L \quad (4.30)$$

The turbulent quantities are then estimated at the system boundaries with equation 3.30 and 3.31.

$$k = \frac{3}{2} (\bar{U} I)^2 \quad (4.31)$$

$$\varepsilon = C_\mu^{3/4} \frac{k^{3/2}}{l} \quad (4.32)$$

5 Geometry and simulation method

The geometry of the swing check valve will be presented along with all the necessary data used in the computer codes. Also a more thorough review will be made regarding the CFD simulation, including numerical settings, mesh generation and UDF (User Defined Function) writing. The RELAP5 system that has been modeled is briefly presented at the end.

5.1 General geometry of the swing check valve

The geometry was first obtained in the form of a CAD drawing which had to undergo some clean up. The result can be seen in Figure 5. 1 where the forward flow enters from the left. The valve is a DN200 swing check valve from the Spanish manufacturer RINGO VALVULAS. The diameter of the disc is approximately 0.2 m and the valve body approx 0.3 m. In addition to the swing check valve itself a straight section of 0.5 m is added at the inlet and outlet in order to have a more fully developed pipe flow entering the valve and well defined flow at the boundaries.

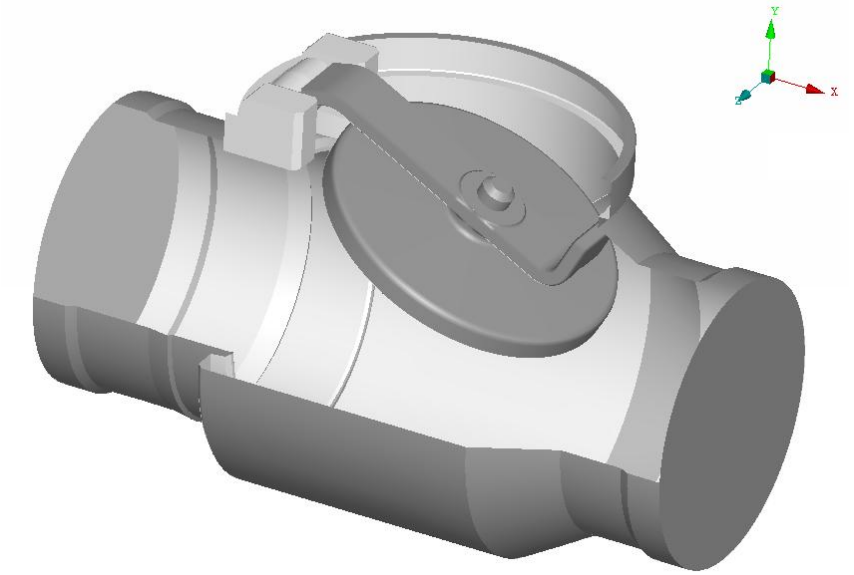

Figure 5. 1. Geometry of the investigated swing check valve with forward flow entering from the left.

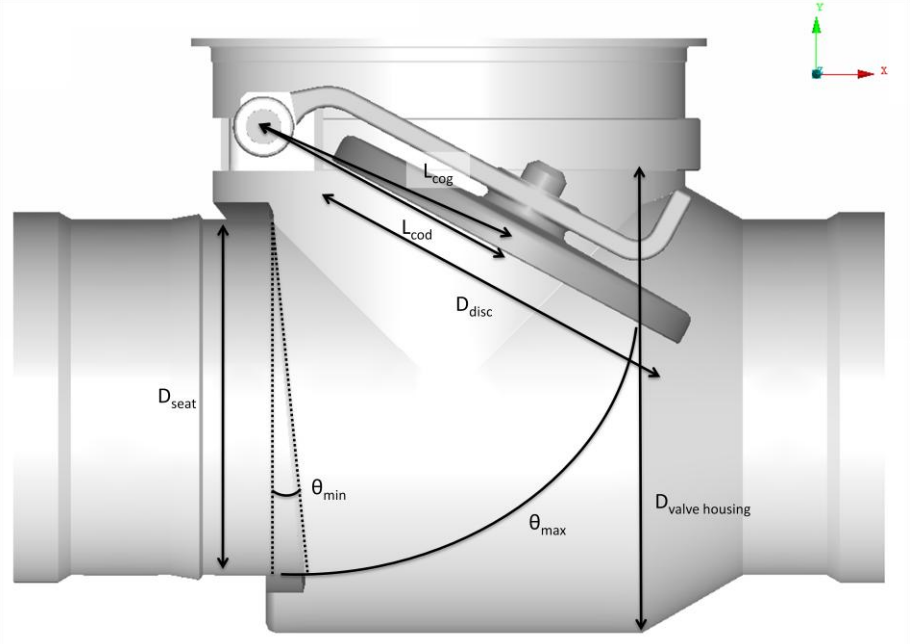

Figure 5. 2. Sketch of the check valve displaying all the important dimensions. The values of the displayed quantities are given in table 5.1.

The exact dimensions and other usable quantities of the geometry are given in Figure 5. 2 are listed in Table 5. 1 below. The rotational inertia is calculated both with equation 3.5 and with the meshing software ANSA v13.05, only the latter is presented but the difference is small. All other quantities are obtained solely from the meshing software.

Table 5. 1. Dimensions and other quantities of the swing check valve.

Quantity	***Abbrevation***	***Value***
Diameter of the disc	D_{disc}	0.224 m
Diameter of the valve seat	D_{seat}	0.203 m
Diameter of valve housing	$D_{valve\ housing}$	0.269 m
Distance to center of disc	L_{cod}	0.155 m
Distance to center of gravity	L_{cog}	0.152 m
Submerged weight of the flapper		6.15 kg
Rotational inertia of the flapper		0.1875 kgm^2
Minimum angle	θ_{min}	5 °
Maximum angle	θ_{max}	62 °

5.2 Numerical settings

Turbulence models
k-ω SST without wall functions
k-ε realizable using non-equilibrium wall functions

Numerical scheme
Second order upwind

Fluid properties
The fluid is water and the density is set to 998.2 kg/m^3 which is the value at 20°C except for the case when compressible fluid is concerned which is described by Tait equation described below.

The P-V-T dependence of a fluid can be described by an equation of state. Typically as the pressure is increased in the system the volume will decrease since the molecules are forces more closely together. A smaller specific volume is the same as a density increase and may affect the torque due to the impinging flow in the CFD simulation.

In the early 19th century Tait formulated a P-V relationship for water written in its integral form as equation 5.1 where C is a constant given by $0.3150/V_0$ and B is approximately 3000 bar (Li, 1967).

$$V = V_0 - C\ log\left(\frac{B+P}{B+1}\right) \tag{5.1}$$

Equation 5.1 can be reformulated to use the density instead and with the coefficient given the Tait equation becomes equation 5.2.

$$\rho = \rho_0 \frac{1}{1-0.3150\ log\left(\frac{3000+P}{3000+1}\right)} \tag{5.2}$$

5.3 Dynamic mesh

The dynamic mesh option is used during transient simulations to maintain a high mesh quality and prevent the formation of negative cell volumes due to mesh quality deterioration. A moving zone will cause the cells in the adjacent zone to adapt in order for the simulation to reach convergence. The requirements of a dynamic simulation are an initial mesh and description of the boundary motion. In this Master's thesis the motion of the boundary is described by a UDF viewed in detail in appendix A.

5.3.1 Dynamic mesh update methods

There are three different mesh motion methods available in FLUENT v12.1 to update the volume mesh. Each of these has their area of appliance and some may also be combined with each other. These three are:

1. Spring-based smoothing
2. Dynamic layering
3. Local remeshing

Spring-based smoothing

This method can be used to update any cell or face zone but may give more accurate results to certain motion and meshes. In the case of non-tetrahedral cells, this method is recommended only if the boundary of the cell zone moves predominately in one direction or the motion is predominately normal to the boundary zone. The smoothing option is used when the motion is small in magnitude but it can also be used in conjunction with remeshing.
In short the spring-base smoothing method sees the mesh as a network of interconnected springs. As the boundary is moving the node closest to the boundary will be displaced and that will generate a force proportional to that displacement along all springs connected to the node. Using Hook's Law the mesh is then updated.

Dynamic layering

The dynamic layering method can only be applied to prismatic mesh zones. The procedure of this method is that it adds or removes layers of cells adjacent to the moving boundary. The user specifies an ideal height of the cells and as the boundary is moving, cell layers are either split or merged with the layer of cells next to it. The layering option is suitable when the boundary motion is perpendicular to the moving boundary.

Local remeshing

In those cases where the boundary displacement is large compared with the cell size the smoothing method is not sufficient since the cell quality can deteriorate. The local remeshing option can be used to handle cells that violate the skewness or size criteria which are set by the user. Those cells are marked for remeshing and if the new cells satisfy the previous criteria the mesh is locally updated with the new cells. If not, the new cells are discarded.

5.3.2 Mesh quality

The quality of the computational domain will play an important role in the accuracy and stability of the calculation. Therefore to control the quality of the mesh a number of criteria can be evaluated in FLUENT such as maximum cell skewness and maximum aspect ratio. Skewness describes the difference between the shape of the cell and the shape of an equilateral cell of equivalent volume. The value of the skewness should be kept low in order to increase the accuracy and stability. For a tetrahedral mesh the maximum value should be below 0.95 and on average below 0.33. The aspect ratio is a measure of how much the cell is stretched. In general this value should be below 5:1 in the bulk flow but with hexahedral cells inside boundary layers this ratio may go up to 10:1.

During a transient simulation using dynamic mesh the quality of the newly updated cells can be specified with respect to the skewness. However as the simulation goes on and the mesh is updated some cells may not fulfill this criterion and the mesh will decrease in quality.

5.4 Meshing

The mesh generation was made in the software ANSA v13.05. Several meshes were constructed in order to be able to analyze the mesh dependence later on. Since the torque is calculated from the pressure force on the swing disc it is important to get as correct value of the pressure as possible. This problem was handled by adding five layers on top of the disc that during the transient weren't marked for remeshing and by doing so obtaining a good quality close to the disc during the whole run. This layers technique can be seen in Figure 5. 3.

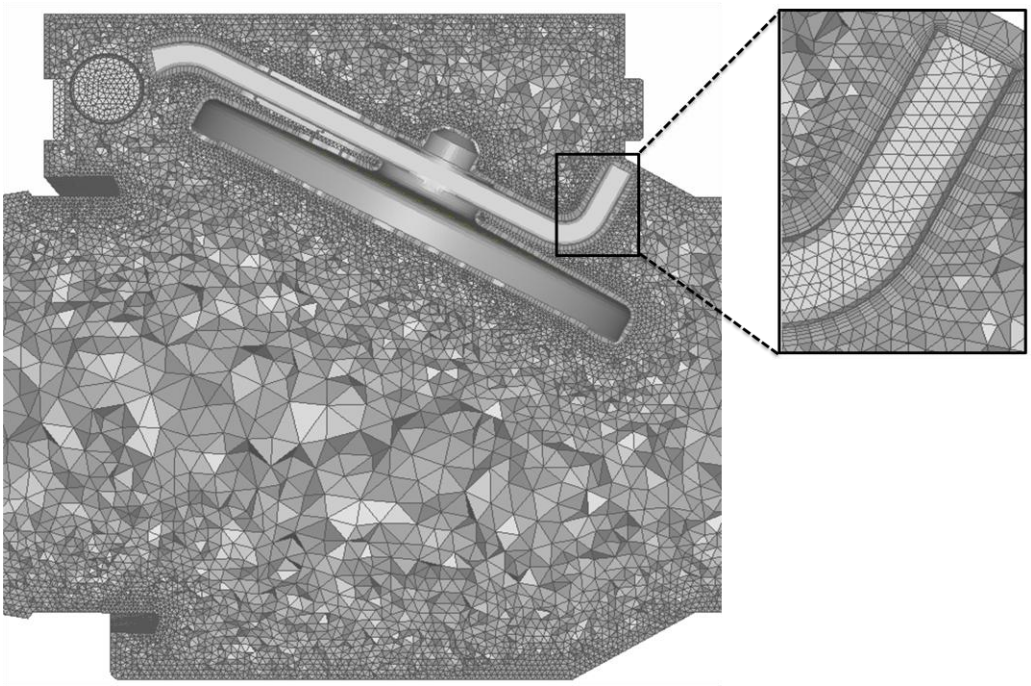

Figure 5. 3. A cross section of the mesh including layers and a tetrahedral grid.

A problem however with the layers technique is that as the valve is about to close the simulation crashed because the program isn't allowed to remesh the layers. Therefore other simulations have been made without layers. The number of cells in the domain varies for the different simulations and these numbers are summarized in Table 5. 2.

Table 5. 2. A summary of the number of cells in the domain for different simulations.

Type of simulation	***Number of cells***
Steady state -different angles	0.65 – 0.72 M
Transient -default	0.7 M
Transient -five layers	0.8 M
Transient -refined mesh	2.1 M
Transient -more refined mesh and five layers	3.9 M
Transient -scaling double	3.4 M
Transient -scaling half	0.7 M
Transient -pipe simulation	1.2 M

5.5 Using UDFs to control the behavior of the swing check valve

A UDF is a function written in the programming language scheme, which is not so different from the C language. These types of functions can be used among many other things to specify boundary conditions, do independent calculations, alter variables in the solver or change fluid properties. UDFs are used mainly in this report to control the flow entering the domain and calculating the pressure force on the flapper and from that calculation move it and remesh the domain. Additional functions are used to change the time step and to simulate complete valve closure. For this last purpose different approaches were made. The valve can not close completely due to constrain in the solver since at least one fluid element must be present between the wall of the valve housing and the wall of the flapper. To circumvent this solver limitation different ways to alter the simulation or domain are proposed:

- Adjust the viscosity of the cells located between the disc and the valve seat to a very large value, and by doing so simulate a wall. This will cause the residuals to increase rapidly and also the calculated pressure force will be incorrect after the alteration.
- Adjust the velocity of the fluid in the same cells by changing the momentum source term.
- Specify the porosity of the same cells to either 1 or 0, where 1 means that no fluid is allowed to go through. These cells must however be specified in advance and this may cause problem with the mesh as the disc is moving closer to this region.
- Stop the simulation right before it crashes and manually change the fluid cells in the discussed region into solid cells. However to know when to stop the simulation beforehand might be difficult.
- In the new version of the CFD software (FLUENT v13) it is possible to load a new mesh during a transient simulation. When this event occurs is determined by a time specified by the user. Thus by loading a new mesh of a closed valve just before the simulation crashes the complete closure may be simulated. However once again the time is unknown beforehand and as far as this writer is concerned it is not possible to load a new mesh with a UDF.

The aim of this report is however not to simulate the final closure of a swing check valve but instead the transient from fully open until closed. Thus during the transient simulations presented in chapter 6 none of the above alterations have been used.

5.6 RELAP5 system

The system modeled in the one-dimensional code is composed of two time-dependent volumes one at the beginning and one at the end. Between these two volumes there are four different components added, a time-dependent junction that specifies the flow velocity, two pipe segments, a valve and a single junction connecting the last pipe to the volume marking the outlet. The node length is set to 0.2 m and each pipe consists of 10 nodes. The check valve itself is modeled as a servo valve where the movement is controlled by control variables. The entire system description can be seen in Figure 5. 4.

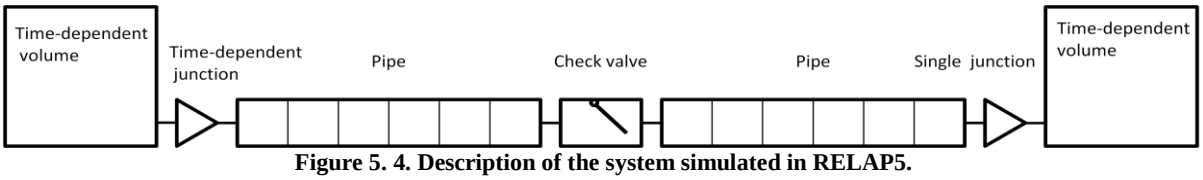

Figure 5. 4. Description of the system simulated in RELAP5.

5.7 Boundary condition

5.7.1 Inlet

At the inlet (upstream of the valve) for both the three dimensional calculations and the one dimensional a velocity inlet is used. For the transient calculations the velocity at the inlet is calculated according to:

$$U = U_0 - at \quad (5.3)$$

Where U is the velocity, a the deceleration and t the time. The following initial velocities and rates of deceleration have been used:

Table 5. 3. Inlet boundary condition for the six different transient cases investigated in this report.

Valve dimension	***Initial velocity (m/s)***	***Deceleration (m/s^2)***
DN100	3	-6
DN200	3	-0.5
DN200	3	-3
DN200	3	-6
DN200	3	-9
DN400	4[2]	-6

5.7.2 Outlet

At the downstream boundary a pressure is imposed with the pressure 101325 Pa (1 atm). For the one dimensional calculations a time dependent volume with a fix pressure is used. In the three dimensional calculations the operating pressure is set to 101325 Pa and the Gauge pressure at the outlet to 0 Pa.

[2] Due to the larger mass of the DN400 valve the initial velocity had to be increased in order for the valve to stay open.

6 Results

6.1 Stationary results

Focus will be on the angular and velocity dependence of the stationary torque coefficient along with a sensitivity analysis.

6.1.1 Flow field plots provided by the CFD simulations

Figure 6. 1 shows the impingement of the flow at a disc angle of 35 degrees and with a forward flow of 3 m/s. A stagnation zone is formed at the surface facing the flow which can be seen by a high pressure zone. The backward flow also creates a high pressure zone seen in Figure 6. 2 but not as significant as in the forward case. The location of the stagnation zones also differs depending of the direction of the flow. The forward flow creates a zone located at a position that is closer to the hinge pin than the backward flow.

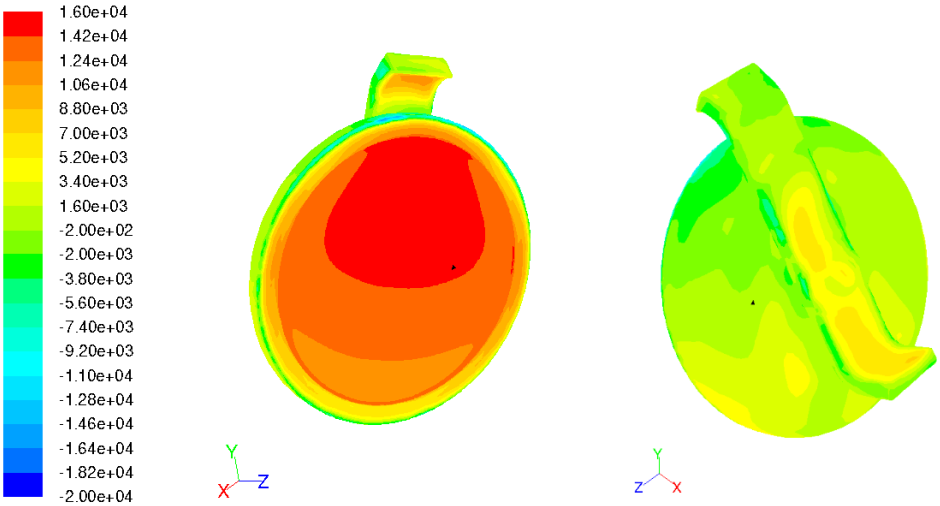

Figure 6. 1. Contour plot of the flapper with forward flow at a disc angle of 35 degrees.

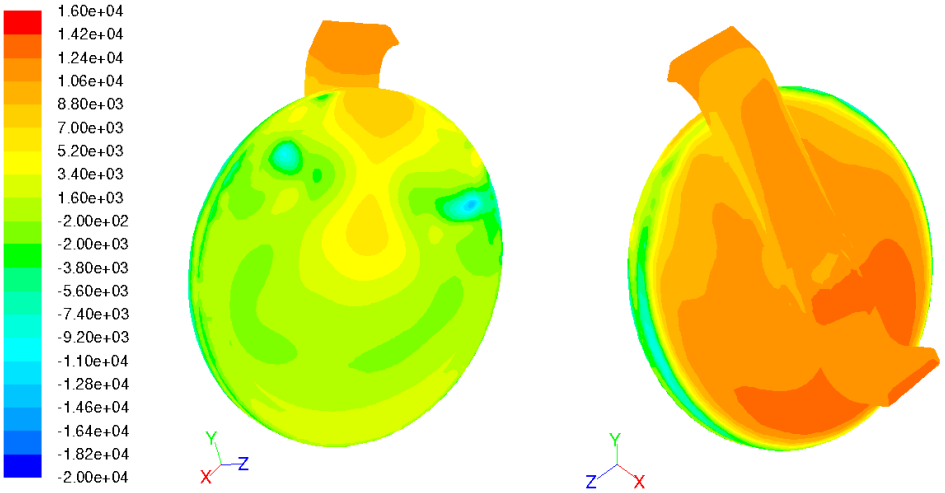

Figure 6. 2. Contour plot of the flapper with backward flow at a disc angle of 35 degrees.

The backward flow is creating a large vortex in the vicinity of the surface facing away from the flow that is not found in the forward case which can be seen by comparing Figure 6. 3 and Figure 6. 4. The flow separation is not complete over the whole disc and the flow reattaches before it has passed the valve in case of backward flow. The vortex created by the forward flow is located in the periphery of the disc and will probably play less of a role on the torque.

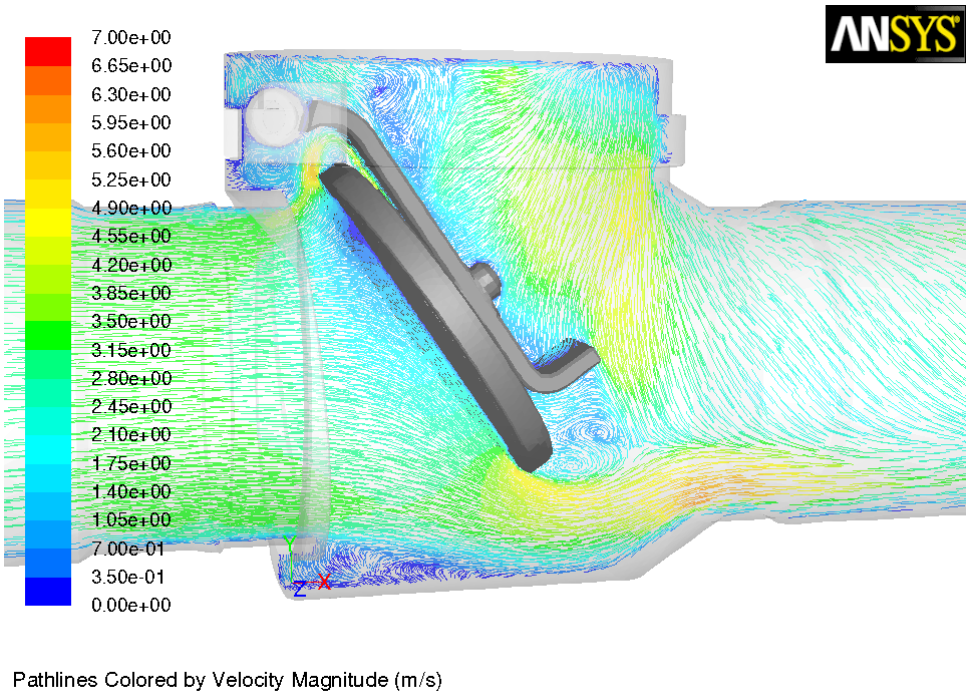

Figure 6. 3. Pathline plot of the flow colored by velocity magnitude for a forward flow of 3m/s and a disc angle of 35°.

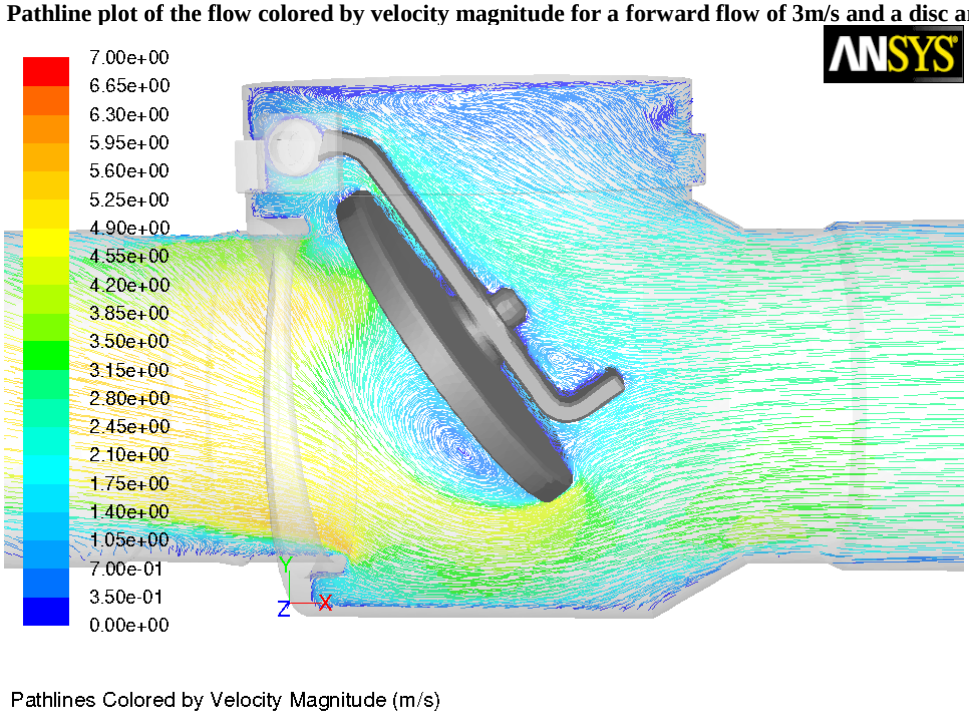

Figure 6. 4. Pathline plot of the flow colored by velocity magnitude for a reverse flow of 3m/s and a disc angle of 35°.

The static pressure of the check valve system is presented in Figure 6. 5 and Figure 6. 6 with forward and backward flow respectively. The distribution of the high pressure zone also visible in Figure 6. 1 can be seen in Figure 6. 5. A larger pressure is thus being built up by the forward flow compared to the backward flow, which will affect the hydrodynamic force and corresponding torque on the flapper.

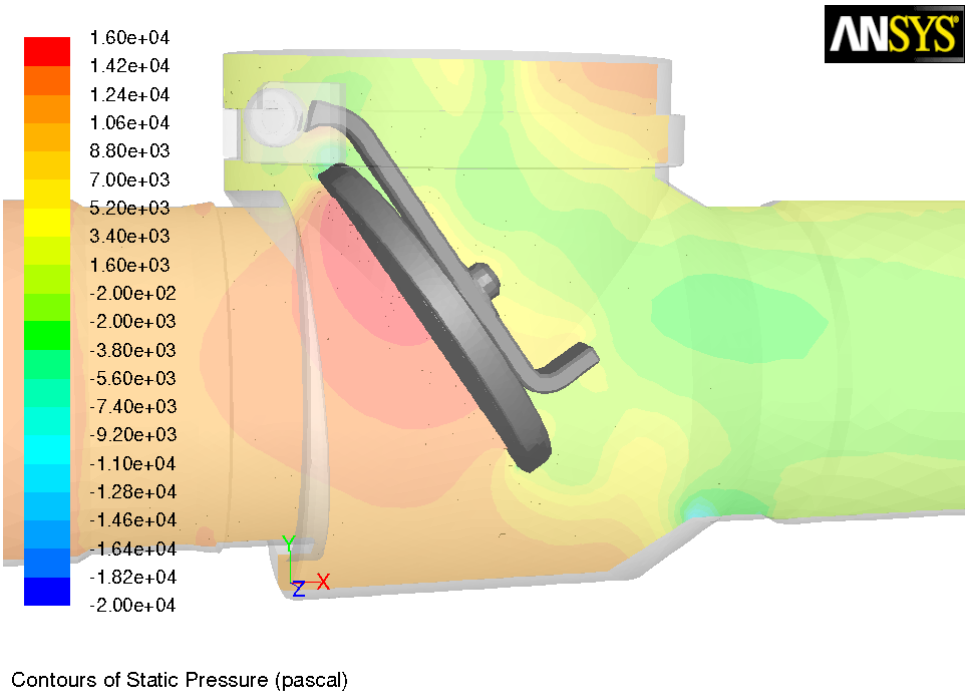

Figure 6. 5. Static pressure for a forward flow of 3m/s and a disc angle of 35°.

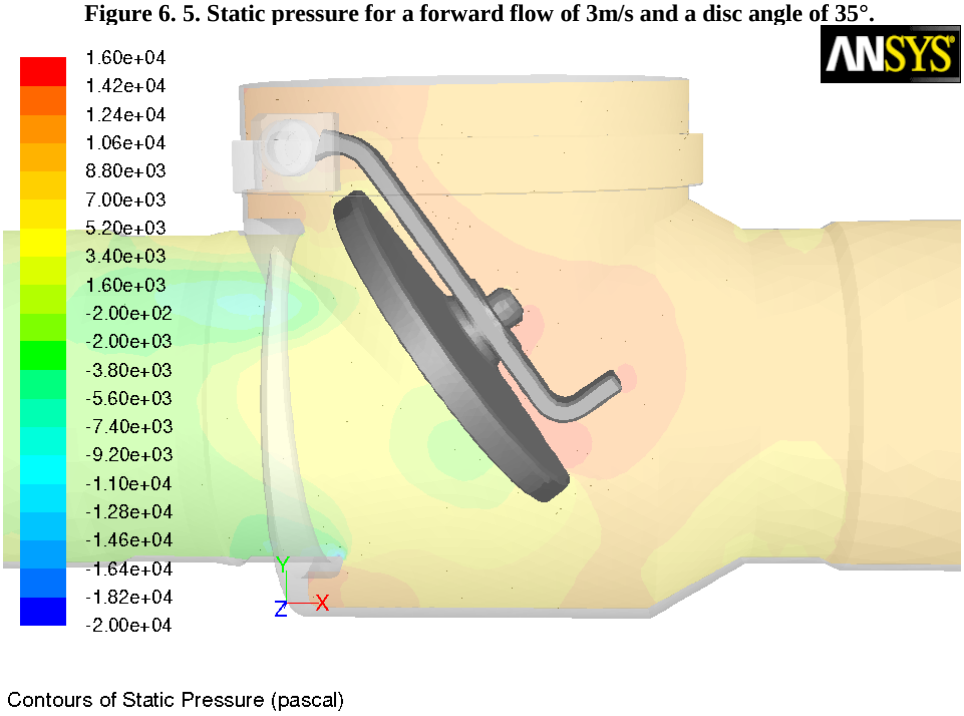

Figure 6. 6. Static pressure for a backward flow of 3m/s and a disc angle of 35°.

The turbulent properties of the forward and backward flow are investigated in Figure 6. 7 and Figure 6. 8 where the turbulent kinetic energy colors the contour plots. The largest values of the turbulent kinetic energy are located after the flow has passed the flapper, which is valid for both forward and backward flow. As the flow travels in the pipe and into the valve house there is little disturbance to the flow but as it strikes the flapper more turbulent eddies will form affecting the flow field and corresponding pressure on the flapper.

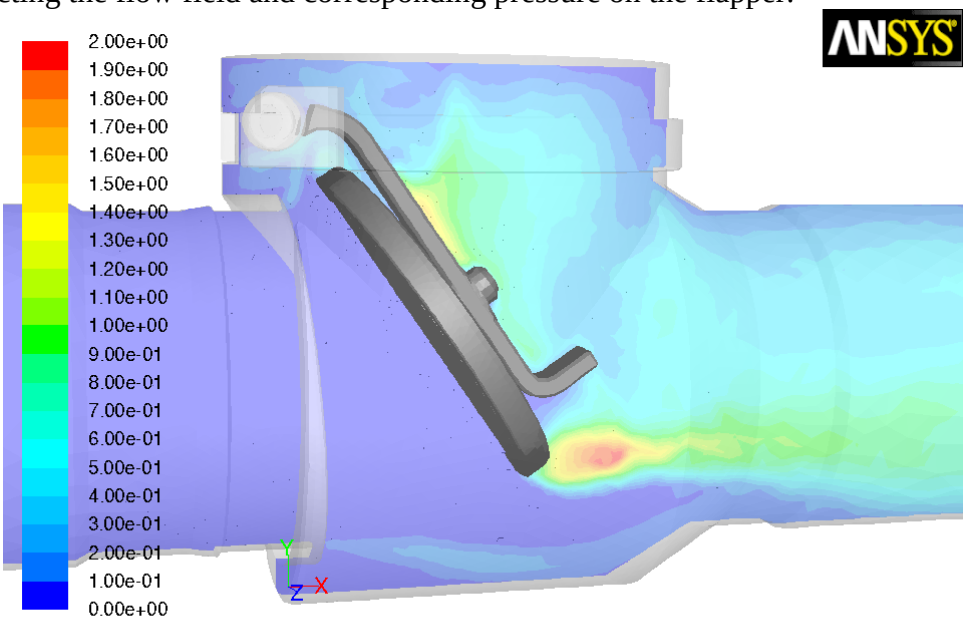

Figure 6. 7. Turbulent kinetic energy for a forward flow of 3m/s and a disc angle of 35°.

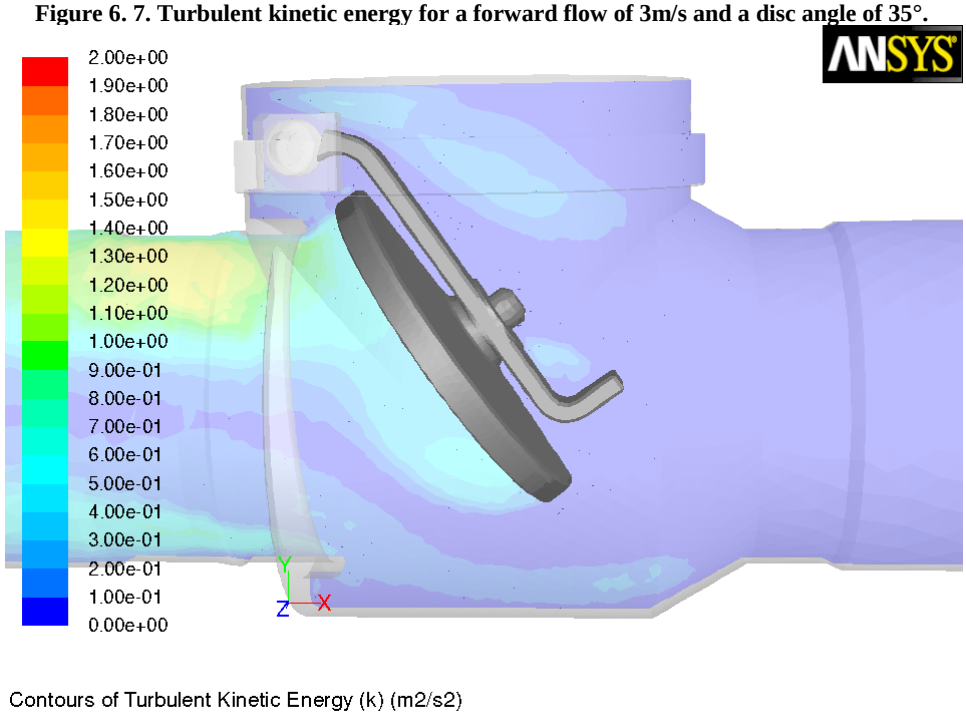

Figure 6. 8. Turbulent kinetic energy for a backward flow of 3m/s and a disc angle of 35°.

6.1.2 Stationary torque coefficient

The stationary torque coefficient is assumed to accurately handle the angle dependence of the stationary torque, thus the torques due to both pressure variation and flow diversion. The general shape of the stationary torque coefficient was first proposed in section 3.4.3. The exact values of the constants X and Y can be seen in equation 6.1 below.

$$C(\theta) = 0.3\,\theta^{-2.2} \tag{6.1}$$

This equation is assumed to both handle the area projection of the swing disc towards the flow and the angle dependence of the diversion of the flow. The constants are fitted for both forwards and backwards flow which can be seen in Figure 6. 9. From the same figure it can be concluded that the coefficient for forward flow is larger than in the case of backward flow. This difference can more clearly be seen in Figure 6. 10, where the ratio between forward and backward torque is displayed. Even though this ratio is above one for all angles there is no other clear trend.

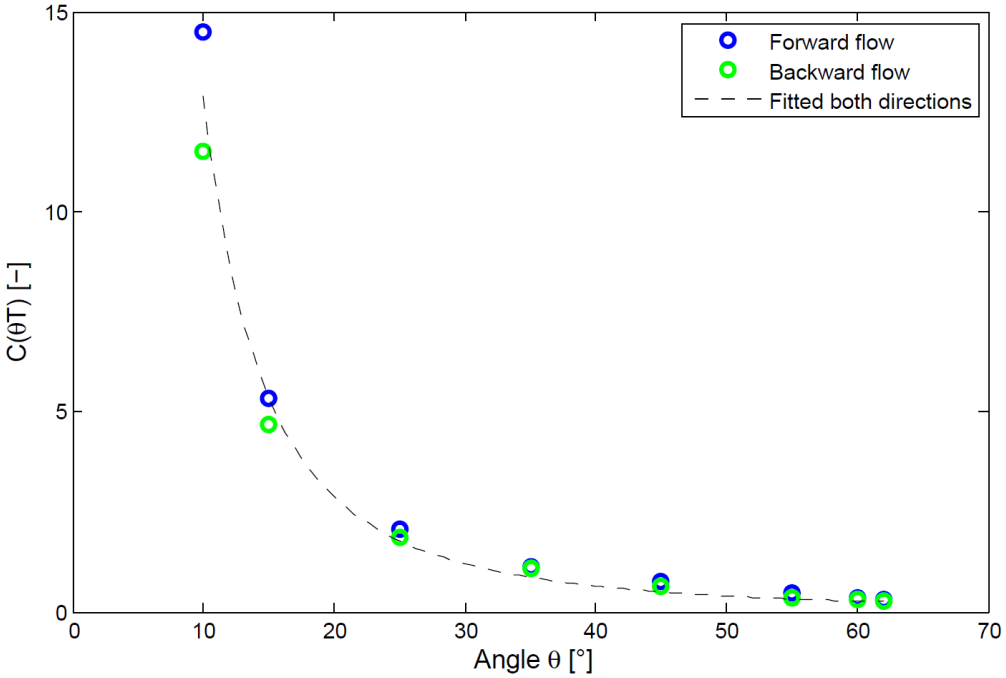

Figure 6. 9. The stationary torque coefficient as a function of angle for forward and backward flow.

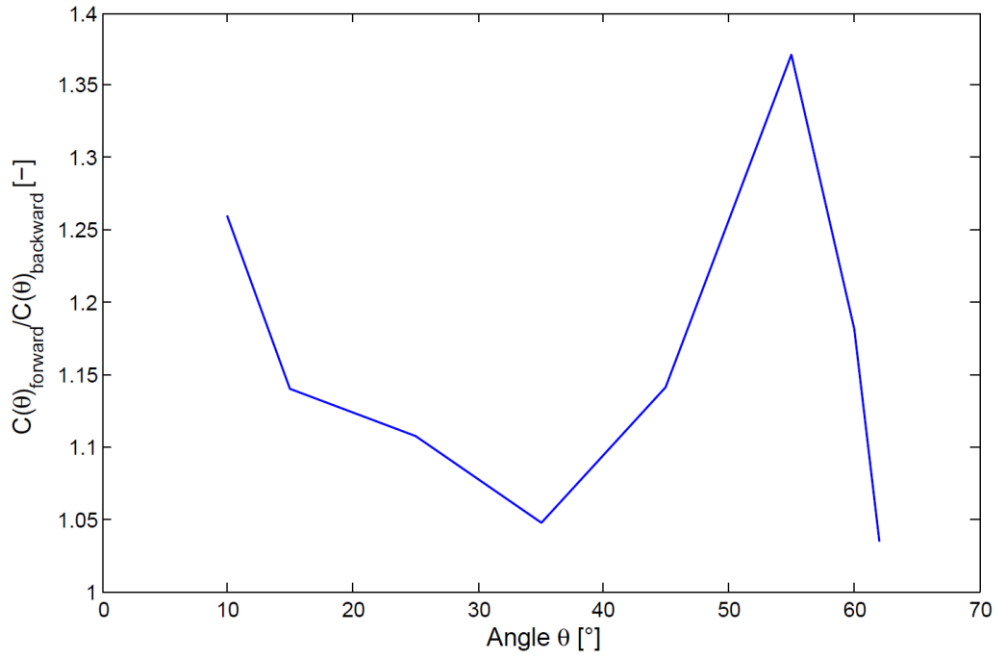

Figure 6. 10. The ratio between the forward and backward torques for different angles.

6.1.3 Velocity dependence of stationary torque coefficient

The velocity dependence of the stationary torque coefficient is given in Figure 6. 11 for a given angle of 35 degrees. The different velocities are +/- 1, 3 and 5 m/s. The trend is that the coefficient for forward flow decreases slightly with higher velocities while the coefficient for backward flow increases. This indicates that as the velocity increases these two coefficients will go towards a certain value. Overall the velocity dependence is small, this includes both the direction and magnitude of the flow. An increase of the kinetic energy of the flow by a factor of 25 results in a decrease of the forward coefficient by 4.7% and an increase of the backward coefficient by 1.2%. The largest difference between forward and backward flow is thus obtained for small velocities, where the difference is 10%. In conclusion the assumption made earlier that the stationary torque coefficient is independent of flow velocity seems correct.

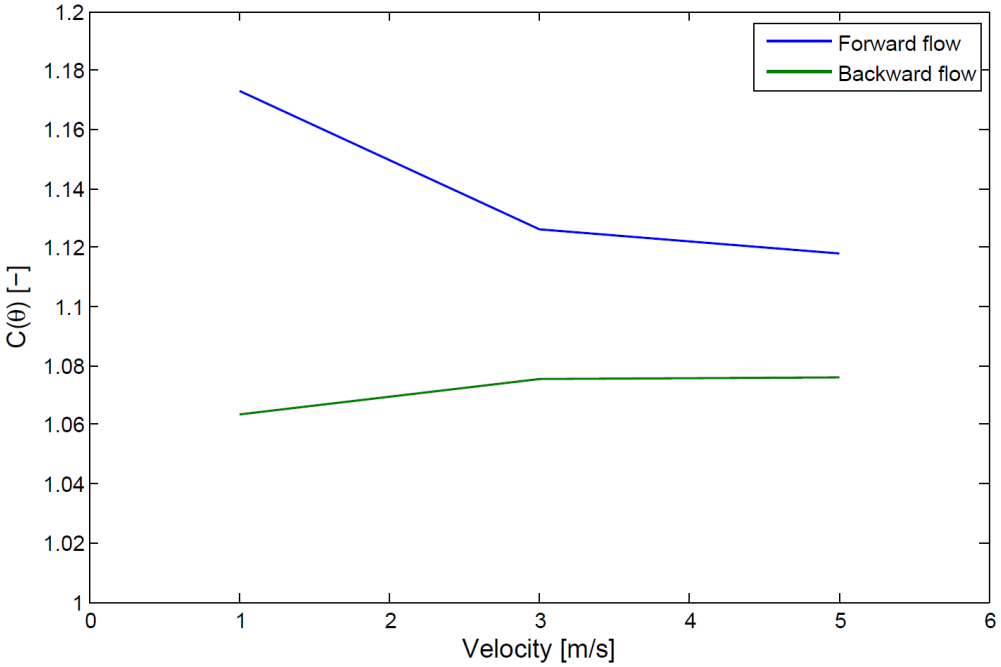

Figure 6. 11. Stationary torque coefficient for forward and backward flow as a function of the velocity.

6.1.4 Simplified way of describing the torque

A simplified way of calculating the hydrodynamic torque is used by the RELAP5 code seen in section 4.6.1. Here the torque is calculated solely by the pressure difference multiplied by the projected area (A_p=Acos(θ)) of the disc in the flow direction. The result of these types of calculations is displayed in Figure 6. 12, where the calculated torque is divided by the torque obtained from CFD simulations. Please observe that the pressure differences are also obtained from the CFD calculations. The pressure drop is calculated both over the valve and over the domain containing 0.5 meters of pipe both downstream and upstream of the valve. Figure 6. 12 shows that for small angles the approximations over-estimate the torque while it under-estimates for larger angles. For comparison the same calculations are performed where the projected area is substituted with the actual disc area. These calculations show more resemblance to the CFD simulations[3] even though the calculated torque is over all larger for both types of pressure drop.

These results can however not be directly compared to the RELAP5 calculations since that code uses an area function to calculate the pressure drop over the valve. The exact behavior of that area function is not investigated in this report and the presented results are more of a general comparison of equations.

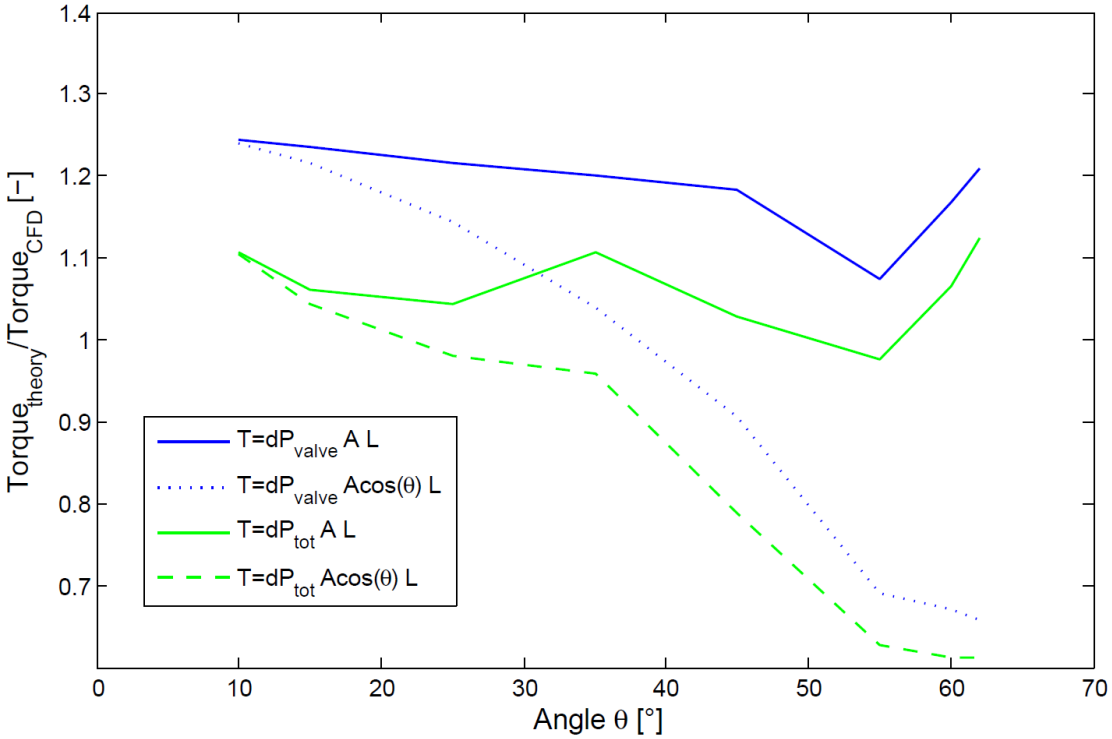

Figure 6. 12. Comparing four ways of approximating the torque with the torque from the CFD simulation.

6.1.5 Sensitivity analysis of CFD simulation

The CFD simulations have been tested regarding turbulence model and cell density.

Turbulence model

The dependence of turbulence model is investigated for a velocity of +3 m/s and plotted in Figure 6. 13. The difference between these two models is overall small, about 3% on average and with one outliner at 9%. The turbulence model that gives the largest torque is k-ω SST for all angles.

[3] Here the CFD simulations refer to the more exact description of the torque given in equation 3.60.

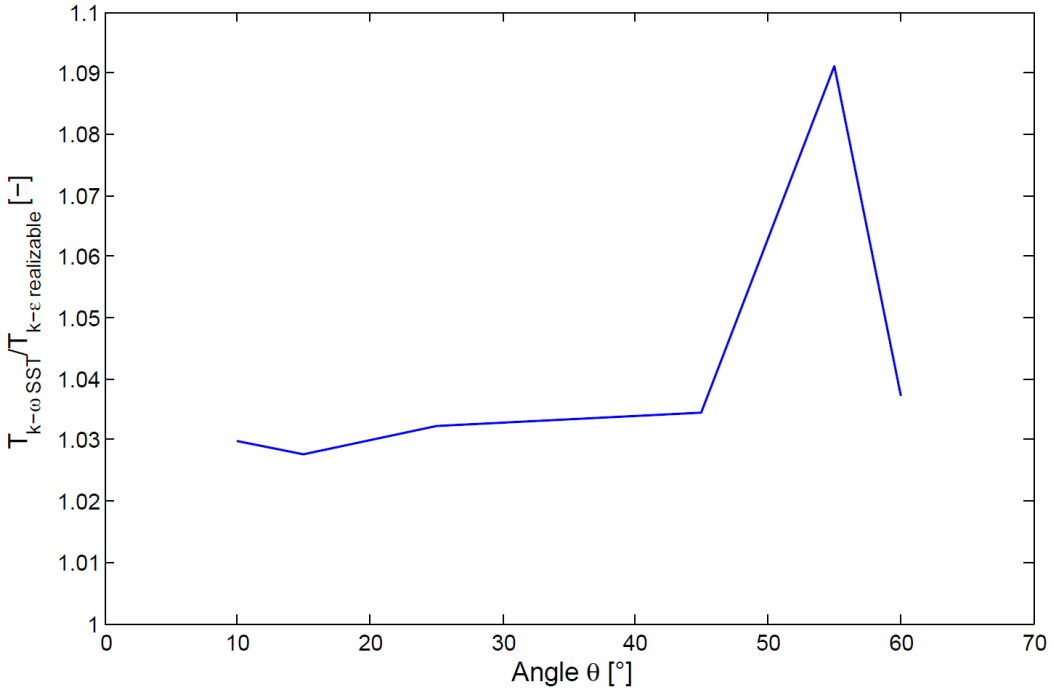

Figure 6. 13. Sensitivity analysis regarding turbulence model.

Cell density

A sensitivity analysis has also been made regarding the cell density for two different opening angles; 5 and 50 degrees. The mesh was in both cases refined by a factor of three from about 0.7 M to 2.1 M cells. The corresponding torques are given in Table 6. 1 for both the refined and the unrefined cases. The difference between the refined and unrefined cases with the smallest angle can be explained by the amount of cells passing the information in the computational domain. The number is much less in the case of a smaller angle and some information might get lost.

Table 6. 1. Data of the sensitivity analysis regarding cell density.

Angle	*Mesh type*	*Torque (Nm)*	*Difference (%)*
5°	Unrefined	796	
	Refined	867	+8.4
50°	Unrefined	26.3	
	Refined	26.2	-0.3

6.1.6 Comparing stationary torques from CFD-calculations to 1D models

The stationary torque of the three swing check valve models are plotted together with the stationary CFD simulation in Figure 6. 14. The inrvlv model over-predicts the torque quite a lot leading to a later start of the closure and as the flow reverses the larger negative torque will result in a quick closure. The DRAKO model with the area curve recommended by the developer of DRAKO (KAE) however shows rather good correlation with the CFD results. The calculated torque is slightly larger than that of the CFD simulation for the angle corresponding to fully open, resulting in an expected later start of the closure. The quasi-stationary model that is developed based on stationary CFD simulation shows good correlation, indicating that the model is implemented correct in the RELAP5 code.

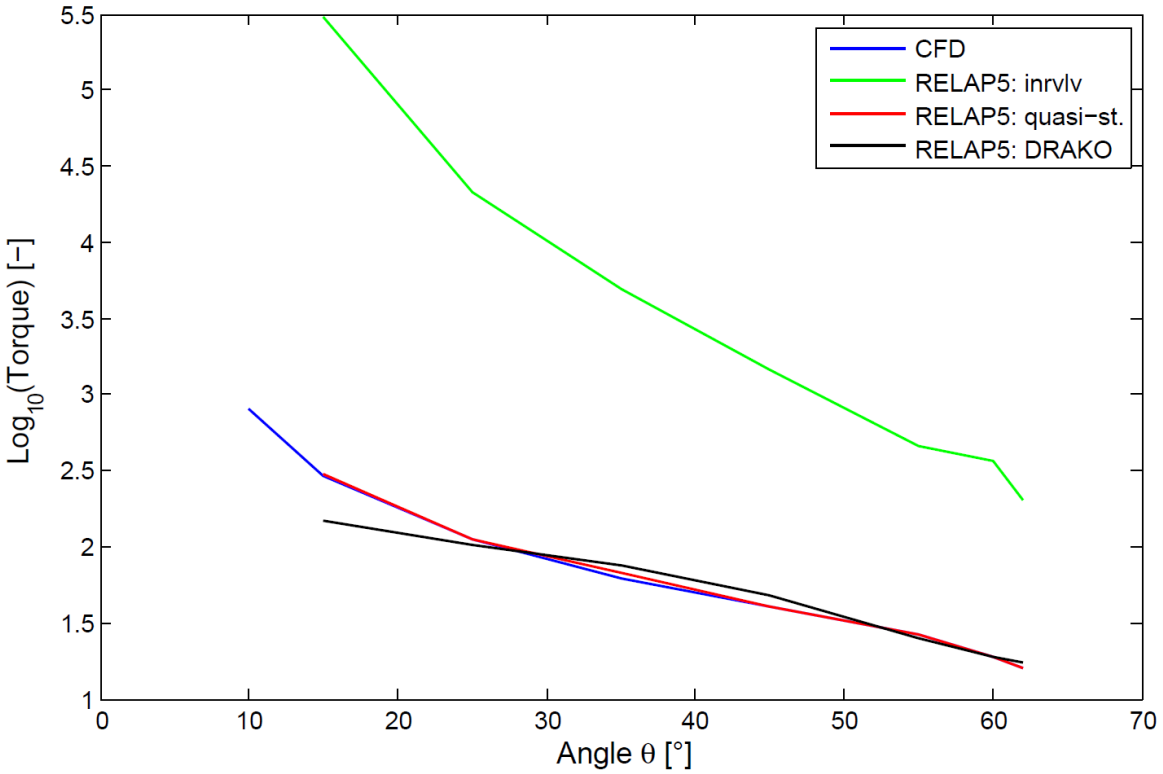

Figure 6. 14. The10- logarithm of the stationary torques from three swing check valve models together with the CFD simulation.

6.2 Transient results

The closing times for the check valve are presented as a plot of the different models along with the CFD result. Thereafter a sensitivity analysis regarding the CFD simulations are performed.

6.2.1 Comparing CFD with RELAP5 models

The most obvious and important result is that all RELAP5 models under-predicts the closing time compared to the CFD simulation as depicted in Figure 6. 15. The quasi-stationary model that showed good results for stationary flow simulations does not handle the rotational movement very well. The model predicts the start of the movement well but as the disc is accelerating towards closure the model differs more and more from the corresponding CFD run. The DRAKO model is the second to move the swing disc as expected from the stationary results in section 6.1.6. The overall behavior of the DRAKO model is similar to that of the quasi-stationary but tends to handle the dynamic behavior of the rotation and flow acceleration better. The inrvlv model was shown to over-predict the stationary torque and this result in a valve closure that starts much later than any other model. On the other hand as the valve begins to close, the closure process is the fastest.

These four different closing times given the same flow deceleration will then lead to four different reverse velocities. The CFD simulation is assumed to be the most correct since no experimental data is available, meaning that the reverse velocity and the corresponding pressure profile is under-estimated for all RELAP5 models.

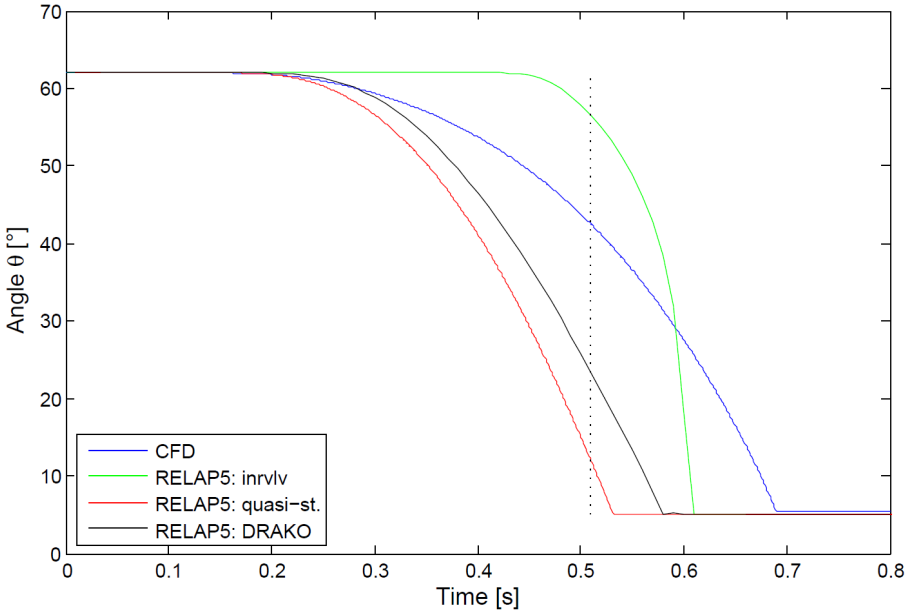

Figure 6. 15. The RELAP5 simulations are compared with the CFD run by analyzing the angle with time. The dashed line corresponds with the point where the flow reverses.

6.2.2 Expanding the quasi-stationary model

The effect of added mass and relative velocity in the quasi-stationary model is investigated in Figure 6. 16. By adding an added mass term to the simulation that is proportional to the angular acceleration the valve will close more slowly. This comes from the fact that as the valve is closing the angular velocity of the swing disc is increasing. Thus a larger angular acceleration gives a larger added mass which slows the movement of the disc. If the torque due to the flow is calculated using the relative velocity instead of the flow velocity the closure will be more slowly. Since the swing disc is moving in the opposite direction of the flow for most of the closure, the relative velocity will be greater than the flow velocity, resulting in a larger forward torque and later closure. This effect can also be found to be the greatest at the end where the angular velocity has its highest value. By using both the added mass and the relative velocity to describe the transient behavior of the swing check valve the result is closer to the CFD simulation but a complete description of the rotation is not achieved.

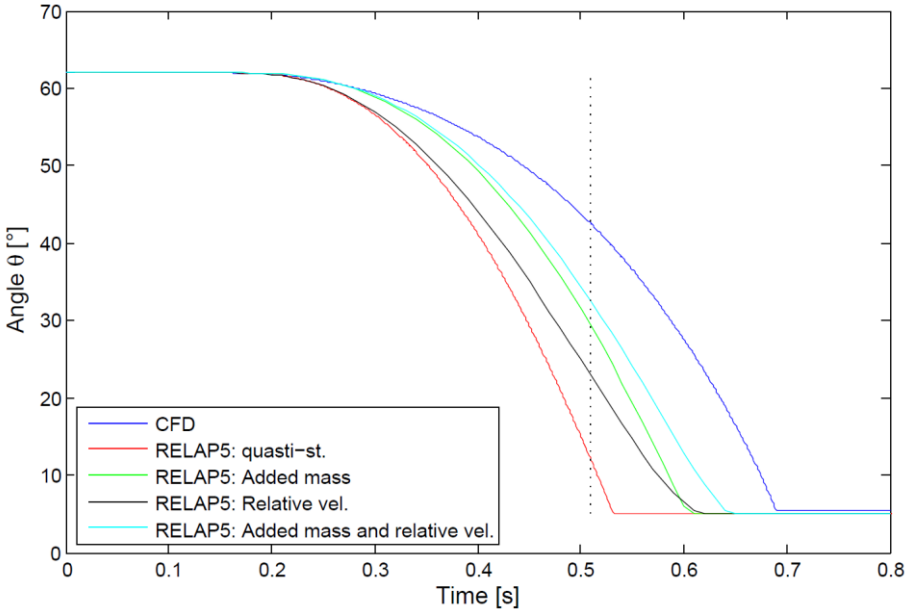

Figure 6. 16. Comparison of the CFD simulation with different RELAP5 models which are based on the quasi-stationary model.

6.2.3 Sensitivity analysis regarding the CFD calculations

A sensitivity analysis regarding cell density, turbulence model, time step and compressibility is presented in this section.

Cell density, effect of layers and serial vs. parallel solver

The sensitivity of cell density and turbulence model is displayed in Figure 6. 17. The solution can be regarded as independent of turbulence models, meaning that the closure process is well described by the mean properties of the flow. In addition the cell density is of small importance to the overall behavior of the flapper. This includes both the number of cells and the option to use layers. Thus the remeshing and smoothing option that is utilized for updating the mesh works well close to the flapper and without the use of layers. As concluded in section 6.1.5 the calculated torque is mesh sensitive at small angles but this behavior will not be noticed since the swing disc moves fast in that region and closure is imminent.

Two simulations have been made which compares the usage of serial or parallel processing. This comparison is of importance since parallel processing will shorten the computational time significantly but requires information to be passed between the nodes and the host. By using parallel processing the domain is divided into sub-domains which might cause some difference to the calculated toque compared to a serial run. This difference is insignificant and parallel processing is recommended.

The usage of layers might give more accurate results but as the swing disc move toward final closure the number of fluid cells between the layers and valve seat is decreasing to zero. Since the layers are not allowed to be remeshed the simulation will crash earlier than without layers. This is however not seen as a problem since complete closure is not simulated anyhow and the dynamic behavior of the transient is assumed to be caught.

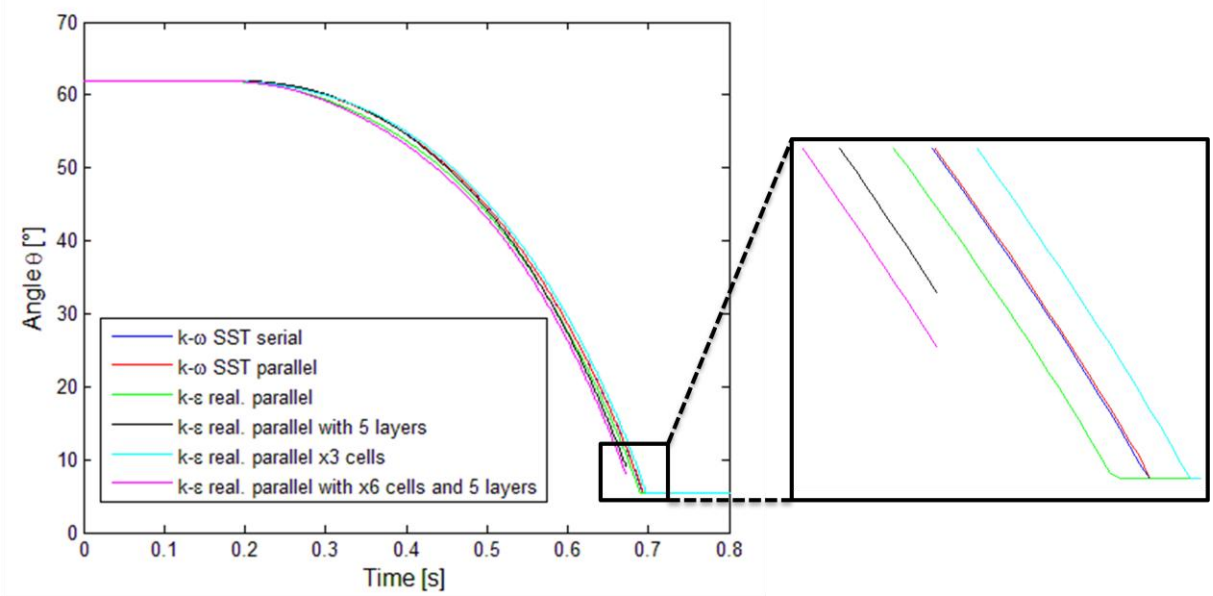

Figure 6. 17. Sensitivity analysis regarding cell density and turbulence models where the legend indicates; name, serial/parallel and other information.

Time step

The time step chosen will affect both the quality of the mesh undergoing update and the movement of the flapper. A smaller time step thus keeps the quality high and the total distance between time steps small. However a small time step will also increase the computational time. As can be seen in Figure 6. 18 the effect of time step on the final solution is small. Also a smaller time discretization results in a slightly longer time for closure. Note that a longer time step gives a larger displacement between time steps and this may result in mesh failure at the end where the cells are highly compressed.

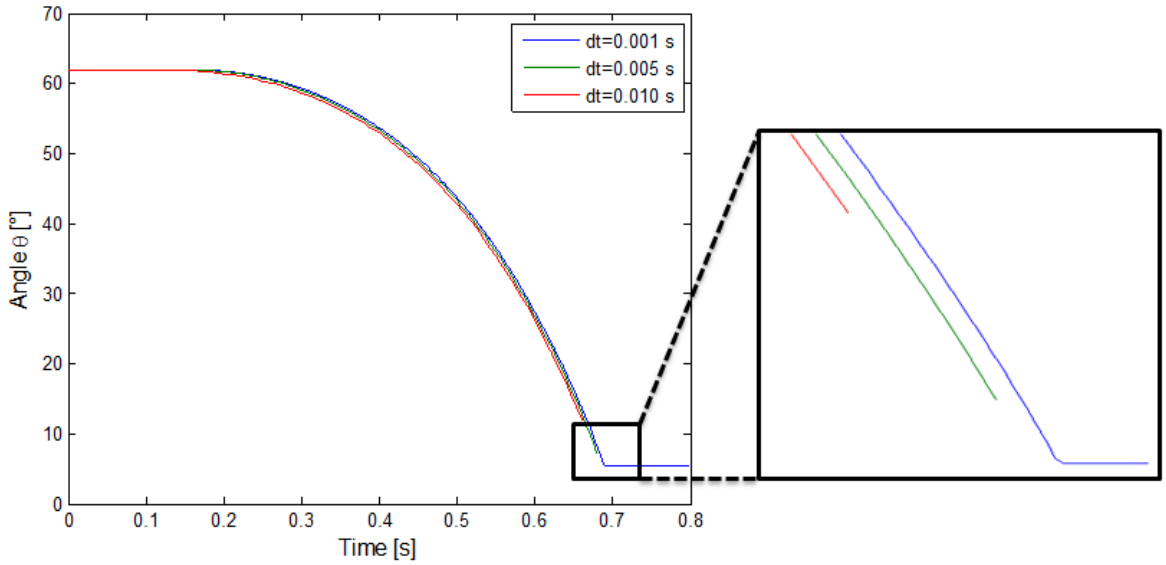

Figure 6. 18. Sensitivity analysis regarding time step.

Compressibility

The fluid is regarded as incompressible water with a density of 998.2 kg/m^3 for all CFD simulations. This simplification is investigated in Figure 6. 19 below where two plots are displayed, one for the incompressible fluid and one using the Tait-equation for compressible fluid. The difference between the two is very small but a slight variation can be seen. The calculation using the incompressible fluid has a lower torque due to the impinging flow and thus tends to close earlier.

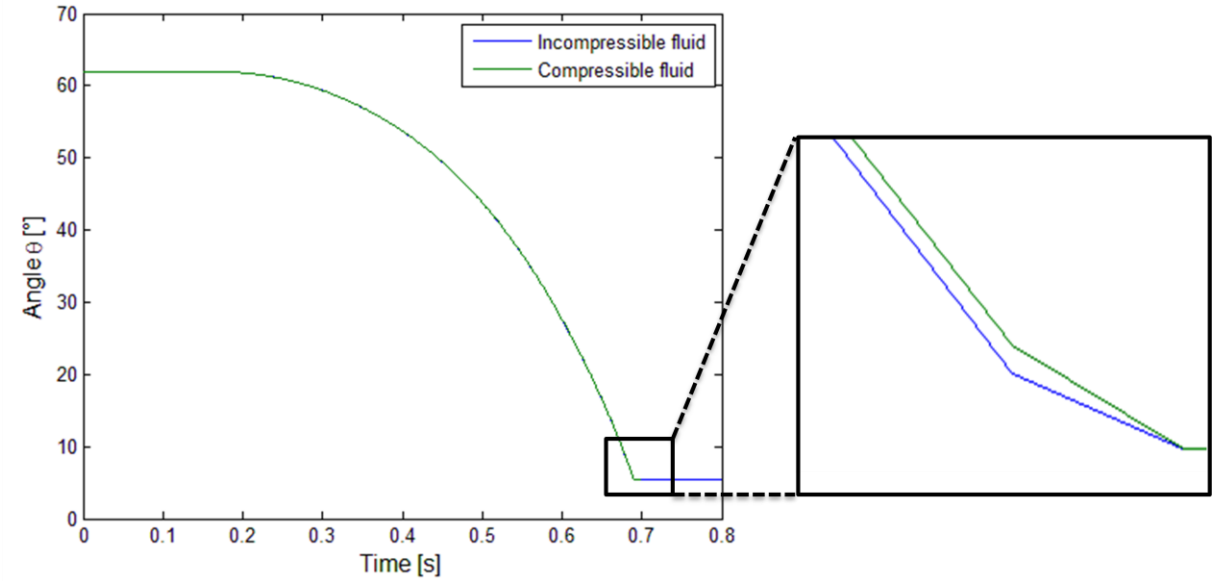

Figure 6. 19. The angular time dependence of an incompressible and compressible fluid.

6.3 Velocity variation

As depicted in Figure 6. 20 (left) the flow deceleration affect the time for the start of the closure as well as the total time. By increasing the deceleration the valve will close faster and also begin its acceleration at a shorter time. The corresponding reverse velocity for the three investigated flow decelerations is displayed in Figure 6. 20 (right). This figure shows that with a faster deceleration the reverse flow will increase. On the contrary to minimize the reverse velocity and by doing so also minimizing the water hammer the flow deceleration should be small.

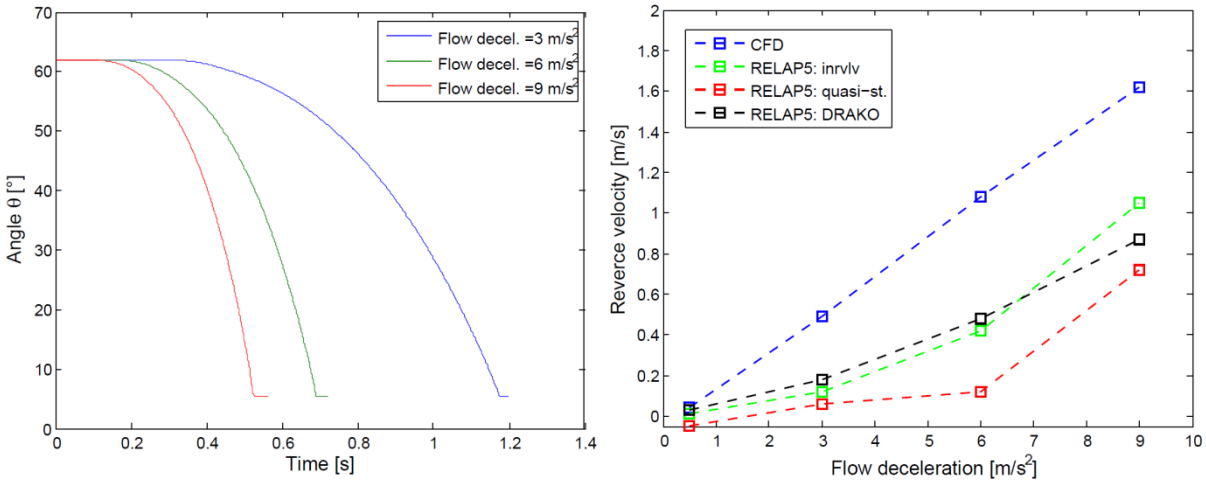

Figure 6. 20. CFD simulations giving the angular change with time for three different flow decelerations (left) and maximum reverse velocity for these decelerations (right).

Figures 6.21 through 6.23 indicate that all check valve models under-estimate the closing time for flow decelerations of 0.5 m/s^2, 3 m/s^2 and 9 m/s^2 compared to the CFD simulation. The trend in these three figures is that the different swing check vale models are getting closer to the CFD simulation as the flow approaches a steady state condition.

The DRAKO model together with the quasi-stationary model seems to behave strange for a flow deceleration of 3 m/s^2. This behavior is enlarged for the even slower deceleration of 0.5 m/s^2 where also the inrvlv model oscillates slightly in the beginning. The code describing the movement is an exact copy of the other decelerations except for the flow profile itself and thus the behavior probably lies within the check valve models, where there seems to lack a dampening term. The quasi-stationary model is expected to behave more correctly as the flow approaches a steady state. This effect can also be seen by following the figures 6.21 through 6.24. Even tough the angle oscillates quite a lot with the slowest deceleration the result is that the quasi-stationary model follows the CFD simulation rather well. Note that the time scales in the figures presented below are different from another.

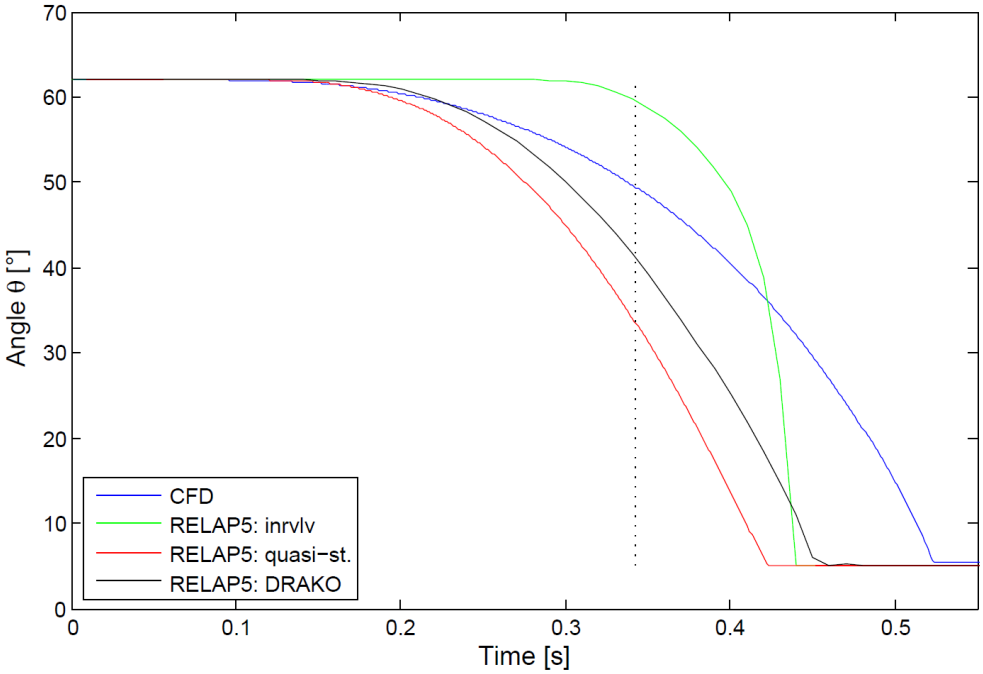

Figure 6. 21. The angular change as a function of time for a flow deceleration of 9 m/s^2. The dashed line corresponds with the point where the flow reverses.

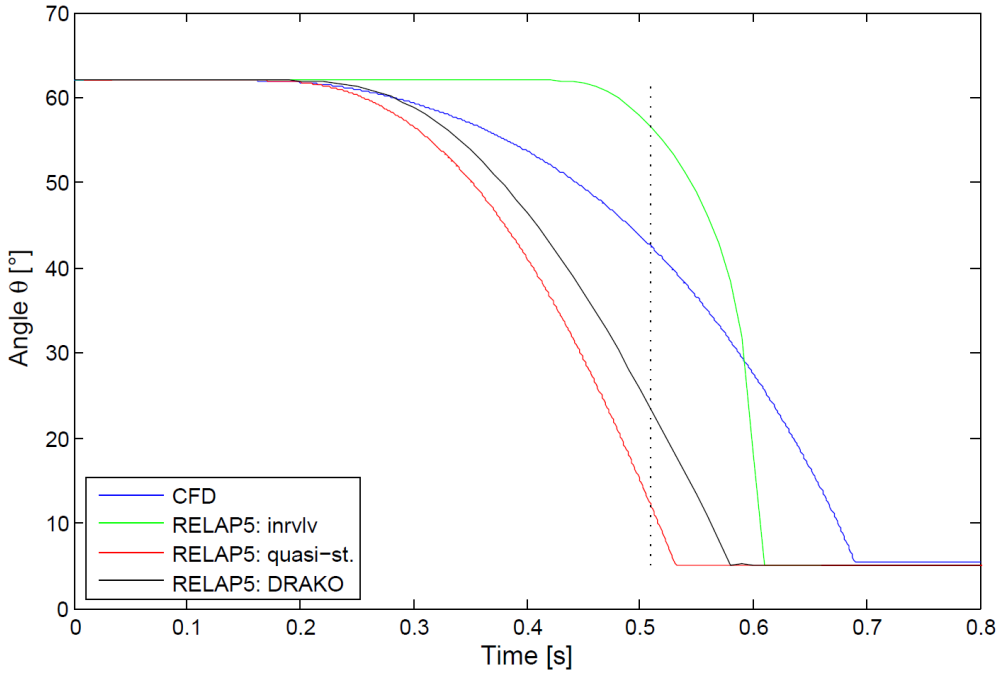

Figure 6. 22. The angular change as a function of time for a flow deceleration of 6 m/s^2. The dashed line corresponds with the point where the flow reverses.

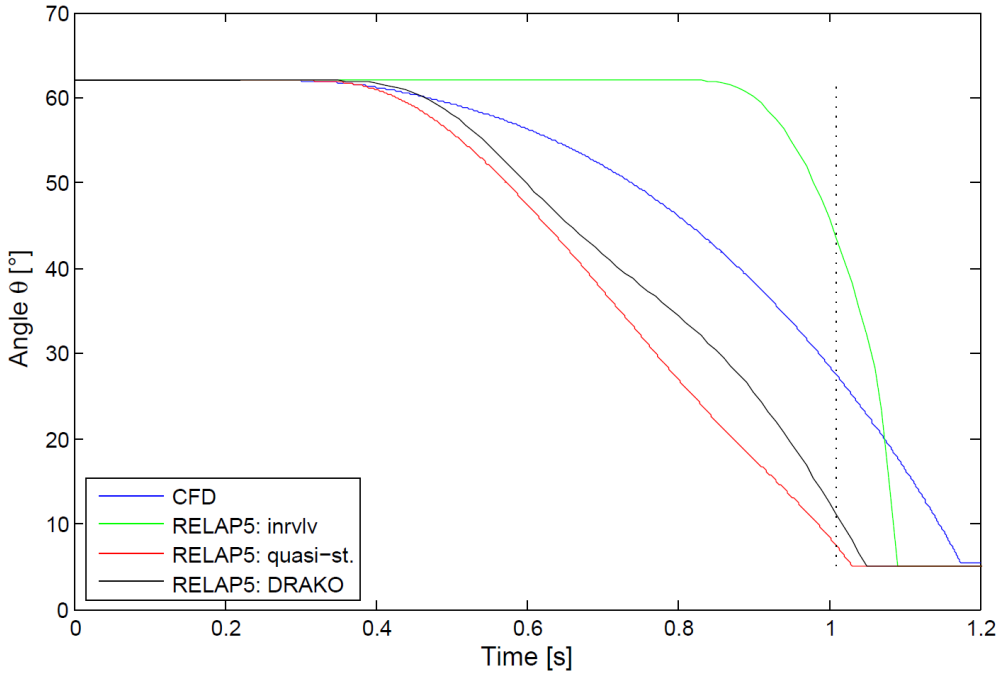

Figure 6. 23. The angular change as a function of time for a flow deceleration of 3 m/s^2. The dashed line corresponds with the point where the flow reverses.

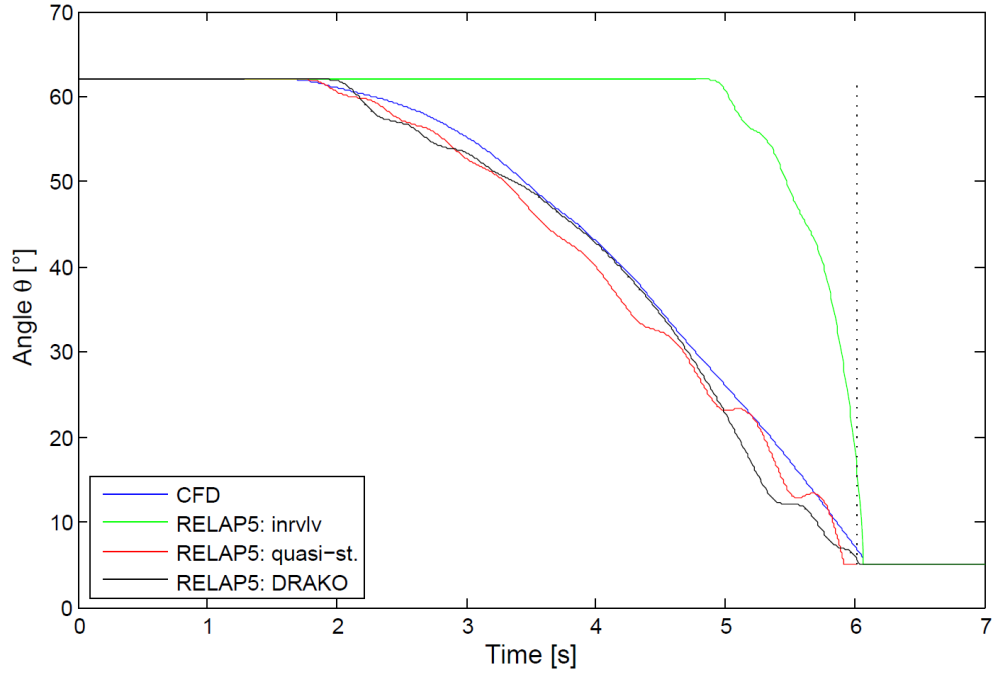

Figure 6. 24. The angular change as a function of time for a flow deceleration of 0.5 m/s^2. The dashed line corresponds with the point where the flow reverses.

6.4 Effect of geometry scaling

In order to investigate the behavior of different check valve sizes the original valve geometry has both been double and halved in size. These new geometries are denoted DN100 and DN400. In case of reducing the size as can be seen in Figure 6. 25 the behavior is slightly different from the DN200 valve. The check valve models all behave the same but the closure itself starts about 0.1 s later. On the other hand the closing process is faster with the smaller geometry, about 0.16 s compared to the DN200 valve.

Regarding the larger valve denoted DN400 and viewed in Figure 6. 27 the figures cannot be compared exactly since another initial velocity was required for this valve due to the larger mass. The initial velocity was in this case increased from 3 m/s to 4 m/s but still the start of the closure is only delayed by 0.05 s compared to the DN200 and 3 m/s. The flow deceleration is however the same and as the larger valve begins to move the closing process is slower than the other sizes, about 0.2 s compared to the DN200 valve and 0.36 s compared to the DN100 valve. Please observe the different time scales on the three figures below.

The different parameters that are change with the geometry are listed in the table below.

Table 6. 2. Summary of the main parameters that are changed for the different valve sizes.

Quantity	***DN100***	***DN200***	***DN400***
Diameter of the disc	0.112 m	0.224 m	0.448 m
Distance to center of disc	0.077 m	0.155 m	0.31 m
Distance to center of gravity	0.076 m	0.152 m	0.303 m
Submerged weight of the flapper	0.77 kg	6.15 kg	49.18
Rotational inertia of the flapper	0.0059 kgm^2	0.1875 kgm^2	6.0 kgm^2

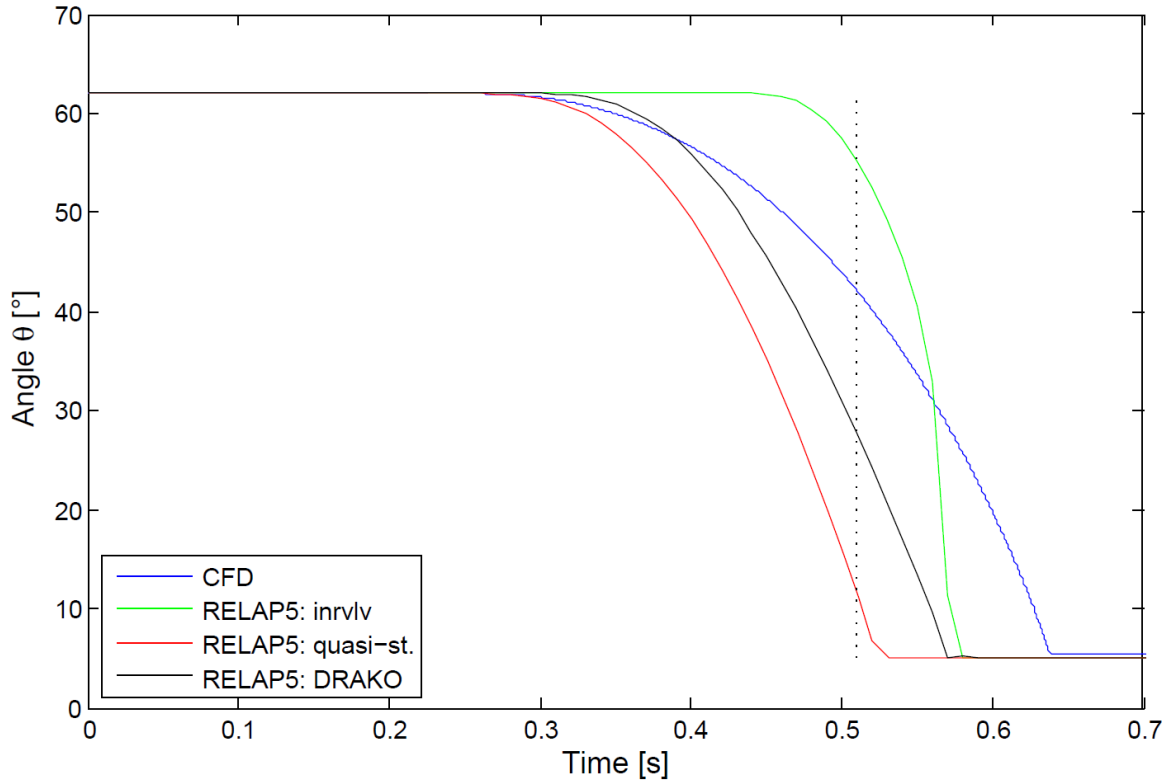

Figure 6. 25. A DN100 valve simulated with a flow deceleration of 6 m/s^2. The dashed line corresponds with the point where the flow reverses.

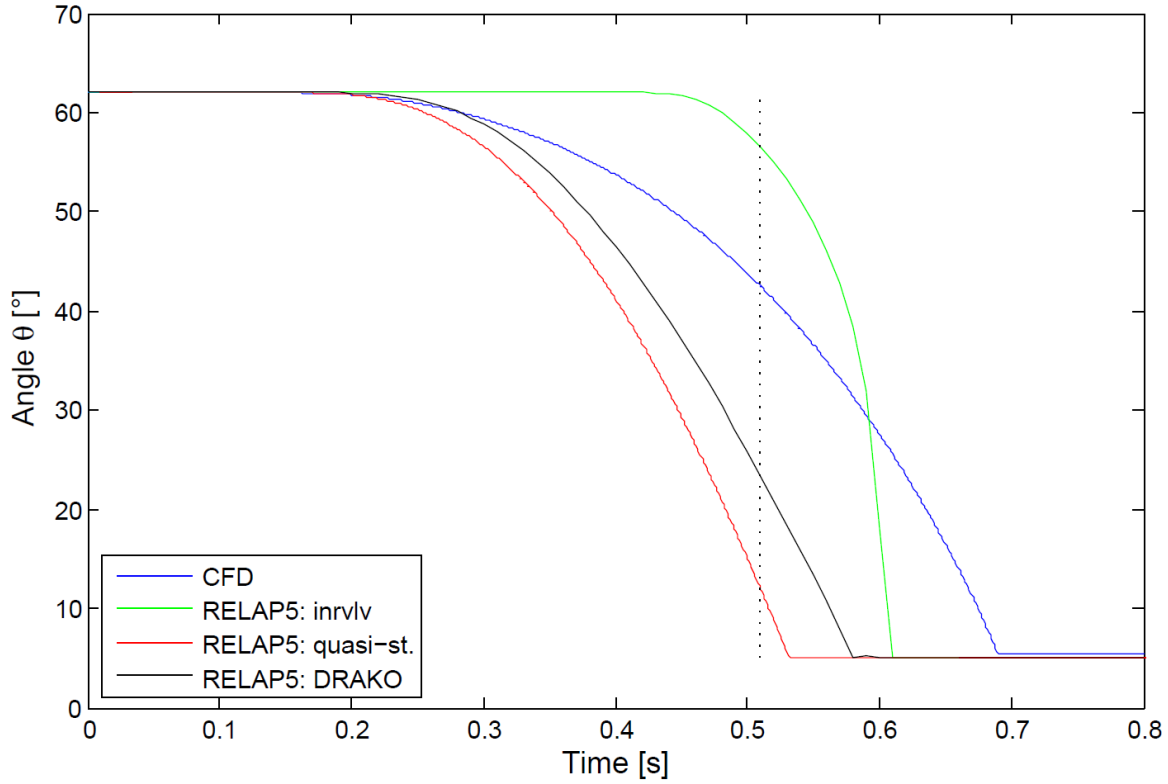

Figure 6. 26. A DN200 valve simulated with a flow deceleration of 6 m/s^2. The dashed line corresponds with the point where the flow reverses.

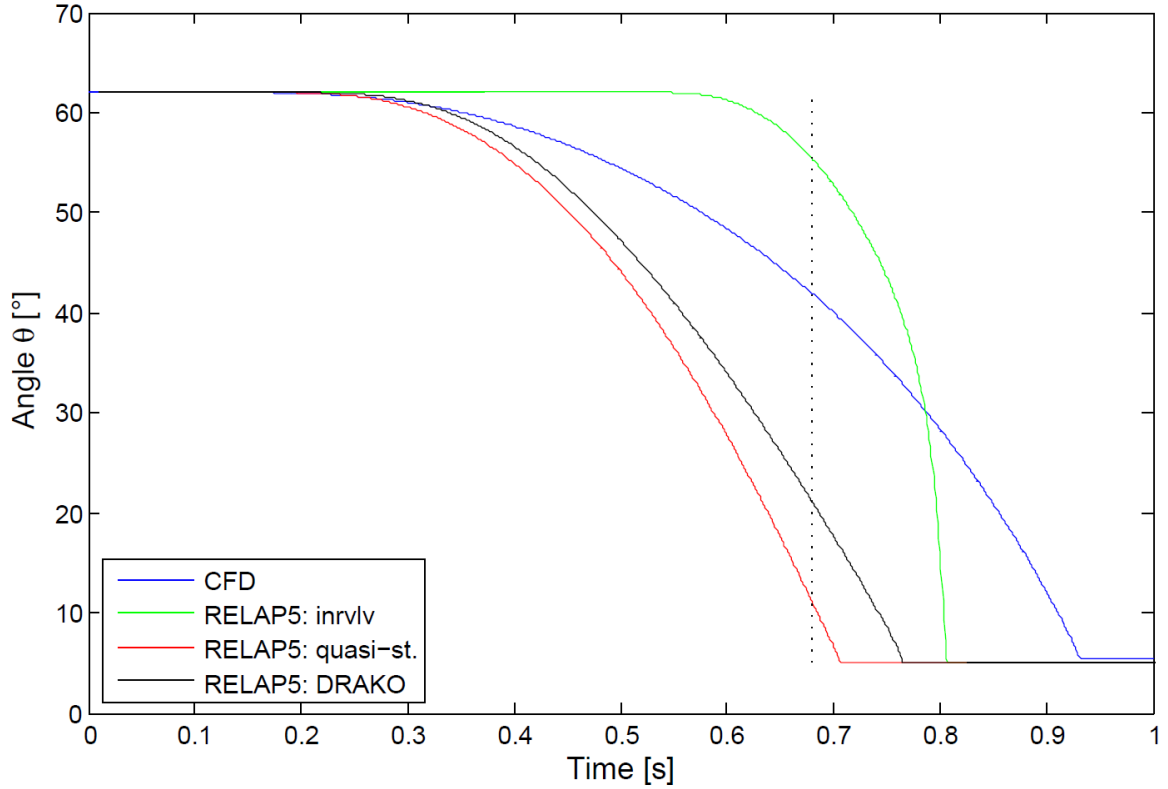

Figure 6. 27. A DN400 valve simulated with a flow deceleration of 6 m/s^2. The dashed line corresponds with the point where the flow reverses[4].

[4] Observe that the dashed line is displaced compared to the previous figure due to a larger initial velocity.

7 Discussion

7.1 Stationary simulations

The stationary calculations is performed to investigate the torque for a stationary valve subjected to a steady flow and to compare this to the values calculated by the one-dimensional check valve models. The DRAKO model with the area table recommended by the manufacturer of DRAKO (KAE) gives reasonable values of the stationary torque. However the stationary torque for the RELAP5 inertial swing check valve model is very high compared to the result from the CFD-calculations.

Also, describing the torque with using a stationary torque coefficient seems to be a good idea. The torque coefficient is nearly constant despite varying flow rate. Different approximations of the torque based on the pressure loss over the valve are also investigated. The inertial swing check valve model approximates the torque as the pressure loss over the valve times the projected area of a disk hinges at the top end. This approach seems to overestimate the torque at low opening angles and underestimate them at high opening angles. Another way of approximating the torque is to, instead of a projected area, using the full disk area. With this assumption the torque is over-estimated by a couple of percent for all angles compared to the more detailed CFD calculation, and thus this simplification seems more correct. Using the disc area instead of the projected area means that the torque will be larger as the opening angle increases. The RELAP5 inertial swing check valve model already over-predicts the torque compared to the CFD calculation and the best way to modify that model based on stationary results are probably to instead change the area function calculating the pressure drop over the valve.

Even though the stationary torque coefficient is regarded as independent of flow velocity, the direction of the flow is shown to have a slight impact. The forward flow results in larger value and the reason lies within the geometry. The valve is unsymmetrical in the flow direction, where the flapper is located closer to the upstream flow. Also the transition between the smaller pipe and the larger valve housing is smoother for the backward flow, creating less of a jet. Since there is an area change as the flow enters the valve the velocity will change given a constant density. The continuity equation states that a larger area results in a lower velocity since the mass flux is constant. In addition the flapper itself looks different to the flow depending on the direction and overall these phenomena will cause different stagnation zones as well as vortexes to form and the torque on the flapper will be different.

7.2 Transient simulations

Even though the inrvlv model and the DRAKO model show great resemblance in the torque balance equation the dynamic behavior is very different. Both models include a torque corresponding to the pressure difference over the valve. In addition the inrvlv model uses a projected area which is smaller than the area used in the DRAKO model. This means that the torque due to the pressure difference should be larger for the DRAKO model compared to the inrvlv model. On top of this the DRAKO model also includes a term that describes the diversion of the flow. If it were not for anything else the DRAKO model should accordingly close later than the inrvlv model. Since this is not the case but instead the opposite, the explanation lies somewhere else, namely the area table describing the flow resistance and by doing so also the pressure drop. The DRAKO model uses an area function that is much nicer to the flow (lower pressure drop), resulting in a smaller pressure drop and thus a smaller torque. The area function of the inrvlv model causes the pressure drop to be large enough to keep the valve open for a longer time. Not until the flow is about to reverse does the swing

disc start to move and then the pressure drop is over-estimates in the backward direction causing the valve to close fast.

The fact that the quasi-stationary model predicts the start of the valve closure is expected since it is based on stationary CFD simulations and the disc is stationary until this event. As the swing disc starts to move however the model does not account for the additional resistance in both the rotation of the flapper and the acceleration of the adjacent fluid. The dependence of these two phenomena is loosely investigated in the sense that both relative velocity and/or added mass are added to the model. To simply use the relative velocity between the fluid and the moving disc is quite unsuccessful and even show unphysical behavior at the end of the closure where the angular acceleration is slowed down instead of increased even further. The rotational part should therefore be modeled in an alternative fashion. This could be a rotational torque coefficient which only depends on the angular velocity of the disc, similar to the stationary torque coefficient. The impact of added mass to slow the rotation down is welcomed but the term is difficult to predict. During the simulation the added mass was approximated with a sphere since this was recommended in the literature. To model the added mass term in this way means that as the disc is accelerating toward complete closure the term is increased. This seems correct since a faster accelerating of the disc will lead to a larger resistance since more fluid is affected. For a complete description however the velocity change of the fluid itself should also be accounted for. The time derivative of the flow is set by the user but the hard part is to model the acceleration over the valve.

7.3 Sensitivity analysis

The sensitivity analysis regarding cell density, turbulence model and time step shows that the modeling of this type of check valve is only loosely affected by these parameters. The time step can be increased to at least 0.01 s and still obtain a satisfying solution except at the end of the closure where the swing disc move too fast and the displacement per time step is too large, resulting in a crash due to mesh problems. It is however no problem at all to alter the time step during the transient using an UDF, where the time step as a suggestion is based either on the position of the valve or on the relative velocity.

The cell density of the solution can be held relative coarse and by doing so still keep the solution accurate and the computational time short. It is also recommended that at least a few layers which are not remeshed during the transient are added on top of the swing disc. This will cause problems as the valve is about to fully close but since only the transient behavior is of interest the simulation is allowed to crash at the end. When using the method with layers it is also important to mark these layers as interior and control the movement of the rotation based on the pressure on the disc, not on the layers.

The simplification of assuming that the fluid is incompressible is found to be correct in these isothermal simulations. As described earlier the formation of bubbles is possible as the pressure is decreased fast at the end of the closure but this possibility is not taken into account and the flow is seen as incompressible one phase flow during the entire simulation.

7.4 Velocity variation

The torque representing the flow is proportional to the velocity squared. Thus if the velocity is decreased quicker the torque acting in the opening direction is reduced quicker. This causes the check valve to start the closure at a shorter time.

The fact that a smaller flow deceleration is better for reverse flow considerations can be explained by the resistance in the rotation of the swing disc. A fast deceleration of the flow causes the valve to close more quickly, but this time is not compensated by the fact that the velocity is decelerating in a quicker pace. The resistance within the system is thus too large to fully respond to the changes in the flow.

7.5 Scaling

The fact that the DN100 check valve stays open for a longer time can be explained by the two torques acting on the stationary disc, namely those due to pressure difference and weight. The torque coming from the impinging fluid is proportional to L^3 and the torque due to weight is proportional L^4, where L is the length unit. Thus by reducing the length by half the positive torque from the flow is reduced to 1/8 and the negative torque from the weight is reduced to 1/16. This generates a net torque in the positive direction compared to the original geometry that keeps the valve fully open for a longer time. As the swing disc begins to move the rotational inertia comes in play and this term is proportional to L^5. This means that the rotational inertia is reduced to 1/32, resulting in that the resistance to the rotation is decreased and the closing process can be faster. The same reasoning can be applied to the larger valve but the result will be the opposite. The forward torque is increased by 8 while the negative torque due to the weight is increased by 16, generating a net negative torque and resulting in an earlier start of the closure. The closing process itself is slower due to an increase of the rotational inertia by a factor of 32 and thus the resistance to the movement is increased quite a lot.

7.6 Comparing CFD with RELAP5

Perhaps the most interesting part of this Master's thesis is the comparison between the different RELAP5 models and the CFD simulation. This comparison does not only include the closing time and corresponding reverse velocities but also the methodology of the two types of simulation. A CFD simulation requires first of all geometry of the check valve, and a generated mesh. This procedure may be time consuming depending whether or not a CAD drawing is available and the level of detail required. The simulation itself is shown not to be too dependent of the solver settings made and the time between a complete mesh and start of a transient simulation should therefore be short. This however requires that the user is familiar with UDF writing or that a working UDF is already provided. The time required for the simulation then depends on the number of CPU's available and the flow transient, but can be measured in hours. The CFD results can be visualized in many ways; a short film of the pressure variation along the piping system or a plot showing the angle of the disc is no problem to obtain. The largest downside of the CFD simulation is the trouble of simulating complete valve closure where the time is unknown. This may lead to the loss of important effects happening at the absolute end.

A RELAP5 simulation is very different to a CFD simulation in many ways. No 3D-CAD drawing is required and instead only the important length parameters is nedded. The RELAP5 code does not require any advanced settings and the simulation is up and running in a short time. Note that this is the case for the inrvlv model, but for the implementation of more advanced models such as the DRAKO and quasi-stationary models some programming is

required. The procedure is simpler than the UDF writing but does require some experience. The time required for the simulation itself is very short and can be measured in seconds even with a time step of 0.0001 and one CPU. A table of water properties is required as input to the RELAP5 solver and the code thus have the possibility to account for the formation of vapor. In addition there are no problems with simulating the entire closure process since there is no mesh that can crash. The largest downsides of these 1-D simulations are the lack of detail and information which leads to a wrongly calculated reverse velocity and corresponding pressure profile in the system.

8 Conclusions

This report has shown that the swing check valve models underestimates the closing time of the investigated check valve when compared to three-dimensional CFD simulations. On the basis that the CFD simulations provide a more accurate result, the working engineers are introduced to a problem. The reverse flow and corresponding pipe forces will then be under-estimated for all the valve dimensions and flow transient that are investigated in this Master's thesis. A structural analysis that uses these results may then under-estimate the stresses acting within the piping system and unless conservative calculations are made unsuspected failure is possible.

Three-dimensional CFD simulations for all kinds of system can nowadays be performed without problem and spending too much time. CFD is thus an excellent tool for detail studies of complex flow situation where moving parts are part of the problem. In the past the CFD calculations were limited to smaller systems due to the slower computational power but that problem is now gone. Larger systems involving hundreds of meters of pipe and different components can now be simulated within a reasonable amount of time. For very large system transients involving many different components the one-dimensional codes will still have a future. These codes are fast but the results are not as accurate. In this specific area the CFD methodology is not yet ready to compete at full strength.

In order to make the CFD calculation complete further work should be made regarding the complete closure of the check valve. Note that only FLUENT v12.1 has been tested to achieve this process but there are many other both free and commercial software capable of simulating a valve closure. Since the complete closure is not simulated the pressure rise and water hammer that is associated with the closure of a swing check valve is neglected and some important properties are lost.

Bibliography

Andersson B [et al.] Computational Fluid Dynamics [Book]. - Gothenburg : Bengt Andersson, 2010. - Vol. 6.

ANSYS FLUENT v12.1 Documentation. - Southpointe : Software guide -bundled with ANSYS FLUENT v12.1, Accessed 2011-03-10.

Boyd J.N. and Raychowdhury P.N. Parallel Axis Theorem. - Richmond : -, 1985. - Vol. 23.

Brennen C.E. A Review of Added Mass and Fluid Inertial Forces. - Port Hueneme : Naval Civil Engineering Laboratory, 1982.

Cummings K [et al.] Understanding Physics [Book]. - NJ : John Wiley & Sons, 2004.

Information Systems Laboratories, Inc RELAP5/MOD3.3 CODE MANUAL. - Rockville, Maryland : Information Systems Laboratories, Inc., 2003.

Janna W.S. Introduction to Fluid Mechanics [Book]. - Boca Raton : Taylor & Francis, 2010.

KAE DRAKO v3.22 Users manual. - Bubenreuth : KAE, 2005.

Li Yuan-Hui Equation of State of Water and Sea Water [Article] // Journal of Geophysical Research. - 1967. - 10 : Vol. 72.

Lim Ho-Gon, Park Jin-Hee and Jang Seung-Cheol Development of a swing check valve model for low velocity pipe flow prediction [Article] // Nuclear Engineering and Design. - 2006. - 236.

Liou Jim C.P and Gouhua Li Swing Check Valve Characterization and Modeling During Transients [Article] // Journal of Fluids Engineering . - 2003. - 6 : Vol. 125.

McElhaney K.L. An analysis of check valve performance characteristic based on valve design [Article] // Nuclear Engineering and Design. - 2000. - 1-2 : Vol. 197.

Menter F.R. Two-Equation Eddy-Viscosity Turbulence Models for Engineering Applications [Article] // AIAA Journal. - Moffett Field : 1994. - 8 : Vol. 32.

Panton R.L. Fluid Dynamics, Equilibrium. - : Encyclopedia of Applied Physics, 2003.

Rahmeyer W Dynamic Flow Testing of Check Valves [Conference] // Nuclear Industry Check Valve Group. - 1996.

Rahmeyer W Sizing swing check valves for satbility and minimum velocity limits [Journal]. - Milwaukee : Journal of Pressure Vessel Technology, 1993. - Vol. 115.

Thorley A.R.D Check Valve Behavior Under Transient Flow Conditions: A State-of-the-Art Review [Article] // Journal of Fluids Engineering. - June 1989. - 2 : Vol. 111.

Thorley A.R.D. Fluid transients in pipeline systems : a guide to the control and suppression of fluid transients in liquids in closed conduits [Book]. - London : Professional Engineering Publishing, 2004.

Val-Matic Valve and Manufacturing Corp Dynamic Characteristics of Check valves. - Elmhurst : Val-Matic Valve and Manufacturing Corp, 2003.

Welty J.R. [et al.] Fundamentals of Momentum, Heat, and Mass Transfer [Book]. - NJ : John Wiley & Sons, 2001.

Wilcox D.C. Turbulence Modeling for CFD [Book]. - La Canada : DCW Industries, Inc, 2006.

Zappe R.W. and Smith P Valve selection handbook: engineering fundamentals for selecting the right valve design for every industrial flow application [Book]. - Amsterdam; Boston : Elsevier Gulf Professional Pub., 2004.

Appendix A: UDFs used to control the motion of the swing check valve

There are three different UDFs presented below that all need to be included in the CFD solver FLUTENT v12.1 in order to get the correct movement. The first one, called torque_calculation is used to calculate the torque to due pressure on the flapper in the different nodes and must be hooked in the solver. The UDF called move_flapper uses the torque from the previously described UDF along with the torque due to weight to calculate the angular velocity and by doing so move the flapper. There are also additional commands in this function which are used to print the calculated data to a txt-file. The last UDF, called inlet_velocity is used to define the inlet velocity profile as a function of time.

```
#include "udf.h"
#include <mem.h>

static real omega_calc = 0.0;
static real theta=1.082104136;
/*extern real omega_out=0.0; */
real torque_p;

DEFINE_ADJUST(torque_calculation,domain)
{
/* Variables used by serial, host, node versions */
 int surface_thread_id=0;
 real total_area=0.0;
torque_p=0.0;


/* "Parallelized" Sections */
#if !RP_HOST   /* Compile this section for computing processes only (serial
                  and node)  since these variables are not available
                  on the host */
 Thread* thread;
 face_t face;
 real area[ND_ND];
 real NV_VEC(A);
 real w[ND_ND];
#endif /* !RP_HOST */


/* Get the value of the thread ID from a user-defined Scheme variable */
#if !RP_NODE /* SERIAL or HOST */
 surface_thread_id = 5;
 /*Message("\nCalculating on Thread # %d\n",surface_thread_id);*/
#endif /* !RP_NODE */

 /*  To set up this user Scheme variable in cortex type */
 /* (rp-var-define 'pres_av/thread-id 2 'integer #f) */
 /* After set up you can change it to another thread's ID using : */
 /* (rpsetvar 'pres_av/thread-id 7) */

 /* Send the ID value to all the nodes */
 host_to_node_int_1(surface_thread_id); /* Does nothing in serial */
```

```
#if RP_NODE
 /*Message("\nNode %d is calculating on thread # %d\n",myid,
          surface_thread_id);*/
#endif /* RP_NODE */

#if !RP_HOST  /* SERIAL or NODE */
 /* thread is only used on compute processes */
 thread = Lookup_Thread(domain,surface_thread_id);

begin_f_loop(face,thread)

/* If this is the node to which face "officially" belongs,*/
/* get the area vector and pressure and increment         */
/* the total area and total force values for this node    */
  if (PRINCIPAL_FACE_P(face,thread)) /* Always TRUE in serial version */
  {
   F_AREA(area,face,thread);
   total_area += NV_MAG(area);

      F_AREA(A,face,thread);
      F_CENTROID(w,face,thread);

                torque_p += F_P(face,thread)*NVD_DOT(A,-w[1],w[0],0);
  }
 end_f_loop(face,thread)

/* Message("Total Area Before Summing %f\n",total_area);
 Message("Total Torque Before Summing %f\n",torque_p); */


# if RP_NODE /* Perform node synchronized actions here
                Does nothing in Serial */
  total_area = PRF_GRSUM1(total_area);
  torque_p = PRF_GRSUM1(torque_p);

# endif /* RP_NODE */

#endif /* !RP_HOST */

/* Pass the node's total area and pressure to the Host for averaging  */
 node_to_host_real_2(total_area,torque_p); /* Does nothing in SERIAL */

#if !RP_NODE /* SERIAL or HOST */
Message("Total Area After Summing: %f (m2)\n",total_area);
Message("Total Torque After Summing %f (Nm)\n",torque_p);

#endif /* !RP_NODE */
}
```

```
DEFINE_CG_MOTION(move_flapper,dt,vel,omega,time,dtime)
{
 NV_S(omega, =, 0.0);
 node_to_host_real_1(torque_p);

  real torque, torque_w, domega, omega_prev, omega_dot, omega_out;
  const real inertia = 0.1875;

/* Compute the torque due to pressure P and weight W */
/*-------------------------------------------------------------------------*/
torque_w= -9.1469 * sin(theta); /* -g*L*W*sin(theta)  */
torque= torque_p + torque_w;
domega = dtime * torque / inertia;
omega_dot= torque / inertia;

/* Calculate the angular velocity */
/*-------------------------------------------------------------------------*/
omega_prev = omega_calc;
omega_calc = omega_calc + domega;
omega_out = omega_calc;

/* Calculate the angle theta  (Taylor expansion) */
/*-------------------------------------------------------------------------*/
theta=theta + 0.5*dtime*(omega_prev+omega_calc);
 #if !RP_NODE
Message ("\ntorque_p = %f,", torque_p);
Message ("\ntorque_W = %f,", torque_w);
Message ("\ntorque = %f,", torque);
Message ("\ndomega = %f,", domega);
Message ("\nomega_calc: %f\n", omega_calc);
Message ("\n---------------------------------------");
Message ("\ntheta: %f\n", theta);
 #endif

/* Resitrictions,  make it stop at the end points*/
/*-------------------------------------------------------------------------*/

if (theta < 0.0872664626*1.1) /* Corresponds to 5.5 degrees */
{
           omega_out=0;
           omega_calc=0;
           domega=0;
           theta=0.0872664626*1.1;
           Message("\nSTOP - Almost closed!!");
}

if (theta > 1.082104136)
{
           omega_out=0;
           omega_calc=0;
           domega=0;
           theta=1.082104136;
           Message("\nSTOP - Fully open!!");
}
```

```
#if !RP_NODE
/* Saving the values*/
/*---------------------------------------------------------------------*/


  FILE *fd_time;
  FILE *fd_torque;
  FILE *fd_omega;
  FILE *fd_theta;


  fd_time = fopen("data_time.txt","a");
  fd_torque = fopen("data_torque.txt","a");
  fd_omega = fopen("data_omega.txt","a");
  fd_theta = fopen("data_theta.txt","a");


  fprintf(fd_time, "%f \n", time);
  fprintf(fd_torque, "%f \n", torque);
  fprintf(fd_omega, "%f \n", omega_out);
  fprintf(fd_theta, "%f \n", theta);


  fclose(fd_time);
  fclose(fd_torque);
  fclose(fd_omega);
  fclose(fd_theta);


Message ("\nomega: %f", omega_out) ;
Message ("\n---------------------------------------\n");
#endif


omega[2]=omega_out;
}


DEFINE_PROFILE(inlet_velocity, thread, position)
{
  face_t f;
  real t = CURRENT_TIME;

  begin_f_loop(f, thread)
  {
  if (t < 0.01)
     F_PROFILE(f, thread, position) = 3.0; /* m/s */
  else
     F_PROFILE(f, thread, position) = 3.0-6*(t-0.01); /* m/s */
  }
  end_f_loop(f, thread)

}
```

Appendix B: Closure coefficients of the turbulence models

There are two turbulence models used in this Master of Science thesis and the closure coefficients of these two are presented below.

k-ε realizable

Table B.1 Constants for the turbulence model k-ε realizable

Constant	value
$C_{1\varepsilon}$	1.44
C_2	1.9
σ_k	1.0
σ_ε	1.2
Pr_t	0.85

$$C_1 = max\left[0.43, \frac{\eta}{\eta+5}\right] \quad , \eta = S\frac{k}{\varepsilon} \tag{B.1}$$

Where S is the modulus of the mean rate-of-strain tensor, defined as:

$$S = \sqrt{2S_{ij}S_{ij}} \tag{B.2}$$

$$C_{3\varepsilon} = tanh\left|\frac{v}{u}\right| \tag{B.3}$$

Where v is the component of the flow velocity parallel to the gravitational vector and u is the component of the flow velocity perpendicular to the gravitational vector

$$C_\mu = \frac{1}{A_0 + A_s\frac{kU}{\varepsilon}} \quad , with\ A_0 = 4.04 \tag{B.4}$$

$$U = \sqrt{S_{ij}S_{ij} + \widetilde{\Omega}_{ij}\widetilde{\Omega}_{ij}} \tag{B.5}$$

$$\widetilde{\Omega}_{ij} = \Omega_{ij} - 2\varepsilon_{ijk}\omega_k \tag{B.6}$$

$$\Omega_{ij} = \overline{\Omega_{ij}} - \varepsilon_{ijk}\omega_k \tag{B.7}$$

Where $\overline{\Omega_{ij}}$ is the mean rate-of-rotation tensor viewed in a rotating reference frame with the angular velocity, ω_k.

$$A_s = \sqrt{6}cos(\phi) \tag{B.8}$$

$$\phi = \frac{1}{3}cos^{-1}\left(\sqrt{6}W\right) \tag{B.9}$$

$$W = \frac{S_{ij}S_{jk}S_{ki}}{\tilde{S}} \quad , with\ \tilde{S} = S_{ij}S_{ij} \tag{B.10}$$

$$S_{ij} = \frac{1}{2}\left(\frac{\partial u_j}{\partial x_i} + \frac{\partial u_i}{\partial x_j}\right) \tag{B.11}$$

k-ω

Table B.2 Constants for the turbulence model k-ω

Constant	value
α	5/9
β	3/40
β^*	9/100
σ_k	1/2
σ_ω	1/2

Appendix C: Input files for the RELAP5 simulations

RELAP5: inertial swing check valve model

```
*------------------------------------------------------------
*         Name       Component
1030000   V         valve
*
*------------------------------------------------------------
*
*     from comp. to comp.   Area       K+      K-  jefvcahs
1030101  102100002 104010001 0.0324 0.0000 0.0000  00000100
*
*  cntrl.word  water flow  vapor flow  Interface-vel.=0
1030201   1           0.0           0.0         0.
*
*         vale type
1030300   srvvlv
*
*          cntrlvar  table_nr
1030301    520        101
*
* Area table
20210100   normarea  0  1.00000  1.0
20210101   0.0000   0.00000
20210102   0.0222   0.00038
20210103   0.0444   0.00150
20210104   0.0667   0.00338
20210105   0.0889   0.00601
20210106   0.1111   0.00939
20210107   0.1333   0.01352
20210108   0.1556   0.01839
20210109   0.1778   0.02401
20210110   0.2000   0.03037
20210111   0.2222   0.03746
20210112   0.2444   0.04530
20210113   0.2667   0.05387
20210114   0.2889   0.06316
20210115   0.3111   0.07320
20210116   0.3333   0.08396
20210117   0.3556   0.09545
20210118   0.3778   0.10765
20210119   0.4000   0.12056
20210120   0.4222   0.13426
20210121   0.4444   0.14873
20210122   0.4667   0.16394
20210123   0.4889   0.17987
20210124   0.5111   0.19660
20210125   0.5333   0.21438
20210126   0.5556   0.23296
20210127   0.5778   0.25232
20210128   0.6000   0.27276
20210129   0.6222   0.29445
20210130   0.6444   0.31703
20210131   0.6667   0.34050
20210132   0.6889   0.36631
20210133   0.7111   0.39320
20210134   0.7333   0.42116
20210135   0.7556   0.45211
20210136   0.7778   0.48489
20210137   0.8000   0.51901
```

```
20210138   0.8222   0.55713
20210139   0.8444   0.59789
20210140   0.8667   0.64033
20210141   0.8889   0.68903
20210142   0.9111   0.74122
20210143   0.9333   0.79556
20210144   0.9556   0.86016
20210145   0.9778   0.92872
20210146   1.0000   1.00000
*
* ------------------------------------------------
* Commands to control the calculation
* ------------------------------------------------
*
* If max angle AND torque positive OR max angle for "the first time"
410  cntrlvar 519  ge null 0 1.082104136 n
411  cntrlvar 513  ge null 0 0.00 n
412  cntrlvar 519  ne cntrlvar  521  0.00 n
610  410      and    411    n
611  410      and    412    n
612  610      or     611    n
*
* If min angle AND torque negative
413  cntrlvar 519  le null 0 0.0872664626 n
414  cntrlvar 513  le null 0 0.00 n
613  413      and    414    n
*
* Time-trip 1
415  time 0  le null 0 0.00 n
614  413      and    415     n
*
* Time-trip 2
416  time 0  ge null 0 100.00 n
615  413      and    416     n
*
* A = 0 If max angle AND torque positive OR max angle for "the first time"
20550000 maxAngle tripunit 1.0 0.0 1
20550001 -612
*
* B = 0 If min angle AND torque negative
20550100 minAngle tripunit 1.0 0.0 1
20550101 -613
*
* C = 0 if trip TRUE
20550200 Custom1 tripunit 1.0 0.0 1
20550201 -614
*
* D = 0 if trip TRUE
20550300 Custom2 tripunit 1.0 0.0 1
20550301 -615
*
* ------------------------------------------------
* Torque calculations
* ------------------------------------------------
* dP = (p1-p2)
20550400 deltaP sum 1.0 0.0 1
20550401 0.00 1.000 p 102100000
20550402 -1.000 p 104010000
*
* Indata
20550500 discArea constant 0.0394
```

```
20550600 Length constant 0.155
20550700 I_tot constant 0.1875
20550800 M_tot constant 5.5542
*
20550900 COSINE stdfnctn 1.0 1.0 1
20550901 cos cntrlvar 519
*
20551000 SINE stdfnctn 1.0 1.0 1  * COS if vertical valve
20551001 sin cntrlvar 519
*
* (p1-p2)*A_disc*cos(theta)*L
20551100 dP_term mult 1.0 0.0 1
20551101 cntrlvar 504 cntrlvar 505 cntrlvar 506  cntrlvar 509
*
* -M*9.82*L*sin(theta)
20551200 Weight mult -9.820 0.0 1
20551201 cntrlvar 508 cntrlvar 506 cntrlvar 510
*
* Sum of torques
20551300 TORQUE sum 1.0 0.0 1
20551301 0.0 1.0 cntrlvar 511
20551302 1.0 cntrlvar 512
*
* ------------------------------------------------
* Calculating angular acceleration
* ------------------------------------------------
*
20551400 ANG_ACC div 1.0 0.0 1
20551401 cntrlvar 507 cntrlvar 513
*
* ------------------------------------------------
* Calculating angular velocity
* ------------------------------------------------
*
20551500 accXdt mult 1.0 0.0 1
20551501 cntrlvar 514 dt 0
*
* w_new = w_old + dw/dt * dT
20551600 OMEGA sum 1.0 0.000000 1
20551601 0.0 1.0 cntrlvar 517
20551602 1.0 cntrlvar 515
*
* w_new*A*B*C*D
20551700 OMEGA mult 1.0 0.000000 1
20551701 cntrlvar 516 cntrlvar 500 cntrlvar 501 cntrlvar 502 cntrlvar 503
*
* ------------------------------------------------
* Calcualting angle
* ------------------------------------------------
*
* theta = theta_old + w_new * dT
20551800 w mult 1.0 0.0 1
20551801 cntrlvar 517 dt 0
*
20551900 theta sum 1.0 1.082104136 1 3 0.0872664626 1.082104136
20551901 0.0  1.0 cntrlvar 519
20551902 1.0 cntrlvar 518
*
* Norm. vinkel (theta/90 deg)*B*C*D     (1/1.571 = 0.636537)
20552000 STEM mult 0.636537 0.0 1
20552001 cntrlvar 519 cntrlvar 501 cntrlvar 502 cntrlvar 503
```

```
*
*Tidsfördröjd vinkel
20552100 thetaOLD delay 1.000 0.00 1
20552101 cntrlvar 519  1.00e-5  1
```

RELAP5: DRAKO swing check valve model

```
*------------------------------------------------------------------------
*         Namn       Komponent
1030000   V     valve
*
* Ritning: Ritn.
*------------------------------------------------------------------------
*
*         From comp  To comp   Area     K+      K-      jefvcahs
1030101   102100002   104010001   0.0324   0.0000  0.0000  00000100
*
*         cntrl.word  Waterflow  Vaportflow  Interface-vel.=0
1030201   1           0.0           0.0         0.
*
*         valve type
1030300   srvvlv
*
*          cntrlvar  table_nr
1030301    211       101

*area table
20210100     normarea
20210101     0.0     0.0
20210102     0.052      0.225
20210103     0.105      0.400
20210104     0.157      0.537
20210105     0.210      0.600
20210106     0.263      0.610
20210107     0.315      0.623
20210108     0.368      0.637
20210109     0.421      0.654
20210110     0.473      0.672
20210111     0.526      0.692
20210112     0.578      0.713
20210113     0.631      0.737
20210114     0.684      0.762
20210115     0.736      0.789
20210116     0.789      0.820
20210117     0.842      0.854
20210118     0.894      0.895
20210119     0.947      0.905
20210120     1.0      0.905

* ------------------------------------------------
* Calcualting relative velocity
* ------------------------------------------------
*
* theta_diversion = theta + 0.0872661626 rad (=5.0 degrees))
20514000 th_str sum 1.0 0.0 0
20514001 0.0872664626 1.0 cntrlvar 210

20514100 cos_thst stdfnctn 1.0 0.0 0
20514101 cos cntrlvar 140


* Flapper velocity in the flow direction
20514200 v_x mult 0.155 0.0 0
20514201 cntrlvar 205 cntrlvar 141
*
* Relative velocity
20514300 v_rel sum 1.0 0.0 0
```

```
20514301 0.0 1.0 cntrlvar 100
20514302 -1.0 cntrlvar 142
*
* ------------------------------------------------
* Calcualting the torque due to the flow
* ------------------------------------------------
*
* Flow velocity
20510000 velfj_25 div 30.83633 0.0 0
20510001 rho 104010000
20510002 mflowj 104010000
*
20510100 cos2th poweri 1.0 0.0 0
20510101 cntrlvar 141 2
*
20510200 absvrel stdfnctn 1.0 0.0 0
20510201 abs cntrlvar 143

* Torque
* M_str = vrel*|vrel|*cos2th*rho*Aseat*L = vrel*|vrel|*cos2th*rho * 0.03243
* 0.155 = vrel*|vrel|*cos2th*rho * 0.00502654
20510300 M_str mult 0.00502654 0.0 0
20510301 cntrlvar 102 cntrlvar 143 * v_rel*|v_rel|
20510302 cntrlvar 101 * cos2th
20510303 rho 104010000 * rho
*
* ------------------------------------------------
* Calcualting the torque due to pressure difference
* ------------------------------------------------
*
* dP
20511000 dp sum 1.0 0.0 0
20511001 0.0 1.0 p 102100000
20511002 -1.0 p 104010000
*
* du/dt=d/dt(velfj_25)
20511100 dudt diffrend 1.0 0.0 0
20511101 cntrlvar 100
*
* dp=-rho*dx*du/dt
20511200 dp mult -0.2 0.0 0   * 0.2 is the node length
20511201 cntrlvar 111
20511202 rho 104010000

* Torque
* M_dp = dp * Adisc * L= dp * 0.0394 * 0.155 = dp * 0.006107)
20511500 M_dp sum 0.006107 0.0 0
20511501 0.00000 1.0 p 102100000
20511502 -1.0 p 104010000
20511503 1.0 cntrlvar 112
*
* ------------------------------------------------
* Calcualting the torque due to weight
* ------------------------------------------------
*
20515000 th_tot sum 1.0 0.0 0
20515001 0.0872664626 1.0 cntrlvar 210

* M_mg=x*Fmg*sin(th_tot) = 9.1469*sin(th_tot)
20515100 Mmg stdfnctn -9.1469 0.0 0
20515101 sin cntrlvar 150
```

```
*
* ---------------------------------------------
* Calcualting the total torque
* ---------------------------------------------
*
20512000 Mtot sum 1.0 0.0 0
20512001 0.0 1.0 cntrlvar 103 * M_str
20512002 1.0 cntrlvar 115 * M_dp
20512003 1.0 cntrlvar 151 * M_mg
*
* ---------------------------------------------
* Calcualting angle
* ---------------------------------------------
*
* Itot=0.1875 kgm2
20519900 Itot constant 0.1875

* omega_dot
20520000 alfa div 1.0 0.0 0
20520001 cntrlvar 199 cntrlvar 120

* domega=alfa*dt
20520100 domega mult 1.0 0.0 0
20520101 cntrlvar 200 dt 0

* domega at the end posiition
20520200 domega mult 1.0 0.0 0
20520201 cntrlvar 201 cntrlvar 605

* domega at the end position
20520300 omega_n mult 1.0 0.0 0
20520301 cntrlvar 205 cntrlvar 606

* new omega
20520500 omega_ny sum 1.0 0.0 0
20520501 0.0 1.0 cntrlvar 203
20520502 1.0 cntrlvar 202

* Disc angle (radianer): Max angle 57 degrees =0.9948376736 rad
20521000 theta integral 1.0 0.9948376736 0 3 0.0 0.9948376736  *
0.0872664626 1.082104136
20521001 cntrlvar 205

* Stem position: theta/theta_max = theta/0.9948376736 = theta * 1.005189114
20521100 vlvstem mult 1.005189114 0.0 0 3 0.0 1.0 **0.6366197724 0.0 1
20521101 cntrlvar 210

* Theta displaced
20521300 o sum 1.0 0.0 0
20521301 0.087266463 1.0 cntrlvar 210
*
* ---------------------------------------------
* Trips
* ---------------------------------------------
*
* Valve position
551 cntrlvar 210 le null 0 0.0 n
552 cntrlvar 210 ge null 0 0.9948376736

* Torque
```

```
553 cntrlvar 120 lt null 0 0.0 n * closing
554 cntrlvar 120 ge null 0 0.0 n * opening
*
* End position
601 551 and 553 n * Valve closed and closing torque
602 552 and 554 n * Valve open and opening torque
603 601 or 602 n * Valve at end position and closing torque
604 551 or 552 n * Valve in end position
*
* Moving valve
605 -603 and -603 n * Flapper not in end position and not looking
606 -604 and -604 n * Flapper not in end position
*
20560500 tr605 tripunit 1.0 0.0 0
20560501 605
*
20560600 tr606 tripunit 1.0 0.0 0
20560601 606
```

RELAP5: Quasi-stationary model

```
*------------------------------------------------------------
*         Name       Component
1030000   V         valve
*
*------------------------------------------------------------
*
*     from comp. to comp.   Area       K+      K-  jefvcahs
1030101  102100002 104010001 0.0324 0.0000 0.0000  00000100
*
*  cntrl.word  water flow  vapor flow  Interface-vel.=0
1030201   1           0.0           0.0         0.
*
*         vale type
1030300   srvvlv
*
*          cntrlvar  table_nr
1030301    520        101
*
* Area table
20210100   normarea  0  1.00000  1.0
20210101   0.0000   0.00000
20210102   0.0222   0.00038
20210103   0.0444   0.00150
20210104   0.0667   0.00338
20210105   0.0889   0.00601
20210106   0.1111   0.00939
20210107   0.1333   0.01352
20210108   0.1556   0.01839
20210109   0.1778   0.02401
20210110   0.2000   0.03037
20210111   0.2222   0.03746
20210112   0.2444   0.04530
20210113   0.2667   0.05387
20210114   0.2889   0.06316
20210115   0.3111   0.07320
20210116   0.3333   0.08396
20210117   0.3556   0.09545
20210118   0.3778   0.10765
20210119   0.4000   0.12056
20210120   0.4222   0.13426
20210121   0.4444   0.14873
20210122   0.4667   0.16394
20210123   0.4889   0.17987
20210124   0.5111   0.19660
20210125   0.5333   0.21438
20210126   0.5556   0.23296
20210127   0.5778   0.25232
20210128   0.6000   0.27276
20210129   0.6222   0.29445
20210130   0.6444   0.31703
20210131   0.6667   0.34050
20210132   0.6889   0.36631
20210133   0.7111   0.39320
20210134   0.7333   0.42116
20210135   0.7556   0.45211
20210136   0.7778   0.48489
20210137   0.8000   0.51901
20210138   0.8222   0.55713
20210139   0.8444   0.59789
20210140   0.8667   0.64033
```

```
20210141   0.8889   0.68903
20210142   0.9111   0.74122
20210143   0.9333   0.79556
20210144   0.9556   0.86016
20210145   0.9778   0.92872
20210146   1.0000   1.00000
*
* ---------------------------------------------
* Command for controlling the calculation
* ---------------------------------------------
*
* If max angle AND torque positive OR max angle for "the first time"
410  cntrlvar 519  ge null 0 1.082104136 n
411  cntrlvar 513  ge null 0 0.00 n
412  cntrlvar 519  ne cntrlvar  521  0.00 n
610  410      and    411    n
611  410      and    412    n
612  610      or     611    n
*
* If min angle AND torque negative
413  cntrlvar 519  le null 0 0.0872664626 n
414  cntrlvar 513  le null 0 0.00 n
613  413      and    414    n
*
* Time-trip 1
415  time 0  le null 0 0.00 n
614  413      and    415     n
*
* Time-trip 2
416  time 0  ge null 0 100.00 n
615  413      and    416     n
*
* A = 0 If max angle AND torque positive OR max angle for "the first time"
20550000 maxAngle tripunit 1.0 0.0 1
20550001 -612
*
* B = 0 If min angle AND torque negative
20550100 minAngle tripunit 1.0 0.0 1
20550101 -613
*
* C = 0 if trip TRUE
20550200 Custom1 tripunit 1.0 0.0 1
20550201 -614
*
* D = 0 if trip TRUE
20550300 Custom2 tripunit 1.0 0.0 1
20550301 -615
*
* E = 0 if trip TRUE (omega= 0)
20550400 Custom3 tripunit 1.0 0.0 1
20550401 -417
* F = 0 if trip TRUE (v<0)
20530100 Custom4 tripunit 1.0 0.0 1
20530101 -418
* G = 0 if trip TRUE (v=>0)
20530200 Custom4 tripunit 1.0 0.0 1
20530201 -419

* ---------------------------------------------
* Data
* ---------------------------------------------
```

```
20550500 A_disc constant 0.0394
20550600 Length constant 0.155
20550700 I_tot constant  0.1875
20550800 R constant  0.112

20550900 COSINE stdfnctn 1.0 1.0 1
20550901 cos cntrlvar 572
*
20551000 th_tot sum 1.0 0.0 1
20551001 0.0 1.0 cntrlvar 572

20551100 SINE stdfnctn 1.0 1.0 1
20551101 sin cntrlvar 510

* ------------------------------------------------
* T_w
* ------------------------------------------------
* T_w= -M*9.82*L*sin(theta)
20551200 T_w mult -9.1469 0.0 1
20551201 cntrlvar 511
*
* wLcos(theta)
20551300 a mult 1.0 0.0 1
20551301 cntrlvar 564 cntrlvar 506 cntrlvar 509
*
20551400 b mult  0.92130  0.0 0 * (A2/A1=0.9213)
20551401 velfj 104010000
*
20551500 ABS_v stdfnctn 1.0 1.0 1
20551501  abs  cntrlvar 514

* ------------------------------------------------
* T_flow
* ------------------------------------------------
* C(theta) instead of using the function the values are interpolated in the
* tables for forward and backeard flow

* C (theta) forward
20531500 F1    function 1.00000 0.0000 0
20531501 cntrlvar 510 315

* C(theta)
20231500 normarea
20231501 0.1745   14.5054
20231502 0.2618   5.32450
20231503 0.4363   2.05770
20231504 0.6109   1.12610
20231505 0.7854   0.74380
20231506 0.9599   0.47930
20231507 1.0471   0.34780
20231508 1.0821   0.29230

* C (theta) backward
20531600 F2    function 1.00000 0.0000 0
20531601 cntrlvar 510 316

* C(theta)
20231600 normarea
20231601 0.1745   11.5091
20231602 0.2618   4.66990
20231603 0.4363   1.85860
```

```
20231604 0.6109   1.07530
20231605 0.7854   0.65190
20231606 0.9599   0.34940
20231607 1.0471   0.29430
20231608 1.0821   0.28260

20552300 A mult 1.0 0.0 1
20552301 cntrlvar 315 cntrlvar 301

20552400 B mult 1.0 0.0 1
20552401 cntrlvar 316 cntrlvar 302

*Cfram*A + Cbak*B
20552700 summa sum 1.0 0.0 1
20552701 0.0 1.0 cntrlvar 523 1.0 cntrlvar 524

*T_flow:   T=C*A*rho*L*abs(v)*v
20553000 T_flow mult 1.0 0.0 1
20553001 cntrlvar 527 cntrlvar 505  rho 104010000 cntrlvar 506 cntrlvar 515
20553002 cntrlvar 514

* ------------------------------------------------
* T_tot
* ------------------------------------------------

*Beräkna totalt vridmoment T=T_flow+T_w
20555600 T sum 1.0 0.0 1
20555601 0.0 1.0 cntrlvar 512
20555602 1.0 cntrlvar 530

* ------------------------------------------------
* Omega_dot
* ------------------------------------------------
*
20555900 alfa div 1.0 0.0 0
20555901 cntrlvar 507 cntrlvar 557
*
20556000 alfa div 1.0 0.0 0
20556001 cntrlvar 507 cntrlvar 556
*
* ------------------------------------------------
* omega
* ------------------------------------------------
20556100 domega mult 1.0 0.0 0
20556101 cntrlvar 560 dt 0

* w_new = w_old + dw/dt * dT
20556300 OMEGA sum 1.0 0.000000 0
20556301 0.0 1.0 cntrlvar 564
20556302 1.0 cntrlvar 561

* w_new*A*B*C*D
20556400 OMEGA mult 1.0 0.000000 1
20556401 cntrlvar 563 cntrlvar 500 cntrlvar 501 cntrlvar 502 cntrlvar 503

* ------------------------------------------------
* Theta
* ------------------------------------------------
* theta = theta_old + 0.5*dt*(omega_prev+omega)
*
* Flapper angle (rad): (min max) angle
```

```
20557200 theta integral 1.0 1.082104136 0 3 0.0872664626 1.082104136
20557201 cntrlvar 564

* Norm. angle (theta/57 deg)*B*C*D     (1.005189114) (theta /
90)=theta*0.6366197724
20557500 STEM mult 0.6366197724 0.0 1 *3 0.0 1.0
20557501 cntrlvar 572 cntrlvar 501 cntrlvar 502 cntrlvar 503

*Time delayed angle
20558100 thetaOLD delay 1.000 0.00 1
20558101 cntrlvar 572  1.00e-5  1
```